



Performance Enhancement of a Household Refrigerator Using Phase Changing Materials (PCMs) and Nanoparticles

A Thesis

Submitted to the Council of the Erbil Technical Engineering College at Erbil Polytechnic University in Partial Fulfillment of the Requirements for the Degree of Master of Science in Mechanical and Energy Engineering.

By:

Darawan Bazyan Dhahir

B.Sc. in Refrigeration and Air -Conditioning Engineering Techniques. 2014

Supervised by:

Prof. Dr. Ahmed Mohammed Adham

ERBIL-KURDISTAN

May-2023

DECLARATION

I declare that the master thesis entitled: “**Performance Enhancement of a Household Refrigerator Using Phase Changing Materials (PCMs) and Nanoparticles**” is my own original work, and hereby I certify that unless stated, all work contained within this thesis is my own independent research and has not been submitted for the award of any other degree at any institution, except where due acknowledgement is made in the text.

Signature:



Student Name: Darawan Bazyan Dhahir

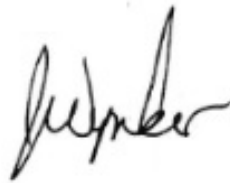
Date:

5 / 6 / 2023

LINGUISTIC REVIEW

I confirm that I have reviewed the thesis titled (**Performance Enhancement of a Household Refrigerator Using Phase Changing Materials (PCMs) and Nanoparticles**) from the English linguistic point of view, and I can confirm that it is free of grammatical and spelling errors.

Signature:

A handwritten signature in black ink, appearing to read 'J. Wynker', written in a cursive style.

Name of Reviewer: Jack C Wynker

Date: 16/04/2023

SUPERVISOR CERTIFICATE

This thesis has been written under my supervision and has been submitted for the award of the degree of Master of Science in Mechanical and Energy Engineering with my approval as a supervisor.

Signature 

Prof. Dr: Ahmed Mohammed Adham
Name

Date 5/6/2023

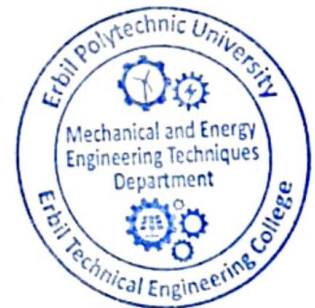
I confirm that all the requirements have been fulfilled.

Signature: 

Name: Prof. Dr. Ahmed Mohammed Adham

Head of Mechanical and Energy Engineering Department.

Date: 5/6/2023



I confirm that all the requirements have been fulfilled.

Signature: 


Name: Byad Abdulqader Ahmed


Postgraduate Office


Date: 6/6/2023


EXAMINING COMMITTEE CERTIFICATION


We certify that we have read this thesis entitled “**Performance Enhancement of a Household Refrigerator Using Phase Changing Materials (PCMs) and Nanoparticles**” and as an examining committee, examined the student (Darawan Bazyan Dhahir) in its content and what related to it. We approve that it meets the standards of a thesis for the degree of Master in Mechanical and Energy Engineering.

Signature: 
Name: Asst. Prof. Dr. Omer Mohammed Hamdoon
Member
Date: 29/5/2023

Signature: 
Name: Prof. Dr. Ahmed Mohammed Adham
Supervisor
Date: 28/05/2023

Signature: 
Name: Prof. Dr. Ayad Z. Saber Agha
Dean of Erbil Technical Engineering College
Date: 05 - 06 - 2023

Signature: 
Name: Asst. Prof. Dr. Banipal Nanno Yaqob
Member
Date: 28/5/2023

Signature: 
Name: Prof. Dr. Omer Mohammed Ali
Chairman
Date: 31/5/2023

DEDICATION

This thesis is dedicated to my father, who passed away seven months ago. Though he is no longer in this world, his memories continue to govern my life.

To my mom who loves me unconditionally and standing with me in all of my happiness and sadness moments, thanks for directing me on to the right path continuously, you have been such an inspiration to me, I couldn't do anything without you.

To my dear wife, for your unending support and encouragement. I sincerely appreciate having you in my life.

To my siblings, my love for you all can never be quantified.

ACKNOWLEDGMENT

In the Name of Allah, the Most Compassionate the Most Merciful, all praise be to Allah, the Lord of the worlds.

Foremost, I am thankful to almighty ALLAH for giving me the strength, knowledge, ability, and opportunity to undertake and complete this research successfully.

My wholehearted thanks go to my supervisor, Prof. Dr. Ahmed Mohammed Adham for his contribution, guidance, and advice, I can never pay you back for all the assistance you have done to me. Thank you for your help and support. I will be thankful to you forever.

I would like to express my wholehearted thanks and appreciation to the General Director of the Scientific Research Center at Erbil Polytechnic University, Asst. Prof. Dr. Hayman Kakakhan Awla, and his colleagues for their technical support and help.

I would like to extend my thanks and appreciation to all of my colleagues and friends, thanks to all of you for the support and real friendship. Your understanding to my situation was one of the major sources of my success.

Lastly, I would like to thank the Erbil Polytechnic University; they give me the opportunity to study my Master.

ABSTRACT

A refrigerator is the most common and efficient method for preserving food and medicine, although its continuous operation consumes a considerable amount of energy. Thus, this study investigated and evaluated the overall performance of a household refrigerator with phase change materials (PCMs) and nanoparticles. The PCMs are applied to the evaporator (evaporator cold storage, ECS) and condenser (condenser heat storage, CHS) individually and simultaneously. Also, a refrigerator with dual energy storage (DES) and combined energy storage (CES) is proposed. The former included CHS and ECS and the latter involved CHS, ECS, and PCM panels in the fridge cabinet. PCMs were organic paraffins, inorganic salt hydrates, and distilled water. The energy consumption of refrigerators is assessed using ISO standards. Isobutane (R600a) was a refrigerant in the system. The experiments included the application of multiple PCMs to the condenser and evaporators. PCM with copper oxide (CuO) nanoparticles is tested on the condenser alone. As a result, through extensive analysis and testing, the overall performance of the refrigerator was optimized. The CHS effectively improved the coefficient of performance (COP) and kept the temperature of the cabinets, while the ECS efficiently saved energy and reduced temperature fluctuation within the cabinets. The most significant optimizations were by DES and CES due to the combination of cons and pros of using PCMs on the condenser, evaporator, and fridge cabinet individually. The energy savings for CHS cases, ECS cases, DES, and CES were 10.87-21.24%, 15.21-23.47%, 24.29%, and 26.42%, respectively. The COP improvements for CHS tests, ECS tests, DES, and CES were 1.58-7.56%, 4.35-5.50%, 8.81%, and 9.10%, respectively. Although their temperatures increased, the fluctuation temperature in the fridge and freezer cabinets dropped by 15.53-56.53% and 0.61-26.46%, respectively.

TABLE OF CONTENTS

DECLARATION	ERROR! BOOKMARK NOT DEFINED.
LINGUISTIC REVIEW	II
SUPERVISOR CERTIFICATE.....	ERROR! BOOKMARK NOT DEFINED.
EXAMINING COMMITTEE CERTIFICATION.....	III
DEDICATION	IV
ACKNOWLEDGMENT	VI
ABSTRACT	VII
TABLE OF CONTENTS	VIII
LIST OF FIGURES.....	XIII
LIST OF TABLES	XVIII
NOMENCLATURE.....	XX
LIST OF SYMBOLS.....	XX
GREEK LETTERS	XXI
SUBSCRIPTS	XXI
LIST OF ABBREVIATIONS	XXII
CHAPTER 1	1
INTRODUCTION.....	1
1.1. INTRODUCTION	1
1.1.1 Vapor compression refrigeration system	2
1.1.2 Household refrigerator	2
1.2. BACKGROUND OF THE RESEARCH.....	3
1.3. THE PURPOSE OF THE RESEARCH.....	5
1.4. THE CONTRIBUTION OF THE RESEARCH.....	5
1.5. THE SCOPE AND LIMITATION OF THE RESEARCH	6
1.6. THE RESEARCH METHODOLOGICAL STAGES	6
1.7. THE OUTLINE OF THE THESIS	7
CHAPTER 2	9
LITERATURE REVIEW.....	9

2.1. INTRODUCTION	9
2.2. PERFORMANCE ENHANCEMENT TECHNIQUES	11
2.3. HEAT EXCHANGER HEAT TRANSFER ENHANCEMENT TECHNIQUES	12
2.4. THERMAL ENERGY STORAGE SYSTEMS	12
2.4.1 Chemical Energy Storage	13
2.4.2. Physical Energy Storage	13
2.5. PHASE CHANGE MATERIALS (PCMs).....	14
2.5.1. Classification of Solid-Liquid PCMs.....	15
2.5.2. Thermal Conductivity Enhancement Methods	17
2.5.3. Nanoparticles	13
2.6. APPLICATION OF PCMS IN HOUSEHOLD REFRIGERATORS AND FREEZERS... 19	
2.6.1. Application of PCMs in Condenser	19
2.6.2. Application of PCM in Evaporator.....	28
2.6.3. Application of PCM in Cabinets.....	40
2.6.4. Application of PCM in Condenser and Evaporator.....	48
2.6.5. Application of PCM in Condenser and Cabinets.....	48
2.6.6. Application of PCM in Evaporator and Cabinets.....	49
2.7. CONCLUSION	50
CHAPTER 3	57
MATHEMATICAL MODELLING AND SYSTEM DESCRIPTION.....	57
3.1. INTRODUCTION	57
3.2. SYSTEM DESCRIPTION	57
3.3. MATHEMATICAL MODELLING	60
3.3.1. Compressor Analysis	61
3.3.2. Condenser Analysis	62
3.3.3. Capillary Tube Analysis	63
3.3.4. Evaporator Analysis.....	63
3.3.5. Freezer and Fridge Cabinets Analysis	64
3.3.6. Coefficient of Performance (COP)	67
3.3.7. Phase Change Material	67
3.3.8. Estimation of Required Mass.....	68
3.3.9. Percentage of Improvement.....	68
CHAPTER 4	69
EXPERIMENTAL WORK	69
4.1. INTRODUCTION	69

4.2. ENERGY DATA LOGGER	69
4.3. PRESSURE GAUGE DATA RECORDER	70
4.4. TEMPERATURE SENSORS AND DATA LOGGER	72
4.5. IMPLEMENTATION AND POSITIONING OF TEMPERATURE SENSORS	72
4.5.1. Sensor Installation on the Condenser	74
4.5.2. Sensor Installation on the Compressor	75
4.5.3. Sensor Installation on the Evaporator.....	76
4.5.4. Sensor Installation in the Cabinets.....	77
4.6. SELECTION OF PCMS	78
4.7. REQUIRED MASS OF PCMS	80
4.8. PREPARATION OF PCMS	83
4.8.1. Preparation of PCM for the Fridge Cabinet.....	83
4.8.2. Preparation of PCM for the Evaporator.....	84
4.8.3. Preparation of PCM for the Condenser	85
4.9. PCM NANOPARTICLE INCLUSION	85
4.10. EXPERIMENTAL PROCEDURES	88
4.10.1. PCM Implementation in the Fridge Cabinet.....	88
4.10.2. PCM Implementation on the Evaporator (Freezer)	88
4.10.3. PCM Implementation on the Evaporator (Fridge).....	89
4.10.4. PCM Implementation on the Condenser.....	90
4.11. EXPERIMENTS.....	91
4.11.1. Application of PCM in Condenser	92
4.11.2. Application of PCM in Evaporator.....	94
4.11.3. Application of PCM in Condenser and Evaporator.....	95
4.11.4. Application of PCM in Condenser, Evaporator, and Fridge Cabinet.....	95
4.12. DATA ACQUISITIONS	96
4.13. UNCERTAINTY ANALYSIS	97
CHAPTER 5	98
RESULTS AND DISCUSSION	98
5.1. INTRODUCTION.....	98
5.2. COMPRESSOR PRESSURES AND TEMPERATURES	102
5.3. EVAPORATION AND EVAPORATOR SURFACE TEMPERATURES	104
5.3.1. ECS Experiments	104
5.3.2. CHS Experiments.....	106
5.3.3. DES and CES Experiments.....	106
5.4. CONDENSATION AND CONDENSER SURFACE TEMPERATURES	108

5.4.1. ECS Experiments	108
5.4.2. CHS Experiments.....	108
5.4.3. DES and CES Experiments.....	112
5.5. TEMPERATURE OF THE CABINETS	113
5.5.1. ECS Experiments	113
5.5.2. CHS Experiments.....	115
5.5.3. DES and CES Experiments.....	116
5.6. ENERGY CONSUMPTION.....	118
5.6.1. ECS Experiments	120
5.6.2. CHS Experiments.....	121
5.6.3. DES and CES Experiments.....	122
5.7. COEFFICIENT OF PERFORMANCE (COP).....	123
CHAPTER 6	127
CONCLUSION AND FUTURE WORK	127
5.1. CONCLUSION	127
5.2. RECOMMENDATIONS FOR FURTHER WORK	129
REFERENCES.....	R ₁
APPENDIX (A).....	A ₁
CALIBRATION OF ENERGY DATA LOGGER.....	A ₁
APPENDIX (B).....	A ₁
CALIBRATION OF PRESSURE GAUGE.....	A ₁
APPENDIX (C).....	A ₂
CALIBRATION OF TEMPERATURE SENSORS.....	A ₂
APPENDIX (D).....	A ₂
DSC GRAPH FOR RT44HC PCM	A ₂
APPENDIX (E)	A ₃
DSC GRAPH FOR RT35HC PCM	A ₃
APPENDIX (F)	A ₃
DSC GRAPH FOR RT28HC PCM	A ₃
APPENDIX (G).....	A ₄
DSC GRAPH FOR RT4 PCM.....	A ₄

APPENDIX (H).....	A4
DSC GRAPH FOR SP-7 PCM	A4
APPENDIX (I).....	A5
DSC GRAPH FOR SP-17 PCM	A5
APPENDIX (J).....	A6
SAMPLE CALCULATION OF MASS FOR CONDENSER.....	A6
J.1 CALCULATION OF MASS REQUIRED FOR THE CONDENSER.....	A6
APPENDIX (K).....	A8
SAMPLE CALCULATION OF MASS FOR EVAPORATORS	A8
K.1 CALCULATION OF MASS REQUIRED FOR THE EVAPORATORS.....	A8
APPENDIX (L).....	A9
ANCERTAINTY ANALYSIS.....	A9
L.1 UNCERTAINTY ANALYSIS OF THE TEMPERATURE SENSORS	A9
L.2 UNCERTAINTY ANALYSIS OF THE ELITECH PGW-500 PRESSURE GAUGE...	A10
APPENDIX (M).....	A11
SAMPLE CALCULATION OF COP.....	A11
M.1 COP CALCULATION	A11
LIST OF PUBLICATIONS	A12

LIST OF FIGURES

Figure 1.1. Vapor compression system (Arora, 2000).....	3
Figure 2.1. The methodical steps involved in reviewing literature.	10
Figure 2.2. Thermal energy storage systems by (Sharma et al., 2009).....	13
Figure 2.3. The operational principle of solid-liquid PCMs (Sidik et al., 2018). 15	
Figure 2.4. Classification of phase change materials by (Dincer and Rosen, 2021).	17
Figure 2.5. PCM's thermal conductivity enhancement methods by (Ibrahim et al., 2017 and Qureshi et al., 2018)	18
Figure 2.6. Condenser heat storage made by (Cheng et al., 2011)..	20
Figure 2.7. Energy consumption vs. time by (Cheng et al., 2011)..	20
Figure 2.8. Condenser equipped with a) Bags of aluminum composite layer containing PCM and b) Copolymer compound by (Sonnenrein et al., 2015).	21
Figure 2.9. Arrangement of PCMs performed by (Pirvaram et al., 2019).....	22
Figure 2.10. PCM setup on condenser tubes made by (Kumar et al., 2020).....	23
Figure 2.11. PCM configuration on the condenser by (Karthikeyan et al., 2021).23	
Figure 2.12. Compressor discharge temperatures by (Kasinathan and Kumaresan, 2021).....	23
Figure 2.13. PCM setup on evaporator (Azzouz et al., 2005)..	29
Figure 2.14. COP vs. melting points for various ambient temperatures (Azzouz et al., 2005).....	29
Figure 2.15. Refrigerator with PCM setup by (Azzouz et al., 2008).....	30
Figure 2.16. COP vs. thermal load made by (Azzouz et al., 2008).	24
Figure 2.17. Experimental setup made by (Azzouz et al., 2009).....	31

Figure 2.18. The average COP for various thermal loads by (Azzouz et al., 2009).....	29
Figure 2.19. Setup procedures of PCM by (Md Imran Hossen and Afroz, 2011).	32
Figure 2.20. PCM setup on the evaporator (Yusufoglu et al., 2015).....	30
Figure 2.21. Design of PCM heat exchanger by (Elarem et al., 2017).....	31
Figure 2.22. PCM arrangement on evaporator by (Cofré-Toledo et al., 2018)...	31
Figure 2.23. VCRS and PCM set up by (Raveendran and Murugan, 2021).....	35
Figure 2.24. Position of PCM panels made by (Gin and Farid, 2010)..	33
Figure 2.25. PCM's effect on temperature swings during power failures (Gin and Farid, 2010)..	41
Figure 2.26. PCM encapsulation container and location by (Oró et al., 2012)..	34
Figure 2.27. Comparison of PCM orientations by (Marques et al., 2013).	34
Figure 2.28. PCM position by (Abdolmaleki et al., 2020).	35
Figure 2.29. Domain modeled by (Pavithran et al., 2021).....	40
Figure 2.30. PCM configuration in the freezer and fridge cabinets (Karthikeyan et al., 2021).....	41
Figure 2.31. Temperature vs. time for (a) condenser upper part, (b) condenser lower part, (c) fridge cabinet, and (d) freezer cabinet by (Karthikeyan et al., 2021).	49
Figure 2.32. PCM arrangements in evaporator (case-1), evaporator and cabinet wall (case-2), evaporator and cabinet racks (case-3), and evaporator and cabinet's wall and racks (case-4) by (Elarem et al., 2017).....	43
Figure 3.1. Household refrigerator prototype.	59
Figure 3.2. A scheme of the household refrigerator system.	59
Figure 3.4. Standard vapor compression refrigeration cycle.	60
Figure 3.5. Standard vapor compression refrigeration cycle on P-h diagram (Arora, 2000).....	61

Figure 3.6. The components of walls and doors.	65
Figure 3.7. One dimensional thermal resistance circuit.....	65
Figure 4.1. Zhurui power recorder (PR10) and its setup.	70
Figure 4.2. The Elitech PGW-500 and Hongsen gauges.	71
Figure 4.3. Set up of Elitech PGW-500 and Hongsen pressure gauges.....	71
Figure 4.4. Temperature sensor and data logger.....	73
Figure 4.5. Location of temperature sensors.....	73
Figure 4.6. Location of temperature sensors on condenser.	75
Figure 4.7. The installation processes of temperature sensors on the condenser.....	75
Figure 4.8. Location of temperature sensors on compressor.	76
Figure 4.9. Location and arrangement of temperature sensors on evaporators.	76
Figure 4.10. Location of temperature sensors in the cabinets.....	77
Figure 4.11. Steps of preparing and installing sensors in the cabinets.	77
Figure 4.12. The parts of the condenser.....	80
Figure 4.13. Cabinets of refrigerator.....	83
Figure 4.14. Rubitherm-manufactured aluminum PCM panel.	84
Figure 4.15. Rubitherm-manufactured aluminum pouches.	84
Figure 4.16. Copper tube fabrication process.	85
Figure 4.17. PCM Nanoparticle inclusion procedures.....	86
Figure 4.18. The position of aluminum PCM panels in the fridge cabinet.....	88
Figure 4.19. PCM configuration on the evaporator (Freezer).	89
Figure 4.20. PCM setup on the evaporator (Fridge).	90
Figure 4.21. Copper tube arrangement on the condenser sections.	91
Figure 4.22. Danfoss Coolselector®2 software version 4.8.2. refrigerant calculator.	96
Figure 5.1. Refrigeration cycle for ECS-1, ECS-2, and ECS-3 vs. HR.....	101
Figure 5.2. Refrigeration cycle for CHS-1, CHS-2, and CHS-3 vs. HR..	101

Figure 5.3. Refrigeration cycle for DES and CES vs. HR.....	101
Figure 5.4. Evaporation and condensation pressures and temperatures.	103
Figure 5.5. Average inlet (T6) and outlet (T7) temperatures vs. time for freezer evaporator.....	105
Figure 5.6. Average inlet (T8) and outlet (T9) temperatures vs. time for fridge evaporator.....	107
Figure 5.7. Average temperature of (T1 and T2) vs. time of section 1 of the condenser.....	109
Figure 5.8. Average temperature of (T2 and T3) vs. time of section 2 of the condenser.....	110
Figure 5.9. Average temperature of (T3 and T4) vs. time of section 3 of the condenser.....	111
Figure 5.10. Average temperature of (T4 and T5) vs. time of section 4 of the condenser.....	112
Figure 5.11. Fridge cabinet temperatures and their improvements in fluctuation	114
Figure 5.12. Freezer cabinet temperatures and their improvements in fluctuation.	116
Figure 5.13. Average of fridge cabinet temperatures (T13, T14, and T15) vs. time.	117
Figure 5.14. Average of freezer cabinet temperatures (T11 and T12) vs. time...	118
Figure 5.15. The energy consumptions per 24h and their savings..	119
Figure 5.16. Energy consumptions vs. time.....	122
Figure 5.17. The COPs and their improvements.....	126
D.1. DSC graph of latent heat of fusion vs. temperature for RT44HC.	A ₂
E.1. DSC graph of latent heat of fusion vs. temperature for RT35HC.....	A ₃
F.1. DSC graph of latent heat of fusion vs. temperature for RT28HC.	A ₃

G.1. DSC graph of latent heat of fusion vs. temperature for RT4.	A ₄
H.1. DSC graph of latent heat of fusion vs. temperature for SP-7.	A ₄
I.1. DSC graph of latent heat of fusion vs. temperature for SP-17.	A ₅

LIST OF TABLES

Table 2.1 List of studies and their results that employed PCM on condenser.....	25
Table 2.2 List of studies and their results that employed PCM on the evaporator.	36
Table 2.3 PCM orientations and locations, covering area by PCM, and compartment variation temperatures of five cases by (Pavithran et al., 2021)....	44
Table 2.4 List of investigations and their outcomes that installed PCM in the cabinets.....	46
Table 2.5 The results of various parameters by (Cheng et al., 2017).....	48
Table 3.1 The specifications of household refrigerator.	58
Table 4.1 Specifications of Zhurui (PR10) power recorder.....	70
Table 4.2 The specifications of the Elitech PGW-500 and the Hongsen gauges.	72
Table 4.3 Specification of temperature sensors and temperature data logger..	72
Table 4.4 Location of temperature sensors.	74
Table 4.5 Specifications of selected PCMs.....	80
Table 4.6 Overall heat transfer gain of fridge cabinet.	83
Table 4.7 Properties of CuO nanoparticles and SDBS.	87
Table 4.8 Thermophysical experimental properties of RT35HC and NCPCM...	87
Table 4.9 The observed temperatures for the first experiment (HR).....	92
Table 4.10 Experiments on the condenser.	93
Table 4.11 Experiments on the evaporator	95
Table 4.12 Results of uncertainty.....	97
Table 5.1 The results of experiments for different parameters.....	99
Table 5.2 The results of experiments for different parameters.....	100
A.1 Results of Calibration of Energy Data Logger.....	A ₁

B.1 Results of Calibration of Pressure Gauges.....A₁
C.1 Results of Calibration of Temperature Sensors.....A₂
L.1. Example of temperature sensor readings.....A₉
L.2. Example of pressure gauge readings.. A₁₀

NOMENCLATURE

LIST OF SYMBOLS

A	Area (m ²)
C _p	Specific heat (kJ/kg. °C)
E	Compressor energy consumption (kJ/s)
Gr	Grashof number (m/s ²)
<i>g</i>	Gravitational acceleration
<i>h_f</i>	Latent heat of fusion (kJ/kg)
<i>h₁</i>	Specific enthalpy of section line of compressor (kJ/kg)
<i>h₂</i>	Specific enthalpy of discharge line of compressor (kJ/kg)
<i>h₃</i>	Specific enthalpy of outlet of condenser (kJ/kg)
<i>h₄</i>	Specific enthalpy of inlet of evaporator (kJ/kg)
<i>h_i</i>	Internal heat transfer coefficient (W/m ² . °C)
<i>h_e</i>	External heat transfer coefficient (W/m ² . °C)
k	Thermal conductivity (W/m. °C)
L _C	Characteristic length (m)
M	Mass (kg)
<i>M_{ref}</i>	Refrigerant mass flowrate (kg/s)
Nu	Nusselt number
P	Perimeter (m)
Pr	Prandtl number
Q _L	Evaporator heat extraction (kW)
Q _H	Condenser heat rejection (kW)
Q _c	Heat gain through cabinet' wall and door (kW)

Q_{pcm}	Amount of stored energy in PCM (kJ)
R_T	Total thermal resistance ($^{\circ}\text{C}/\text{W}$)
Ra	Rayleigh number
T	Temperature ($^{\circ}\text{C}$)
U	Overall heat transfer coefficient ($\text{W}/\text{m}^2 \cdot ^{\circ}\text{C}$)
w	Compressor work (kJ/kg)

GREEK LETTERS

β	Thermal expansion coefficient
ρ	Density (kg/m^3)
ν	Kinematic viscosity (m^2/s)

SUBSCRIPTS

sub	Subcooling degree
suc	Suction line of compressor
interval.ph.	Interval phase change temperature of PCM
on	On time cycle of compressor
off	Off time cycle of compressor
∞	Air
s	Surface
f	Fusion
ph	Phase change
a	Ambient
m	Mean

LIST OF ABBREVIATIONS

CuO	Copper oxide
CHS	Condenser heat storage
CES	Combined energy storage
COP	Coefficient of performance
DES	Dual energy storage
DSC	Differential scanning calorimetry
ECS	Evaporator cold storage
FS	Full scale
HDPE	High-density polyethylene
HIPS	High-impact polystyrene
HR	Household refrigerator
in	Inlet
NCPCM	Nano composite phase change material
out	Outlet
PCM	Phase change materials
PT 100	Platinum 100
PUR	Polyurethane foam
ΔP	Difference between condenser and evaporator pressure
RTD	Resistance temperature detector
SDBS	Sodium dodecylbenzene sulfonate
SSPCM	Shape stabilized phase change material
VAC	AC voltage

CHAPTER 1

INTRODUCTION

1.1. General

Global warming is a threat that our planet is currently challenged with. It is driven by an increase in the concentration of greenhouse gases in the atmosphere, such as carbon dioxide, methane, nitrous oxide, and fluorinated gases (Kumar et al., 2021). Burning fossil fuels like coal, oil, and gases to generate electricity is primarily responsible for the growth in atmospheric concentrations of greenhouse gases (Mohamed et al., 2017). Even though, the backbone of modernization is electricity since virtually all appliances require electricity to perform specific tasks or operations. As a consequence of speedy industrialization and advancements in the quality of life, electricity use is undoubtedly rising daily (Hosseini and Wahid, 2016). The rising worldwide environmental consciousness, combined with the increasing electricity costs, is pushing the requirement for the creation of environmentally efficient cooling systems.

Thus, efforts to reduce electricity consumption or produce electricity from renewable energy sources are imperative. In light of this, many countries are working to significantly minimize household energy use through consumer information initiatives, innovative labels, and guidelines (Vine et al., 2001). For instance, in 1998, the United States energy star program saved about 500 billion kWh of electricity, which prevented 39 billion dollars in energy costs and the release of 390 million metric tons of greenhouse gases (ENERGY, 1998).

Additionally, appliances in Europe are labeled with an energy efficiency rating ranging from the best (A+++), to the worst (G) (Directive, 1992). Currently, stronger energy consumption standards are required, mandating the manufacturing of appliances with an A+ or higher rating to significantly improve energy savings in household electrical products (Yusufoglu et al., 2015). Together with the frightening rise in energy usage, these efforts are compelling production companies to develop and manufacture better-efficient appliances.

Household refrigerators and freezers consume the most energy of household appliances because of their continual running (Raveendran and Sekhar, 2016). Efforts to improve the energy efficiency of household refrigerators will directly result in a reduction in residential energy consumption (Yusufoglu et al., 2015). According to a study by (Dupont et al., 2019), around two billion domestic refrigerators are in operation globally, accounting for a significant portion of the total electricity consumption and releasing greenhouse gases. Therefore, many researchers are currently focusing their efforts on finding novel technical solutions to optimize the energy efficiency and performance of household refrigerators (Khan and Afroz, 2011).

1.1.1 Vapor compression refrigeration system

Vapor compression refrigeration systems are widely used for household refrigerators, freezers, air conditioner units, cold storage, etc. In the below section, the household refrigerator will be discussed thoroughly.

1.1.2 Household refrigerator

A refrigerator is an essential appliance in most houses. Compressor, condenser, expansion valve for large systems and capillary tube for small systems,

and an evaporator are the main components of the refrigeration system, as displayed in Fig. 1. The compressor is the starting and ending point of the refrigeration process. A majority of the energy used during the cooling cycle is absorbed in the compressor (Arora, 2000).

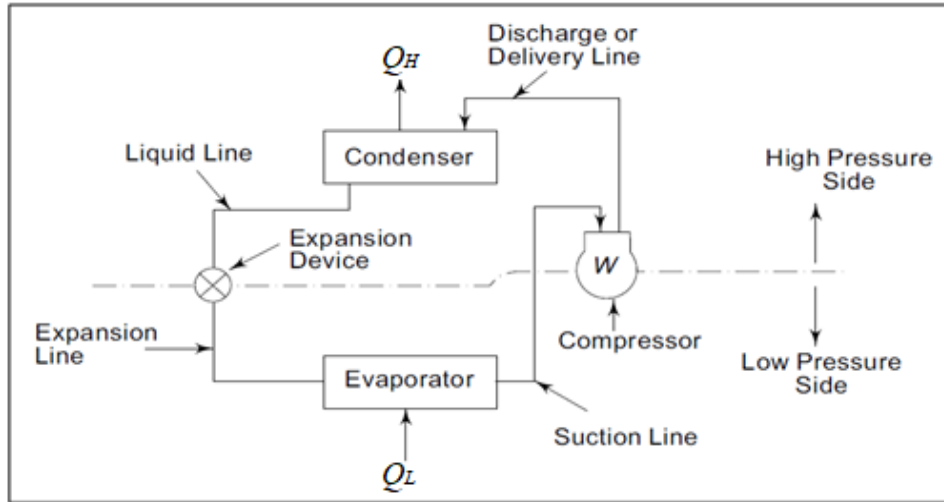


Figure 1.1. Vapor compression system (Arora, 2000).

1.2. Background of the Research

Phase change material (PCM) was first discovered in the early 20th century by Yale University physicist Alan Tower Waterman. Waterman studied the thermionic emission of some hot salts and observed certain irregularities in the conductivity of molybdenite (MoS_2). He found that the conductivity of the chalcogenide could be gradually changed (Waterman, 1917). Based on the literature, direct and indirect PCM applications have gained research attention since the 1980s (Abhat, 1983). There was a gradual increase in the number of publications until 2016. However, between 2016 and 2020, comprehensive efforts have been made to investigate PCM technologies to meet rising energy consumption requirements. This growth in PCM publications was based on their use in fields including construction, air conditioning and refrigeration systems,

micro-electro-mechanical systems, smart textiles, etc (Hamad et al., 2021). From 2020 to the present, the publications on the application of PCMs in the abovementioned areas remain extensive.

Since PCMs have been used until the present, many studies have investigated the PCMs for different purposes in appliances working on the refrigeration system, most notably in household refrigerators. Because household refrigerators relate significantly to global energy utilization and the emission of greenhouse gases (Maiorino et al., 2019). They experimentally and numerically assessed the use of PCMs in household refrigerator components and cabinets to improve COP, reduce energy consumption, and minimize temperature fluctuations within the cabinets (Bista et al., 2018).

Related to the improvements aforementioned, the utilization of PCMs in household refrigerators could improve some other aspects (Omara and Mohammedali, 2020). For instance, greenhouse gas emissions could be mitigated by minimizing energy consumption, like the US energy star program, which eliminated the emission of 390 million tons of greenhouse gases in 2019. Moreover, using PCMs in domestic refrigeration systems increased the initial costs. Nonetheless, when the system runs, the total cost has been reduced (Oró et al., 2012). (Oró et al., 2014) stated that the cost savings based on the benefits of PCM cold potential in European household appliances might range from 1081 to 4682 million euros annually. Lastly, the operation and refrigerant circulation through the tubes generated refrigerator noise (Hartmann and Melo, 2013). Hence, PCMs were applied to reduce it by extending the off-time cycle and shortening the on-time cycle (Joybari et al., 2015).

1.3. The Purpose of the Research

The purpose of this research is to make a household refrigerator more optimized. This optimization will make use of PCMs and nanoparticles. The modified household refrigerator will consume less energy and provide a higher coefficient of performance (COP) than the household refrigerator. Besides that, it will have fewer temperature fluctuations inside the fridge and freezer cabinets.

1.4. The Contribution of the Research

The primary contribution of this research is the overall performance enhancement of a household refrigerator through the use PCMs and nanoparticles. The contribution will involve the number of PCMs, the shape of containers for carrying PCMs, the material of the container for the condenser PCMs, and the arrangement of PCMs. In addition, it will include boosting the thermal conductivity of the PCM with metal oxide nanoparticles. Furthermore, the most significant contribution will be the application of PCMs to multiple refrigerator components. The findings of this study will lead to the following significant improvements:

- I. Reduction in residential electricity consumption because over two billion domestic refrigerators are in operation globally.
- II. Minimizing the environmental pollution since the primary source of this pollution is the combustion of fossil fuels to generate electricity.
- III. Decreasing the cost of electricity utilization thanks to the modified household refrigerator will operate at a lower total on-time cycle than the ordinary one.

- IV. A significant role in food quality preservation by minimizing temperature fluctuations inside the refrigerator compartments and improving refrigerator COP.

1.5. The Scope and Limitation of the Research

The following aspects are covered in this research:

- i. This research provides a comprehensive literature review regarding thermal efficiency and technical solutions for improving the overall performance of a household refrigerator.
- ii. A new, efficient, cost-effective, and environmentally sustainable optimization technique, based on PCMs and PCM nanoparticle inclusion, was implemented to enhance the thermal performance of the household refrigerator components.

1.6. The Research Methodical Stages

The following points are the major stages in this research.

- i. An extensive review of the relevant existing literature to understand the under investigation system and the use of PCMs and nanoparticles to enhance its performance.
- ii. The selection and adoption of an appropriate experimental technique.
- iii. The choosing and using proper supplemental heat transfer correlations.
- iv. Utilizing PCMs and PCM nanoparticle inclusion as the mechanism for optimization.

- v. The graphical and tabular presentation of data and results.
- vi. The analysis and discussion of the outcomes.

1.7. The Outline of the Thesis

This thesis contains six chapters, each with a concise summary described below.

Chapter 1 provides the general introduction and background of the study. The objectives and research questions of this research are explained in detail. The contributions, scope and limitations, and methodological stages are presented.

Chapter 2 presents an extensive and detailed literature review. The literature involved the classification of PCMs and their thermal conductivity enhancement methods. In addition, the optimization mechanisms are thoroughly discussed, along with their advantages and disadvantages. Moreover, this chapter addressed the employment of PCMs in the condenser, evaporator, and compartments to acquire various improvements.

Chapter 3 covers the utilization of heat transfer correlations. The correlations calculated the amount of refrigerant mass flow rate discharged by the compressor, the COP, the refrigeration capacity, and the quantity of integrating PCMs on each component.

Chapter 4 is the experimental work. The specifications of data logger, instruments, and temperature sensors are described. The arrangement of data loggers and temperature sensors on the refrigerator components is shown. The experimental procedure of inserting nanoparticles into the PCM is demonstrated. The concept of measuring and collecting data is analyzed. The amount of mass

required for each component is determined. The selection of PCMs based on the temperature of the refrigerator components is executed. The method and arrangement of PCMs in each experiment are explained.

Chapter 5 represents the overall results of the experiments. The final results are discussed and analyzed in detail using tabular and graphical forms.

Chapter 6 includes a summary of the findings and recommendations for further study.

CHAPTER 2

LITERATURE REVIEW

2.1. Introduction

Globally, energy consumption and refrigerator sales are increasing. As per (Dong et al., 2021), worldwide refrigerator unit sales have continuously grown from 177.9 million in 2014 to 201.1 million units in 2016 and are predicted to exceed 235.5 million units by 2025. Likewise, there has been a significant increase in the desire to preserve fresh foods, fruits, vegetables, and medications from the chance of quality degradation recently (Pingali, 2007). As a result, different solution techniques to optimize the overall performance of household refrigerators and freezers have been tested. Nowadays, most household refrigerators and freezers use a vapor-compression refrigeration cycle as the basis for their operation. This system has a COP better than the absorption and thermoelectric systems (American Society of Heating, 2018). Thus, most of the studies focused on the vapor compression refrigeration cycle.

This chapter covered an extensive review of the existing literature. In this review, performance enhancement techniques, thermal energy storage systems, PCM types, PCM's thermal conductivity enhancement methods, and the use of PCMs in the components and cabinets of household refrigerators and freezers have been discussed. The stages involved in conducting the literature review and the various subjects addressed are presented in Figure 2.1. In the following section, the different performance enhancement techniques will be thoroughly explained.

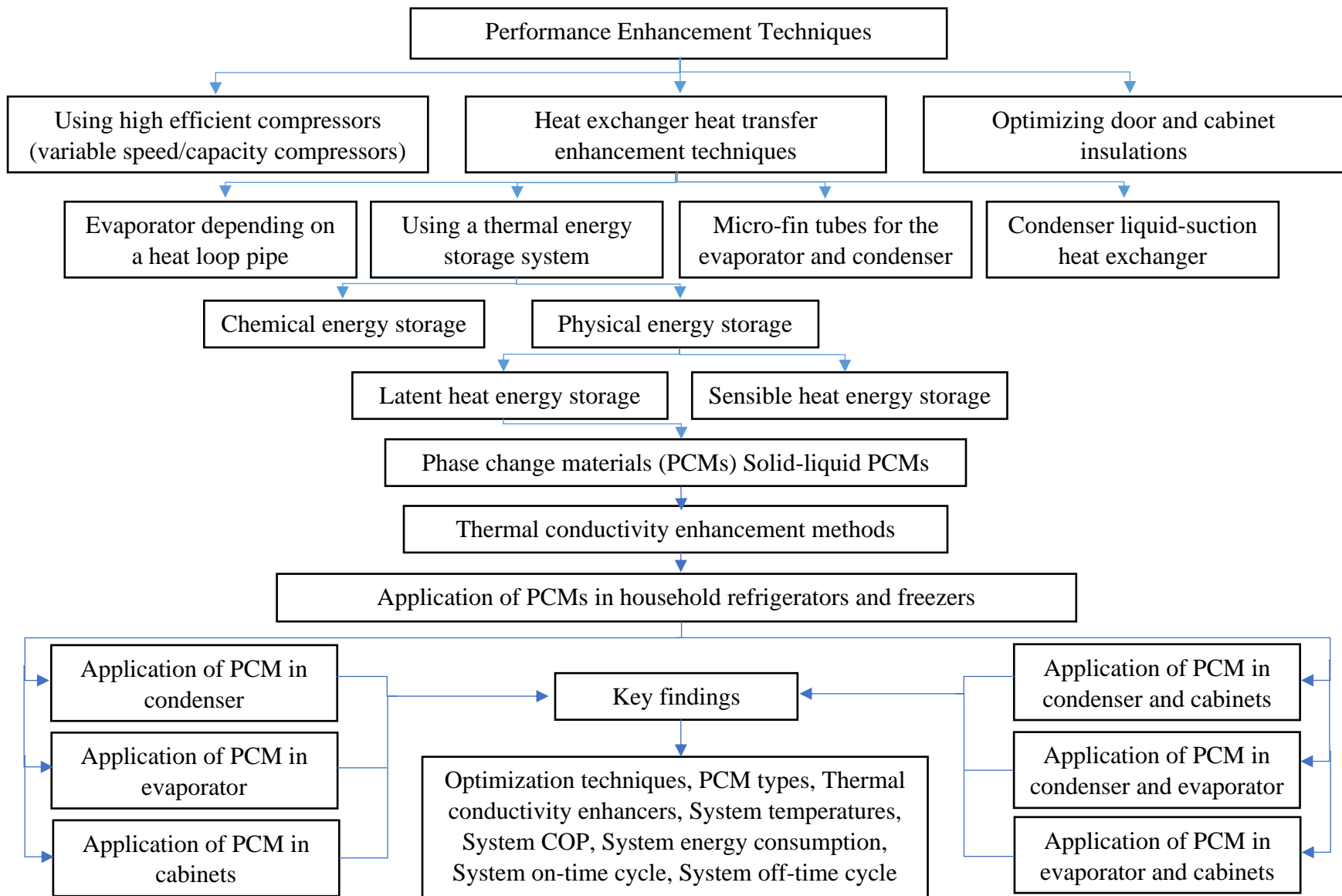


Figure 2.1. The methodical steps involved in reviewing literature.

2.2. Performance Enhancement Techniques

Since the last century, household refrigerators and freezers have been primarily utilized to keep the quality of food products and medicines. Thus, for many years, more studies have been focused on increasing the overall performance of household refrigerators and freezers due to the increased number of these appliances in operation and their wide range of uses through the following common practical methods (Kumar et al., 2016):

- Using high-performance (variable speed/capacity) compressors.
- Improving refrigerator door and cabinet insulation.
- Improving heat exchangers' (condenser and evaporator) heat transfer rates.

(Aprea et al., 2003 and Liang et al., 2010) tested a variable-capacity compressor (VCC), while (Ekren et al., 2013) evaluated a variable-speed compressor (VSC). These compressors were efficient at controlling cooling capacity because they constantly matched thermal loads with the compressor speed. Hence, cycling losses were minimized (Cuevas and Lebrun, 2009). Nonetheless, such compressors have some disadvantages, including a longer payback period, concerns regarding performance maintenance, and a higher initial cost (Bansal et al., 2011).

A thicker layer of insulation or innovative insulation methods for the refrigerator's door and cabinet could reduce compressor energy use in proportion to cabinet heat reduction (Trias et al., 2018). Nevertheless, expanding the insulating layer was limited to production companies because it reduced the interior volume of the refrigerator cabinet. Thus, advanced insulation layers were developed. Baffle form panels that contained low thermal conductivity materials (Bansal et al., 2011) and vacuum insulation panels (VIPs) (Verma and Singh,

2020) were examples of advanced insulation alternatives. The drawback of this alternative insulator was that it was hard to use in corners where blown foam was required to support the construction. They also may need an appropriate production process, which will incur additional labor costs (Manini, 2001).

The enhancement of heat transfer in evaporator and condenser heat exchangers received the most consideration of the practical techniques mentioned previously (Md Imran Hossen and Afroz, 2011).

2.3. Heat Exchanger Heat Transfer Enhancement Techniques

To improve the heat transfer rate of heat exchangers, researchers worked on several techniques (Omara and Mohammedali, 2020), including the following.

- Developing an evaporator depending on a loop heat pipe.
- Utilizing micro-fin tubes for the evaporator and condenser.
- Utilizing condenser liquid-suction heat exchanger.
- Using a thermal energy storage system.

According to the literature, the first three arrangements were either difficult or expensive to implement. Therefore, using a thermal energy storage system has received significant research interest as a new method.

2.4. Thermal Energy Storage Systems

The addition of thermal energy to a substance, followed by the retrieval of the energy when required, is known as thermal energy storage. In the procedure of charging, the accessible thermal energy can be stored in the storage substance. This accumulated thermal energy can be removed and delivered for use in the discharging procedure. Thermal energy is stored in a substance by changing its phase or internal energy (Veerakumar & Sreekumar, 2016 and Zhang et al., 2016).

Chemical and physical storages are the most commonly used thermal energy storage systems, as displayed in Figure 2.2.

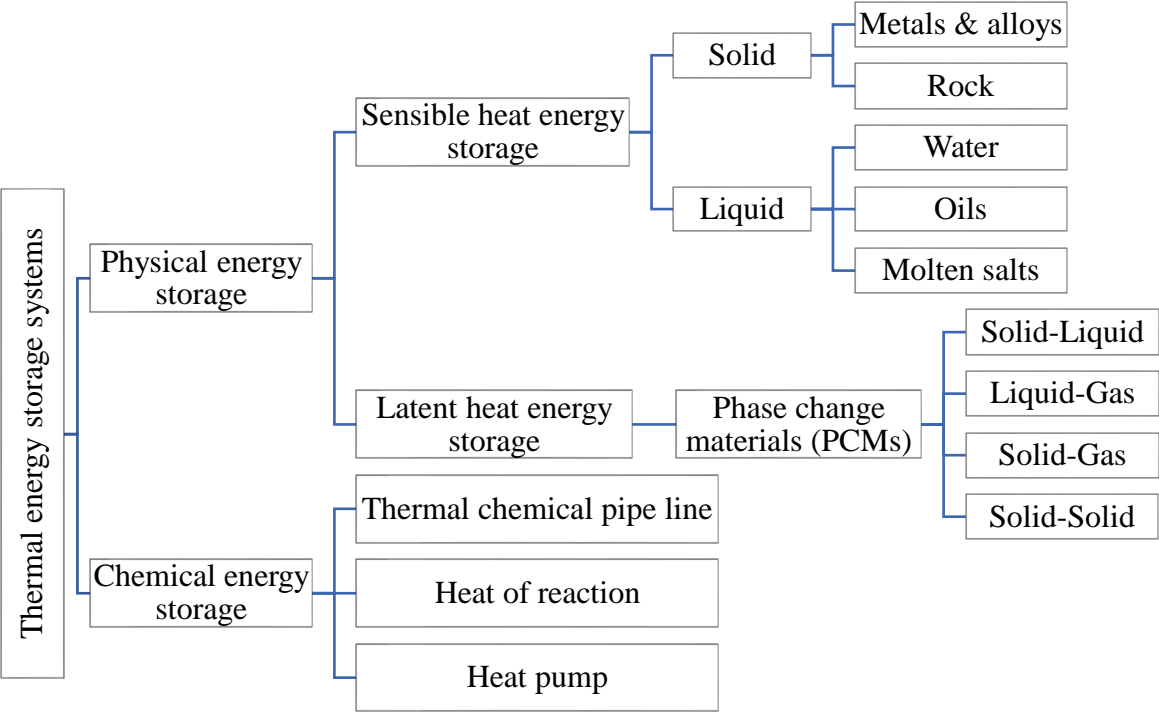


Figure 2.2. Thermal energy storage systems by (Sharma et al., 2009).

2.4.1 Chemical Energy Storage

A chemical or thermochemical energy storage system focuses on the energy stored and discharged in a chemical reaction that arises when molecular bonds are broken and reformed (Wang et al., 2016). This system was not a suitable option for energy storage due to the high cost of the storage medium and associated equipment compared to other systems (Kato, 2007).

2.4.2. Physical Energy Storage

Sensible and latent heat energy storage systems are frequently utilized in physical energy storage (Kürklü, 1998). The sensible method concerns storing

thermal energy in a medium by a specific heat capacity and temperature variations because of adding or removing heat. During charging and discharging energy, the medium does not undergo a phase transition. The temperature of the storage substance decreases when the energy is released and vice-versa (Li, 2016). Complete reversibility is projected for both charging and discharging processes. In both liquid and solid states, the storage substance is accessible (Fernandez et al., 2010), as shown in Figure 2.2. Sensible heat storage offered two key advantages: it is reasonably inexpensive and poses little hazard due to the use of less hazardous substances.

On the other hand, the latent method depends on the phase change of the material in the energy charging and discharging processes (Cabeza et al., 2021). At a constant temperature, materials experience a phase transition. This method accumulates energy as latent heat forms. The latent heat of materials determines the quantity of stored energy (Cabeza et al., 2021). The density of latent method is 5 to 14 times greater than that of sensible method (Sharma et al., 2009). Therefore, this system was more attractive (Mehling and Cabeza, 2008). This mechanism allows for phase changes from solid to liquid, liquid to gas, solid to gas, solid to solid, and vice versa. Thus, materials that are utilized in this storage system are known as phase change materials (PCMs) (Sharma et al., 2009).

2.5. Phase Change Materials (PCMs)

Phase change materials (PCMs) can absorb or release significant quantities of latent heat depending on their state. In other words, when undergoing a phase transition from liquid to solid and vice versa (Dincer and Rosen, 2021). They can store and release excess heat to enhance the thermal performance of a wide range of applications. In the cooling or heating method, the phase transition exists when

the material achieves a specified phase change temperature. The temperature of the phase change material remains unchanged in the latent heat charging or discharging. The amount of latent heat consumed by a PCM is collected within it (Abhat, 1983). PCMs exhibit solid to solid, liquid to gas, solid to gas, solid to liquid, and vice versa phase transitions (Zeinelabdein et al., 2018), as represented in Figure 2.2.

For practical uses, only PCMs with solid-liquid and solid-solid phase transitions were effective. Hence, in many latent heat storage systems, the heat accumulation and retrieval processes are controlled by a material that performs a phase transition from solid to liquid and conversely (Wang et al., 2000). Despite this, PCMs with solid-liquid phase shifts are widely implemented in refrigeration systems (Mastani Joybari et al., 2015). The basic principle of latent heat storage systems (solid-liquid PCMs) is represented in Figure 2.3.

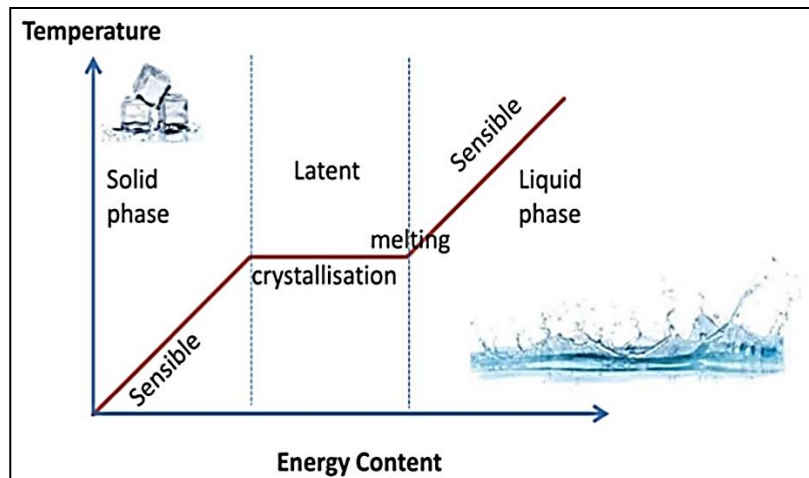


Figure 2.3. The operational principle of solid-liquid PCMs (Sidik et al., 2018).

2.5.1. Classification of Solid-Liquid PCMs

Solid-liquid PCMs are classified as organic, inorganic, and eutectic (Dincer and Rosen, 2021), as shown in Figure 2.4. The structure of organic PCMs is

carbon-dependent. Organic PCMs have high latent heat and chemical stability (Nazir et al., 2019). They are commonly divided into two types: paraffin and non-paraffin compounds. The advantages of these PCMs are a short phase change temperature zone, no supercooling and phase segregation, high thermal energy density, consistent melting, and non-corrosive (Kenisarin, 2014). They also have a self-nucleation benefit, which confirms that they crystallize with little or no supercooling (Magendran et al., 2019). Organic PCMs are convenient although they have high flammability and low thermal conductivity, which are the main drawbacks of these PCMs (Omara et al., 2018).

Inorganic PCMs primarily include metallics and salt hydrates (Zhang et al., 2016). In comparison to organic PCMs, they feature lower degradation phenomena, lower cost, low flammability, higher density, higher thermal conductivity, and store twice as much latent heat per unit volume. Nonetheless, some drawbacks are encountered with these PCMs, including corrosion of the container materials, phase segregation, and sub-cooling (Manting et al., 2019).

Eutectic PCMs are crystal combinations. They are developed during the crystallization process of mixing two or more kinds of PCMs, including organic-organic, inorganic-inorganic, and organic-inorganic combinations (Baetens et al., 2010). No separation occurs during either their melting or solidification processes (Wahid et al., 2017). These PCMs are advantageous for achieving the desired phase change temperature by varying the mass proportions of their components (Yanping et al., 2011).

Due to their weak thermal conductivity, the theoretical and experimental mechanisms have been developed to increase the thermal conductivity of solid-liquid PCMs, as briefly described in the next section.

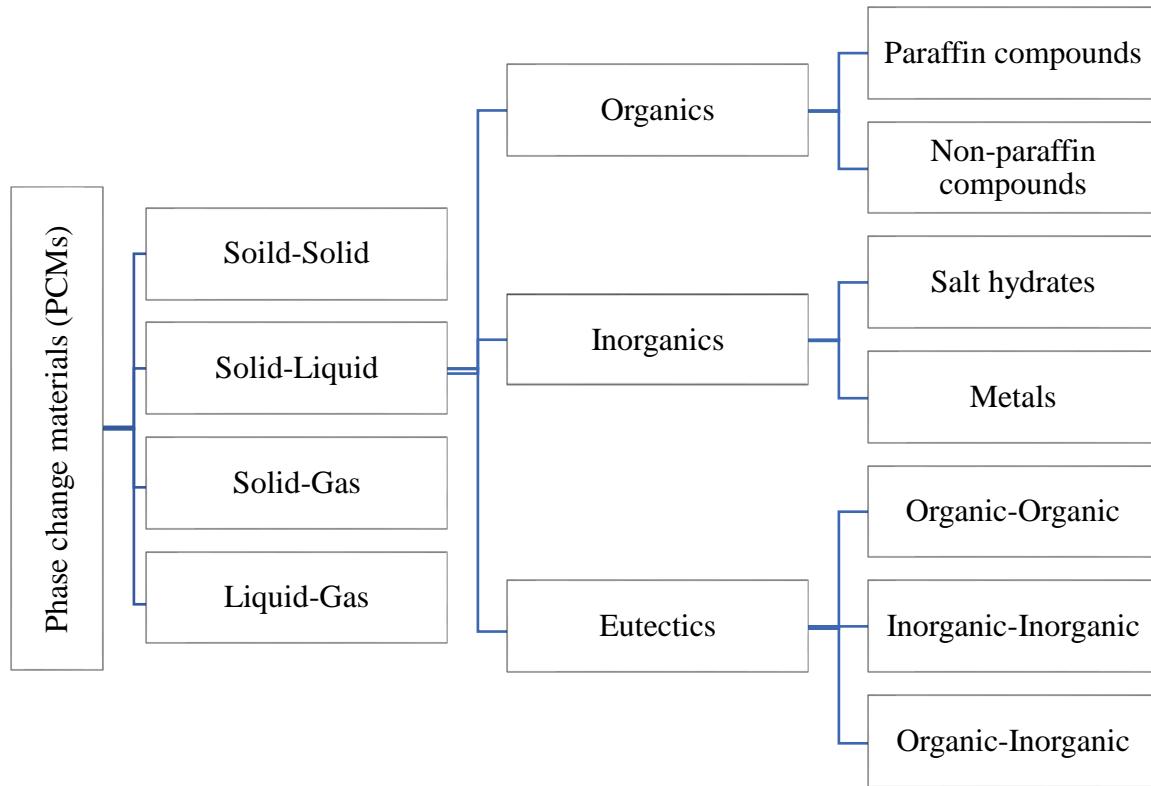


Figure 2.4. Classification of phase change materials (Dincer and Rosen, 2021).

2.5.2. Thermal Conductivity Enhancement Methods

Poor thermal conductivity was the significant limitations of solid-liquid PCMs. It is a crucial property that affected the heat transfer rate of PCMs (Rostami et al., 2020). Therefore, some techniques were proposed by researchers to enhance thermal conductivity, which can be shown in Figure 2.5. The shape stabilization PCM (SSPCM) by (Cheng et al., 2010), encapsulation by (Sonnenrein et al., 2015), the addition of metallic foam by (Opolot et al., 2020), the addition of nanoparticles by (Arshad et al., 2020) were performed.

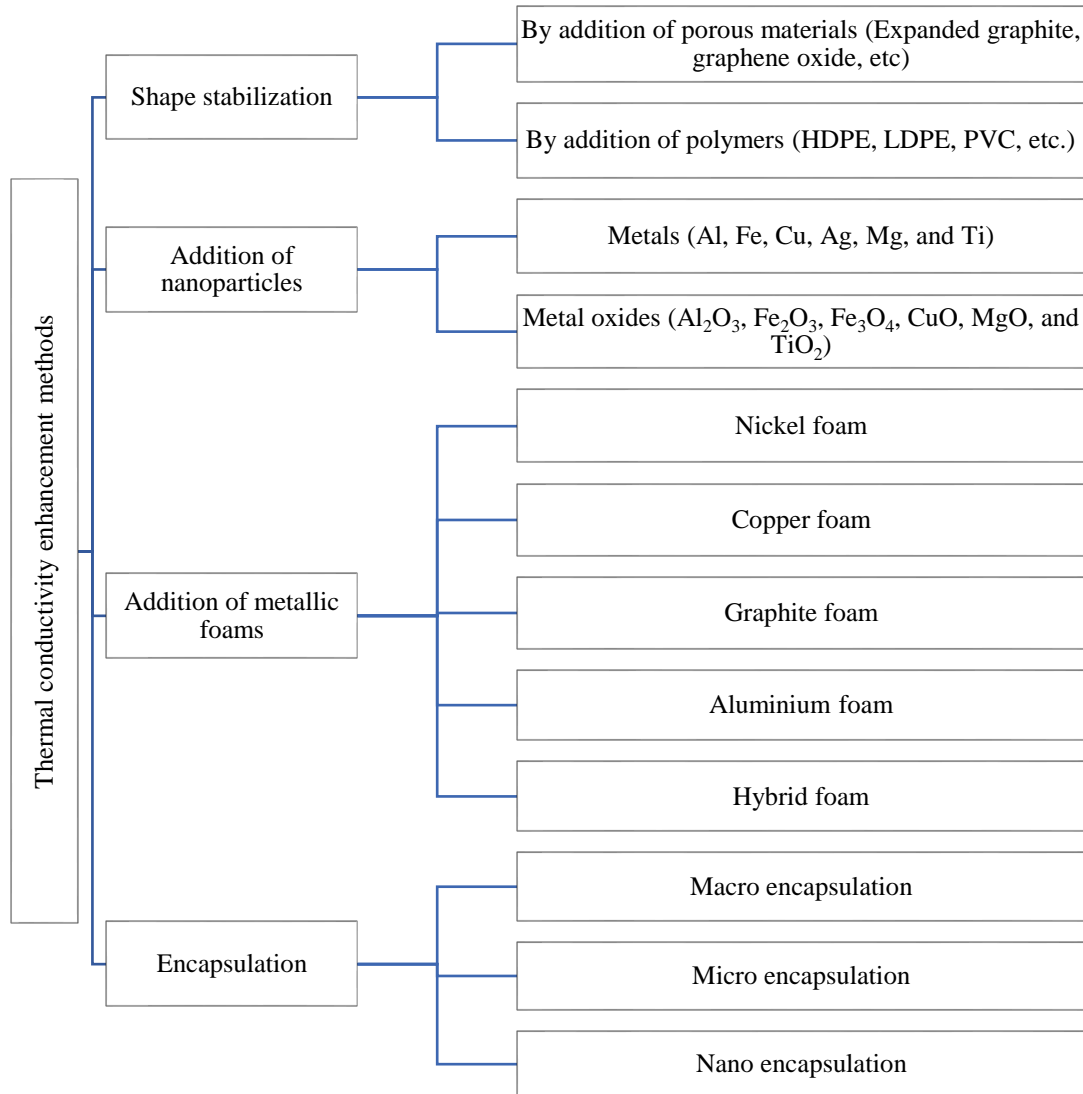


Figure 2.5. PCM’s thermal conductivity enhancement methods by (Ibrahim et al., 2017 and Qureshi et al., 2018)

2.5.3. Nanoparticles

Nanoparticles are tiny materials having size ranges from 1 to 100 nm. They can be classified into different classes based on their properties, shapes or sizes. There are three main types of nanoparticles: metal-based, carbon-based, and nanocomposites (Khan et al., 2019).

2.6. Application of PCMs in Household Refrigerators and Freezers

The experimental and numerical investigation of PCMs in household refrigerators and freezers has been described in this section, which is divided into subsections below.

2.6.1. Application of PCMs in Condenser

The application of PCMs to the condenser could improve condenser heat transfer rate, allowing the condenser to reject more heat during the compressor's off period and attain a lower condensation temperature. The primary goal of using PCM for the condenser was the reduction of the condenser temperature, which leads to significant energy savings (Sonnenrein et al., 2015). Therefore, many studies examined PCM on the condenser, as reported below.

To begin with, (Han et al., 2017) described the shape stabilized phase change material SSPCM, which was a type of PCM. It was made via the encapsulation of PCM in a porous and shell-supporting matrix to create composite materials with specified characteristics. The primary disadvantage of common SSPCMs was their low thermal conductivity, which reduces their heat storage capacity. Therefore, (Cheng et al., 2010) optimized the thermal conductivity of conventional SSPCM composed of paraffin and HDPE by adding expanded graphite and called it heat conduction enhanced SSPCM (HCE-SSPCM). They improved the thermal conductivity by 4 times higher than the common SSPCMs without impacting the melting point and latent heat. The HCE-SSPCM exhibited two peak points of phase change at temperatures of 30.5°C and 50.3°C.

In addition, (Cheng et al., 2011) experimentally created a heat storage condenser by packing the HCE-SSPCM around the condenser tubes, as depicted in Figure 2.6. The findings confirmed that the ordinary and modified refrigerators

consumed 0.51 kWh and 0.45 kWh of energy, respectively, as shown in Figure 2.7. Temperature variations have been substantially reduced in the modified refrigerator freezer and fridge cabinets, leading to a shorter compressor on time. The new refrigerator had an improved COP of 18% because it showed a greater subcooling degree and evaporation temperature but a lower condensation temperature.

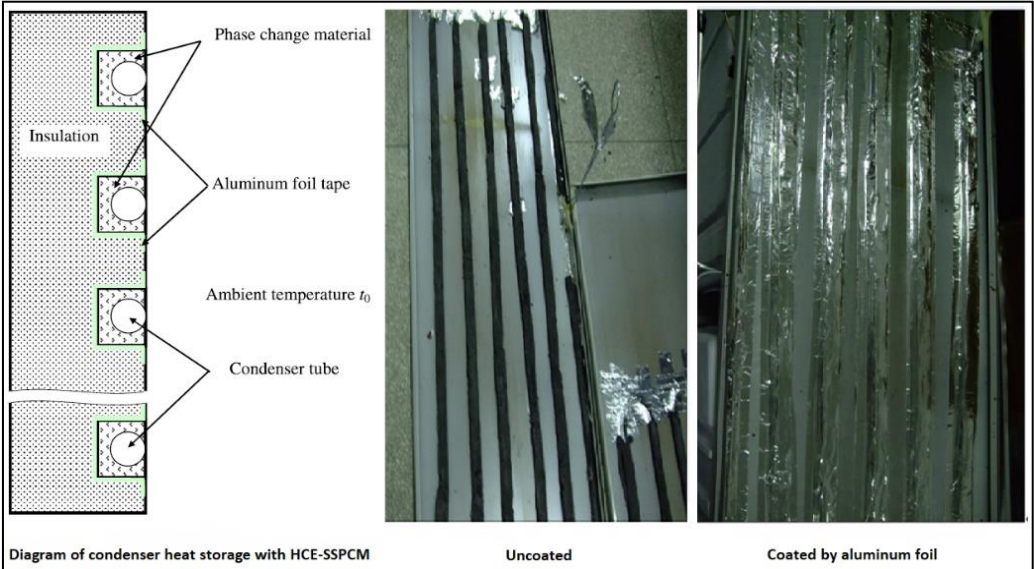


Figure 2.6. Condenser heat storage made by (Cheng et al., 2011).

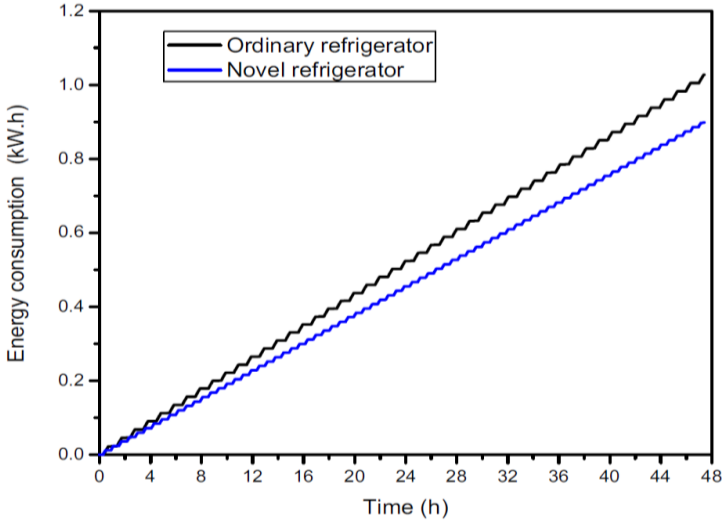


Figure 2.7. Energy consumption vs. time by (Cheng et al., 2011).

In later work by (Cheng and Yuan, 2013), they investigated a numerical model of a household refrigerator based on the work of (Cheng et al., 2011). The results were amazingly close to the experimental data, as demonstrated in Table 2.1. The boosted COP and energy saving growth rates were 18.7% and 12.2%, respectively. The COP and energy saving rates were raised as the ambient temperature rose and the freezer temperature fell.

Furthermore, (Sonnenrein et al., 2015) experimentally examined the refrigerator's performance with water, paraffin, and copolymer compound as PCMs on the condenser, as seen in Figure 2.8. As a result, the copolymer compound dramatically lowered condenser temperatures, resulting in a significant reduction in energy consumption because it had a higher melting point than water and higher thermal conductivity than paraffin. The refrigerator's energy savings with water, paraffin with PE-HD foil, paraffin with aluminum composite layer, and copolymer compound were 3%, 5%, 7%, and 10%, respectively, as shown in Figure Table 2.1.

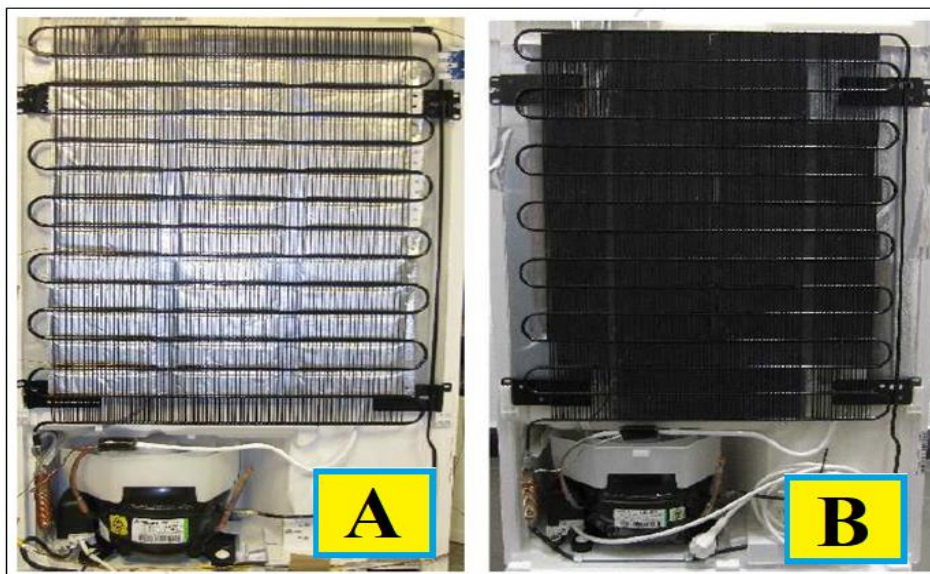


Figure 2.8. Condenser equipped with a) Bags of aluminum composite layer containing PCM and b) Copolymer compound by (Sonnenrein et al., 2015).

Moreover, (Pirvaram et al., 2019) tested the performance of a household refrigerator integrated with single and double eutectic PCMs on the condenser, as represented in Figure 2.9. Double PCMs were arranged in a cascade design. Four tests were performed. The energy consumption by refrigerators with single and double PCMs was 8.72% and 13.38%, respectively, compared to a refrigerator without PCM and thermal load (M-pack). They also reported that the cascaded PCM design offered lower condenser surface temperatures than the other three tests, which led to significant energy savings and better COP, as shown in Figure Table 2.1.

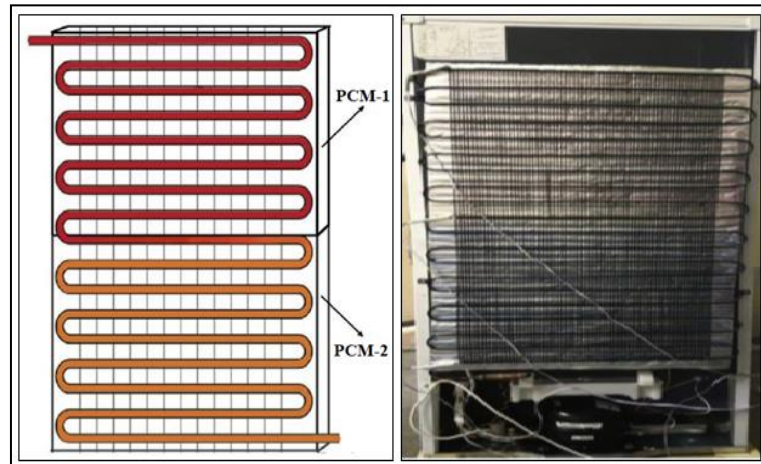


Figure 2.9. Arrangement of PCMs performed by (Pirvaram et al., 2019).

Later, (Kumar et al., 2020) developed a nano-enhanced phase change material (NEPCM) by adding 0.6% wt of multi-walled carbon nanotube (MWCNT) into paraffin wax PCM, which enhanced paraffin wax's thermal conductivity. Then, in a different case, they eliminated the condenser fins and wrapped (NEPCM) and paraffin wax around the condenser tubes, as shown in Figure 2.10. As a result, the paraffin wax and NEPCM cooled the condenser midpoint temperature by 3°C and 7°C, respectively. They also minimized energy

consumption by 13.06% and 18.6% for paraffin wax and NEPCM, respectively, as indicated in Table 2.1. The on to total cycle time ratio was shortened by 8.2% and 17.95% for paraffin wax PCM and NEPCM, respectively.

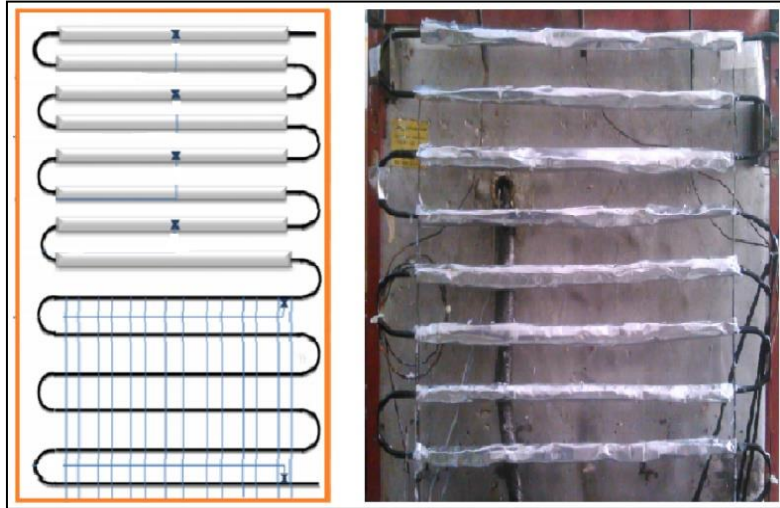


Figure 2.10. PCM setup on condenser tubes made by (Kumar et al., 2020).

(Karthikeyan et al., 2021) also employed the OM-32 and OM-29 organic commercial paraffins in a cascade set up on the upper and lower parts of the condenser, which can be seen in Figure 2.11. Consequently, the condenser inlet and outlet temperatures were greatly minimized by 3.8°C and 3.1°C , respectively.



Figure 2.11. PCM configuration on the condenser by (Karthikeyan et al., 2021).

Comment below, (Kasinathan and Kumaresan, 2021) assessed a household refrigerator's performance with organic commercial paraffin OM-46 on the condenser and deionized water containing 3% wt of natural graphite on the evaporator (inside the freezer cabinet). The experiment of PCM inside the freezer cabinet was described in Section 2.6.5. Due to the PCM on the condenser, the compressor discharge temperature was cooled, as shown in Figure 2.12. This reduction could improve the lifespan of the compressor and its energy usage. For various thermal loads, this refrigerator with PCM on the condenser saved 16–22% of energy, as illustrated in Table 2.1.

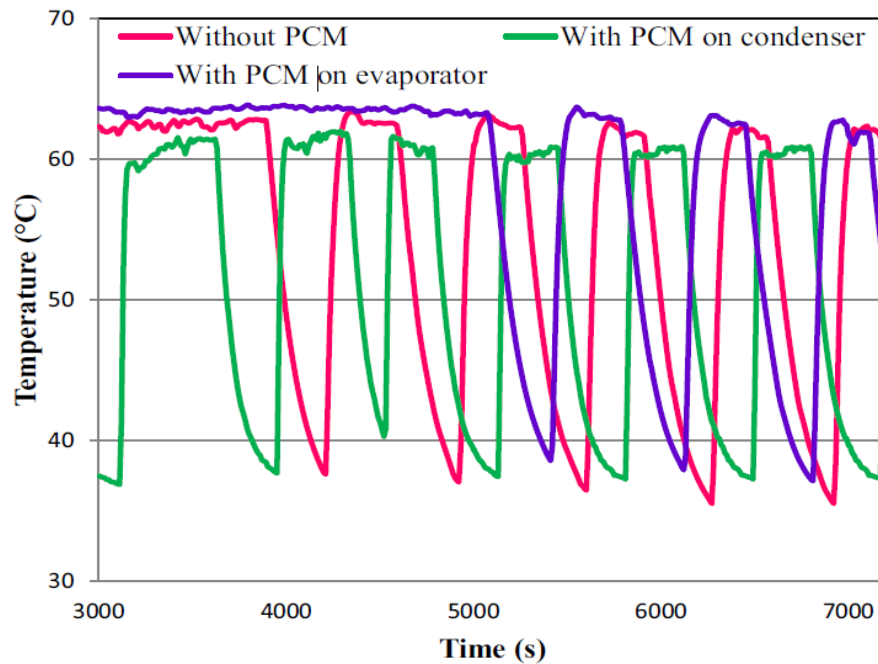


Figure 2.12. Compressor discharge temperatures by (Kasinathan and Kumaresan, 2021).

The results of the abovementioned studies and some others that employed PCM on the condenser are shown thoroughly in Table 2.1.

Table 2.1 List of studies and their results that employed PCM on condenser.

Researcher	Appliance type and volume (L)	PCM types	Mass of PCM (kg)	PCM properties			T _a °C	Condenser temperatures °C						Compressor on and off times (min.)				Improving in %	
				T _{Ph} °C	k $\frac{w}{m \cdot ^\circ C}$	h _f $\frac{kJ}{kg}$		Without PCM			With PCM			Without PCM		With PCM		COP	E
								in	mid	out	in	mid	out	on	off	on	off		
(Cheng et al., 2011)	Refrigerator 220	Organic HCE-SSPCM (Paraffin+ HDPE + EG)	0.5	25 to 60	1.35	17 to 103	25	-	34.8	31.3	-	32.5	25.9	21	40.6	11.9	26.4	18	12
(Cheng and Yuan, 2013)	Refrigerator 220	Organic HCE-SSPCM (Paraffin+ HDPE + EG)	0.5	25 to 60	1.35	17 to 103	25	-	35.5	32.4	-	33	28.5	20	41	12	26	18.7	12.2
(Sonnenrein et al., 2015)	Refrigerator 152	Distilled water	0.5	0	0.6	331	25	47	47	39	44	42	34	-	-	-	-	-	3
(Sonnenrein et al., 2015)	Refrigerator 152	Organic paraffin	0.5	34	0.19	251	25	47	47	39	-	-	-	-	-	-	-	-	7
(Sonnenrein et al., 2015)	Refrigerator 152	Copolymer compound	0.5	34	0.64	182	25	47	47	39	39	37	31	-	-	-	-	-	10

Table 2.1 (Continued)

Researcher	Appliance type and volume (L)	PCM types	Mass of PCM (kg)	PCM properties			T _a °C	Condenser temperatures °C						Compressor on and off times (min.)				Improving in %	
				T _{Ph} °C	k $\frac{w}{m \cdot ^\circ C}$	h _f $\frac{kJ}{kg}$		Without PCM			With PCM			Without PCM		With PCM		COP	E
								in	mid	out	in	mid	out	on	off	on	off		
(Dandotiya and Banker, 2017)	Refrigerator 175	Organic easter	5	18 to 23	-	143	27	-	-	46	-	-	43	-	-	-	-	3	15
(Pirvaram et al., 2019)	Refrigerator 285	Eutectic 36% PEG1000 + 64% PEG600	0.5	32	0.25	151	25 to 43	39.5	37.2	37	39	37.9	36.5	11.6	23.5	12	29.1	-	8.72
(Pirvaram et al., 2019)	Refrigerator 285	Eutectic 36% PEG1000 + 64% PEG600	0.25	32	0.25	151	25 to 43	39.5	37.2	37	37	35.1	34.5	11.6	23.5	9.6	30.2	-	13.3
		Eutectic 32% PEG1000 + 68% PEG600	0.25	29	0.23	149													
(Kumar et al., 2020)	Refrigerator 165	Organic Paraffin wax	-	57.5 to 60	0.24	140 to 145	31	-	55	-	-	52	-	29.6	8.5	20.4	8.8	-	13

Table 2.1 (Continued)

Researcher	Appliance type and volume (L)	PCM types	Mass of PCM (kg)	PCM properties			T _a °C	Condenser temperatures °C						Compressor on and off times (min.)				Improving in %		
				T _{Ph} °C	k $\frac{w}{m \cdot ^\circ C}$	h _f $\frac{kJ}{kg}$		Without PCM			With PCM			Without PCM		With PCM		COP	E	
								in	mid	out	in	mid	out	on	off	on	off			
(Kumar et al., 2020)	Refrigerator 165	Organic (Paraffin wax + MWCNT)	-	57.8 to 60.2	0.28	140 to 147	31	-	55	-	-	48	-	29.6	8.5	13.9	9.3	-	18	
(Kasinathan and Kumaresan, 2021)	Refrigerator 180	Organic paraffin OM-46	1.250	47.8	0.2	250	28	64.4	52.2	36	60	51.8	43.8	310	360	300	380		16 to 22	
(Karthikeyan et al., 2021)	Refrigerator 185	Organic paraffin OM-32	-	32	0.14	157	-	46	-	43.8	42.2	-	40.7	-	-	-	-	-	-	-
		Organic paraffin OM-29	-	29	0.17	194														

2.6.2. Application of PCM in Evaporator

A refrigerator with PCM on the evaporator ran at a higher evaporator temperature and pressure than one without PCM. This caused an increase in the density of the vapor refrigerant. Also, the constant volumetric rate of the compressor removed a larger mass flow from the evaporator. Because of this, refrigerators could attain a greater capacity for refrigeration (Md Imran Hossen and Afroz, 2011). This technique could extend the compressor's on and off times. However, the off-time extension was greater than the on-time. The off-time extension caused a reduction in total electricity usage, a decrease in the number of compressor's starts and stops, and an improvement in food quality (Gin and Farid, 2010). As a result, various technical studies on this enhancement have been published, as described below.

(Cerri et al., 2003) simulated and evaluated the impact of PCM integration in the evaporator, which resulted a 12% increase in the COP. Later, in a series of studies, Azzouz and coworkers examined the use of PCM on evaporators to improve the performance and refrigeration capacity of refrigerators, as followed.

At the outset (Azzouz et al., 2005) loaded eutectic salt solutions PCM with melting points ranging from -6 to 0 °C on one side of the evaporator in a dynamic model study, as displayed in Figure 2.13. The household refrigerator was the refrigerator without a freezer cabinet. For various PCM melting points and ambient temperatures, a considerable rise in COP from 1.09 to a range between 1.9 and 2.22 was recorded, as shown in Figure 2.14. Researchers determined that an improvement in COP could decrease energy consumption because of the decrease in the pressure compression ratio.

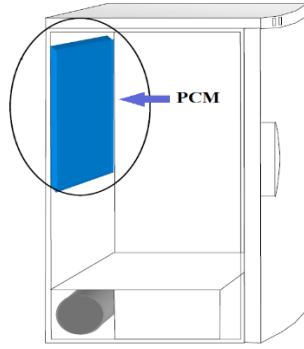


Figure 2.13. PCM setup on evaporator (Azzouz et al., 2005).

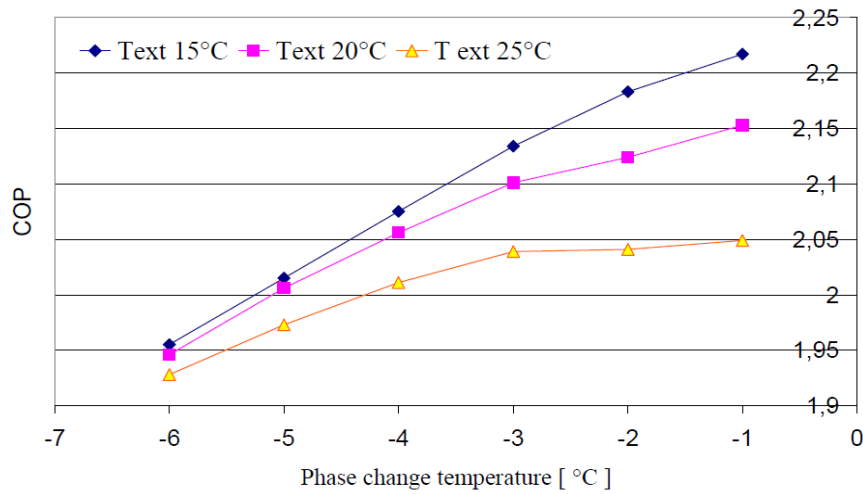


Figure 2.14. COP vs. melting points for various ambient temperatures (Azzouz et al., 2005).

Further, (Azzouz et al., 2008) performed another research by numerical simulation. They employed a slab shape of a eutectic salt solution PCM between the evaporator coils of a single fridge cabinet refrigerator and its wall, as presented in Figure 2.15. The simulation found that variable PCM melting points, PCM thicknesses, and different thermal loads (ambient temperature and door openings) resulted in a 5–15% increase in COP. The results of COP are shown in Figure 2.16. The fluctuating temperature in the refrigerated cell was considerably reduced. A refrigerator equipped with PCM had a threefold increase in on-cycle time and a sevenfold increase in off-cycle time compared to a standard

refrigerator. Lastly, researchers revealed that, based on thermal load, food quality could be protected for 4 to 8 hours without electricity.

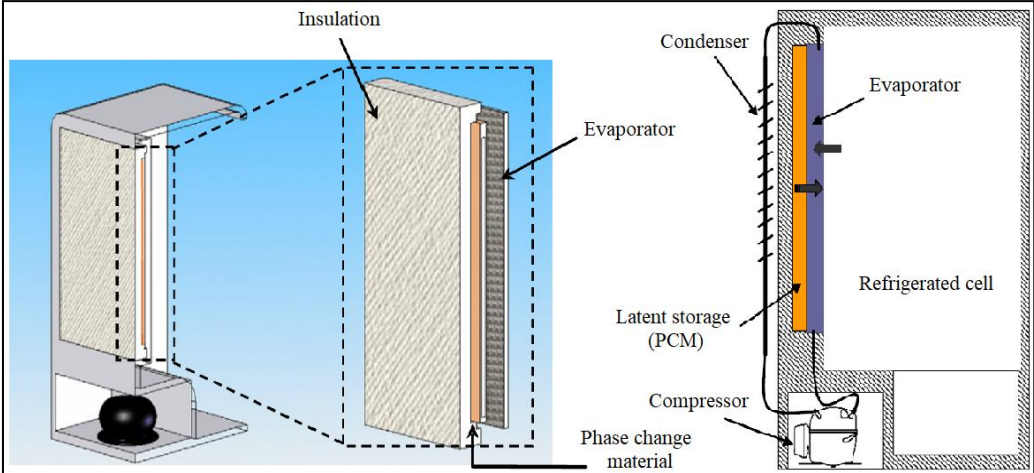


Figure 2.15. Refrigerator with PCM setup by (Azzouz et al., 2008).

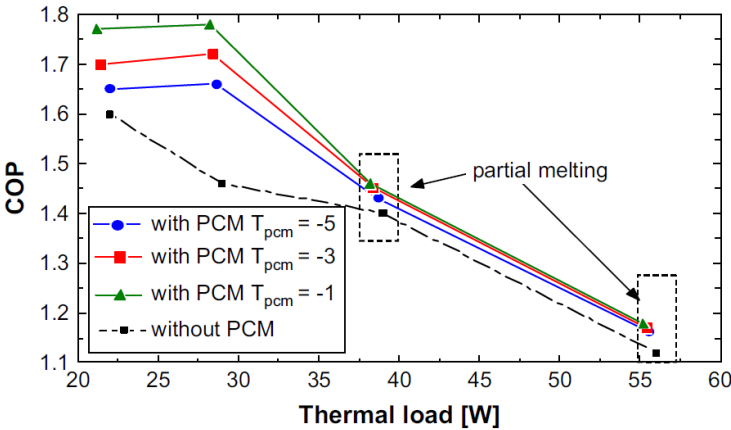


Figure 2.16. COP vs. thermal load made by (Azzouz et al., 2008).

Finally, based on their previous simulation results in 2008, (Azzouz et al., 2009) experimentally incorporated a 5 and 10-mm thick slab form of water and eutectic mixture as a PCM on the same evaporator's back face, as shown in Figure 2.17. Water and eutectic mixture that had a 0°C and -3°C freezing points were used in weights of 1.4 kg and 1.3 kg, respectively. The study findings highlighted that the improved COP was between 10% and 30% based on thermal loads and

PCM thicknesses, as seen in Figure 2.18. In comparison to 1–3 hours without PCM, the refrigerator with PCM supported 5–9 hours of continuous running without a power supply. Water enhanced the COP and refrigeration capacity at a higher rate than the eutectic mixture. However, the eutectic mixture had a better potential to sustain the air temperature in the refrigerator compartment at suitable ranges than the water.

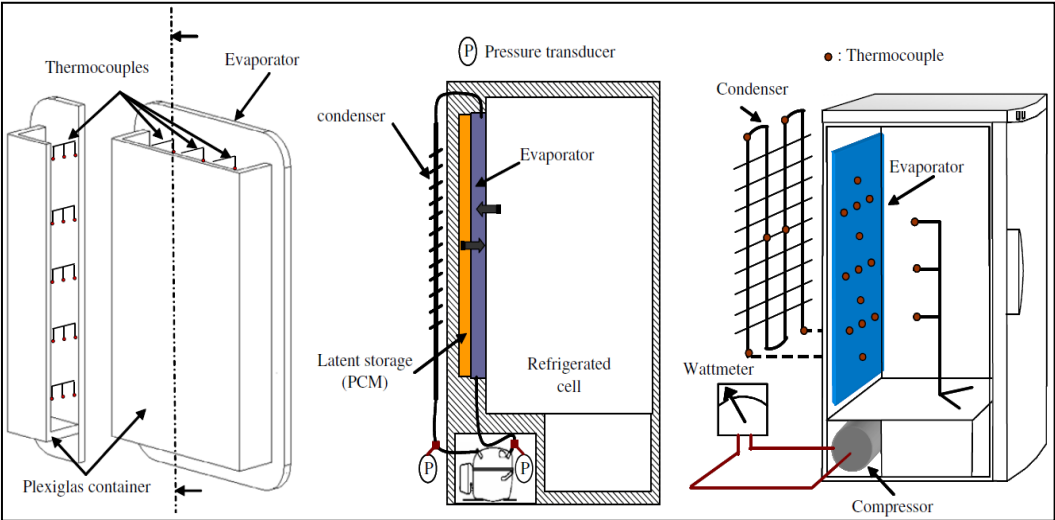


Figure 2.17. Experimental setup made by (Azzouz et al., 2009).

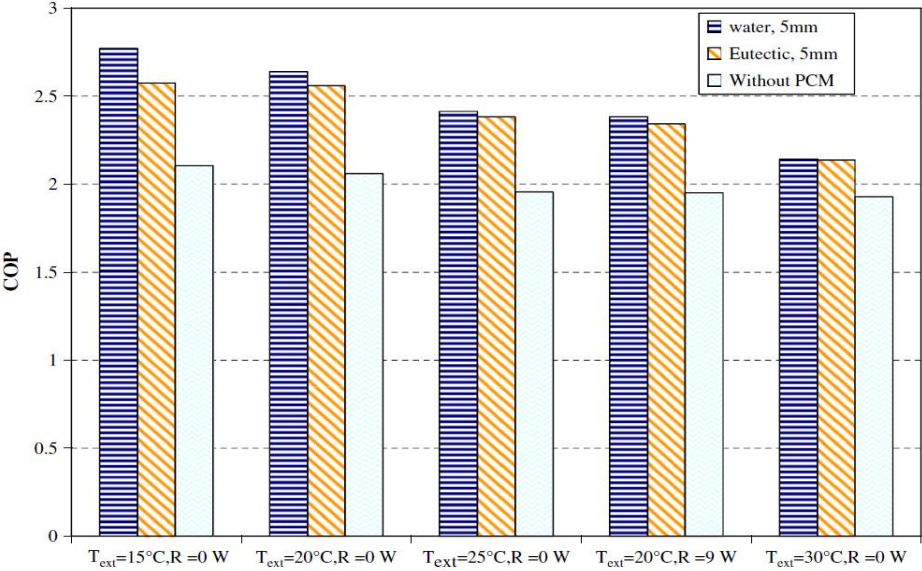


Figure 2.18. The average COP for various thermal loads by (Azzouz et al., 2009).

(Md Imran Hossen and Afroz, 2011) experimentally applied three PCMs to the evaporator in different cases, as detailed in Table 2.2. The PCM arrangement was on the five faces of the evaporator, where submerged the evaporator coil in a PCM box, as shown in Figure 2.19. As a result, the COP was enhanced with PCM by 21% to 34% for different thermal loads, in comparison with no PCM, as provided in Table 2.2. Furthermore, the COP rose by about 6% when the PCM volume was increased from 3L to 4.25L.

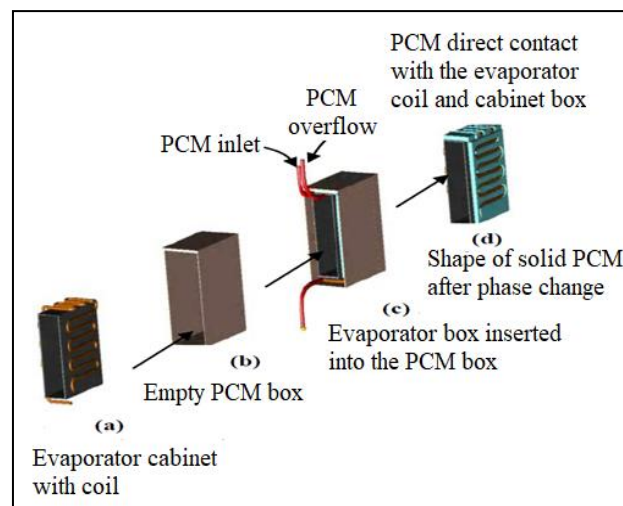


Figure 2.19. Setup procedures of PCM by (Md Imran Hossen and Afroz, 2011).

Also, (Rahman et al., 2014) numerically investigated the submerging evaporator in a box that contained water as a PCM. The COP of a refrigerator with a PCM box was enhanced by 55% to 60%.

(Yusufoglu et al., 2015) experimentally improved the overall performance of two refrigerators. 1.8 kilogram of distilled water as a PCM in a slab form was placed between the first refrigerator's evaporator coils and its wall, as illustrated in Figure 2.20a. This refrigerator saved energy usage by 8.8% and improved the COP from 2.33 to 2.53. While in the second refrigerator, they implemented 0.950

kg for each of four PCMs with different melting points on the evaporator tubes in flexible metallic film packs. This is seen in Figure 2.20b. In conclusion, this refrigerator saved between 0.3% and 5.0% of energy. Additionally, they stated that expanding the second refrigerator condenser's surface area by 20% could save 9.4% of energy.

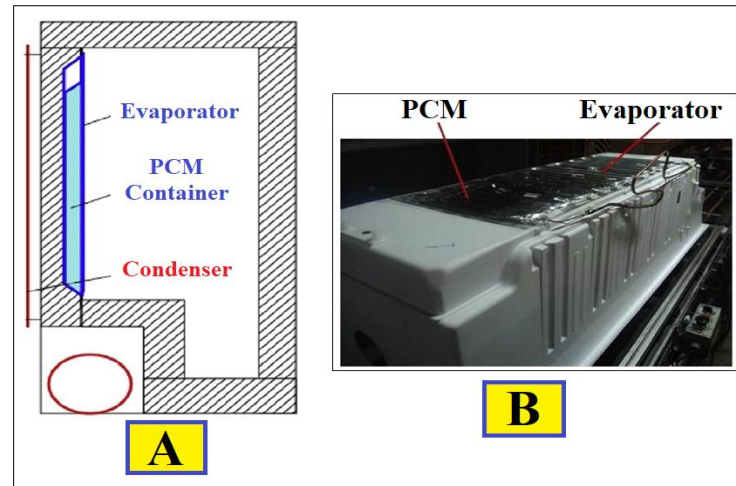


Figure 2.20. PCM setup on the evaporator (Yusufoglu et al., 2015).

(Elarem et al., 2017) experimentally implanted a PCM heat exchanger on the evaporator of a household refrigerator. A PCM heat exchanger was formed by utilizing a system of twelve U-shaped standard copper tubes. It completely covered the non-functional evaporator side, as displayed in Figure 2.21. A PCM was a Plus-ICE with a 4°C melting temperature. In contrast with no PCM, less energy usage (12%) and improved COP (8%) were observed in the household refrigerator with a PCM heat exchanger.

(Cofré-Toledo et al., 2018) incorporated two PCMs with different freezing points in different scenarios, as explained in Table 2.2. Figure 2.22 represents the arrangement of PCM in the form of tubes parallel to evaporator tubes.

Consequently, PCMs reduced compressor work time in the range of 3.71% to 9.1%. Also, they decreased energy consumption by 1.74% – 5.81%, as highlighted in Table 2.2.

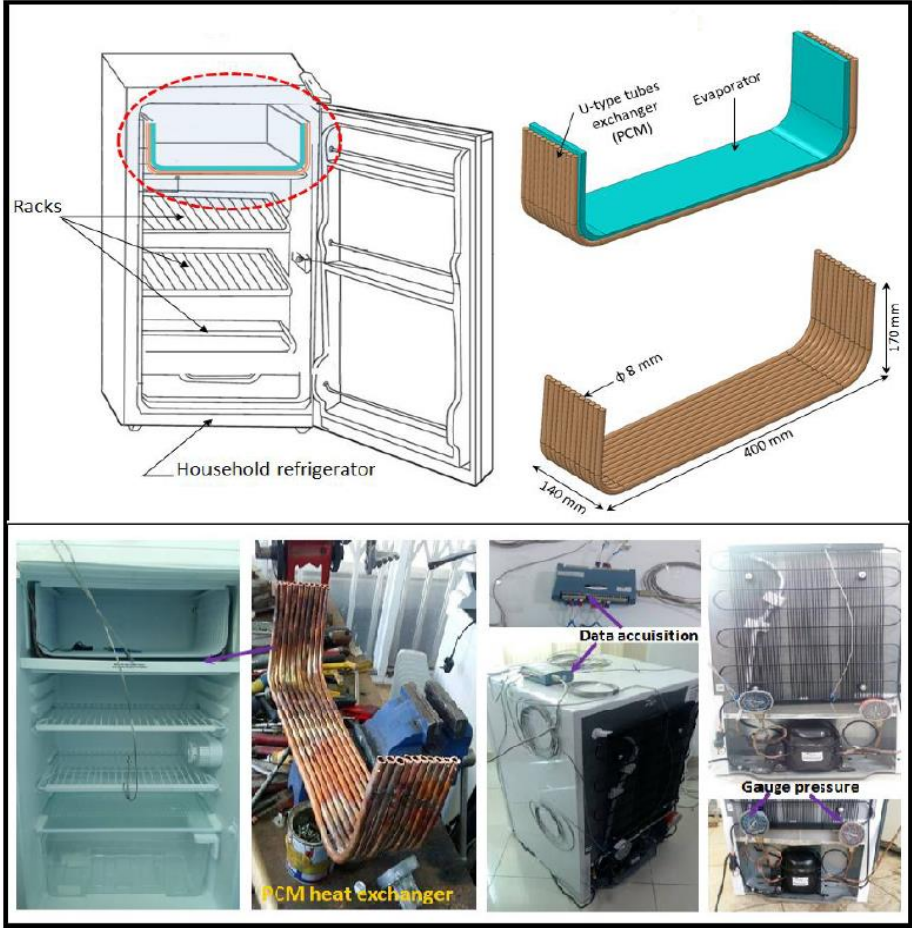


Figure 2.21. Design of PCM heat exchanger by (Elarem et al., 2017).

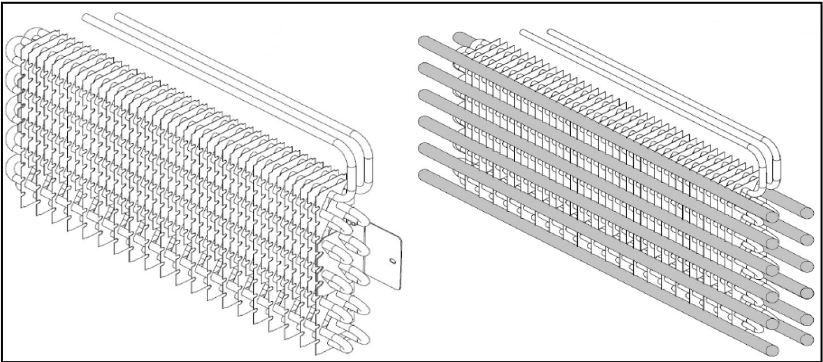


Figure 2.22. PCM arrangement on evaporator by (Cofré-Toledo et al., 2018)

(Raveendran and Murugan, 2021) experimentally incorporated an organic PCM between the evaporator coil and the cabinet insulating wall of a vapor compression refrigeration system (VCRS), as displayed in Figure 2.23. The data indicated that the COP and energy utilization improved by 7.1% and 6.7%, respectively.

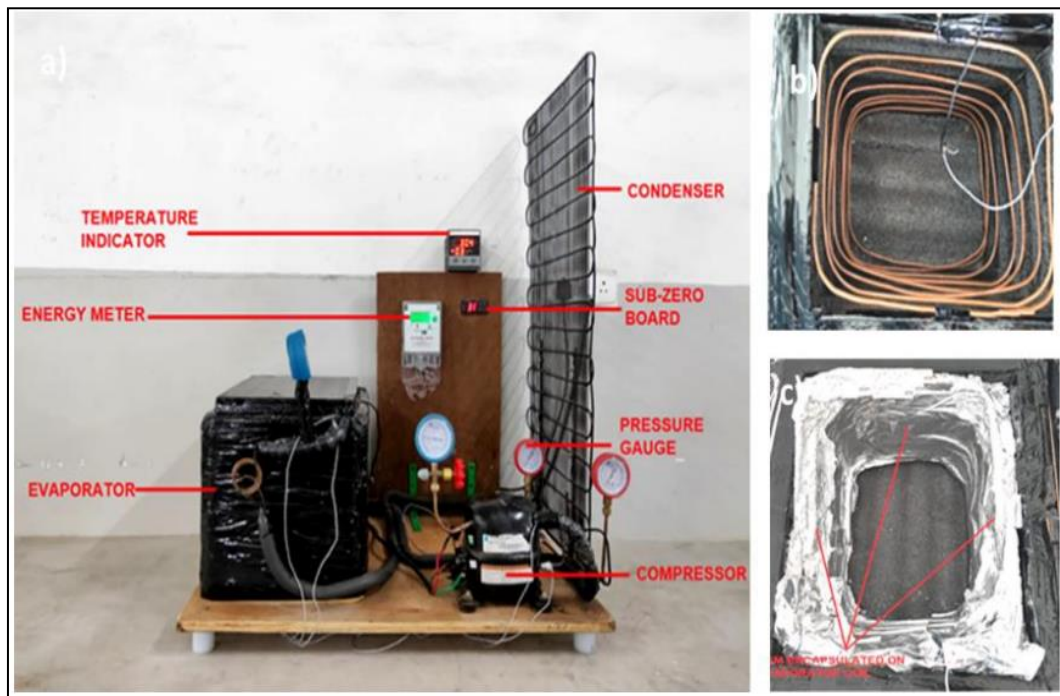


Figure 2.23. VCRS and PCM set up by (Raveendran and Murugan, 2021).

The summary of findings from the aforementioned investigations that used PCM on the evaporator is summarized in Table 2.2.

Table 2.2 List of studies and their results that employed PCM on the evaporator.

Researcher	Household appliance type and volume (L)	PCM types	Mass Of PCM (kg)	PCM properties			T _a °C	Evaporation temperature °C		Freezer temperature °C		Compressor on and off times (min.)				Improving in %	
				T _{ph} °C	k $\frac{w}{m \cdot ^\circ C}$	h _f $\frac{kJ}{kg}$		Without PCM	With PCM	Without PCM	With PCM	Without PCM		With PCM		COP	E
												on	off	on	off		
(Cerri et al., 2003)	Refrigerator -	Eutectic	-	-3	-	-	-	-	-	-	-	-	-	-	-	12	-
(Azzouz et al., 2005)	Single cabinet (fridge) Refrigerator -	Eutectic salt solutions	10	-6 to 0	0.6	280	20	-	-	-19	-7	60	60	180	600	74	-
(Azzouz et al., 2008)	Single cabinet (fridge) Refrigerator 290	Eutectic aqueous solution	-	-9 -7 -5 -3 -1	0.6	280	15 20 25	-20.4	-18	-	-	~20	~40	20 to 72	110 to 258	5 to 15	-
(Azzouz et al., 2009)	Single cabinet (fridge) Refrigerator 290	Eutectic mixture	1.3	-3	-	310	15 20 25 30	-17.39 -15.93 -14.81 -13.21	-14.3 -13.2 -11.9 -10.7	-	-	31 to 37	66 to 180	65	318 to 528	10 to 28	-
(Azzouz et al., 2009)	Single cabinet (fridge) Refrigerator 290	Distilled Water	1.4	0	0.6	330	15 20 25 30	-17.39 -15.93 -14.81 -13.21	-13.7 -12.4 -11.2 -9.97	-	-	31 to 37	66 to 180	78 to 131	323 to 570	11 to 30	-

Table 2.2 (Continued)

Researcher	Household appliance type and volume (L)	PCM types	Mass of PCM (kg)	PCM properties			T _a °C	Evaporation temperature °C		Freezer temperature °C		Compressor on and off times (min.)				Improving in %	
				T _{ph} °C	k $\frac{w}{m \cdot ^\circ C}$	h _f $\frac{kJ}{kg}$		Without PCM	With PCM	Without PCM	With PCM	Without PCM		With PCM		COP	E
												on	off	on	off		
(Md Imran Hossen and Afroz, 2011)	Single cabinet (freezer) Refrigerator 30	Distilled Water	3 and 4	0	0.6	333	22.8 to 23.8	-17.5	-14	-	-	4	16	6	32	21 to 28	-
(Md Imran Hossen and Afroz, 2011)	Single cabinet (freezer) Refrigerator 30	Eutectic solution 90% H ₂ O + 10% NaCl	3 and 4	-5	-	289	22.8 to 23.8	-17.5	-13	-	-	4	16	7	88	21.5 to 30.8	-
(Md Imran Hossen and Afroz, 2011)	Single cabinet (freezer) Refrigerator 30	Eutectic solution 80% H ₂ O + 20% KCl	3 and 4	-10	-	284	22.8 to 23.8	-17.5	-12	-	-	4	16	8	90	22.8 to 34	-
(Rahman et al., 2014)	Refrigerator -	Distilled Water	-	0	0.6	330	-	-	-	-	-	-	-	-	-	55 to 60	-
(Yusufoglu et al., 2015)	Single cabinet (fridge) Refrigerator 130	Distilled water	1.8	0	0.6	331	25.7	-	-	-	-	80	130	105	215	8.6	8.8

Table 2.2 (Continued)

Researcher	Household appliance type and volume (L)	PCM types	Mass of PCM (kg)	PCM properties			T _a °C	Evaporation temperature °C		Freezer temperature °C		Compressor on and off times (min.)				Improving in %	
				T _{ph} °C	k $\frac{w}{m \cdot ^\circ C}$	h _f $\frac{kJ}{kg}$		Without PCM	With PCM	Without PCM	With PCM	Without PCM		With PCM		COP	E
												on	off	on	off		
(Yusufoglu et al., 2015)	Single cabinet (fridge) Refrigerator 350	PCM-1 Eutectic aqueous mixtures	0.95	-5.6	-	228	25	-20	-16	-18	-14.2	32	64	133	306	-	2.4
(Yusufoglu et al., 2015)	Single cabinet (fridge) Refrigerator 350	PCM-2 Eutectic aqueous mixtures	0.95	-3.3	-	251	25	-20	-16	-18	-15.7	32	64	139	298	-	1.4
(Yusufoglu et al., 2015)	Single cabinet (fridge) Refrigerator 350	PCM-3 Eutectic aqueous mixtures	0.95	-3.9	-	201	24.6	-20	-16	-18	-14.5	32	64	136	319	-	1.6
(Yusufoglu et al., 2015)	Single cabinet (fridge) Refrigerator 350	Distilled water	0.95	0	0.6	331	25.1	-20	-16	-18	-16	32	64	145	315	-	4
(Elarem et al., 2017)	Single door Refrigerator 136	Organic Plus ICE A4 solution	-	4	0.21	200	22	-	-	-16	-12	-	-	-	-	8	12

Table 2.2 (Continued)

Researcher	Household appliance type and volume (L)	PCM types	Mass of PCM (kg)	PCM properties			T _a °C	Evaporation temperature °C		Freezer temperature °C		Compressor on and off times (min.)				Improving in %	
				T _{Ph} °C	k $\frac{w}{m \cdot ^\circ C}$	h _f $\frac{kJ}{kg}$		Without PCM	With PCM	Without PCM	With PCM	Without PCM		With PCM		COP	E
												on	off	on	off		
(Cofré-Toledo et al., 2018)	Refrigerator 363.32	Eutectic Plus ICE E-10 solution	0.217	-11.2	0.56	294	5 to 48	-	-	-	-	-	-	-	-	-	1.74
(Cofré-Toledo et al., 2018)	Refrigerator 363.32	Eutectic (19.5 wt.% NH ₄ Cl aqueous solution)	0.270	-15.6	0.57	289	5 to 48	-	-	-	-	-	-	-	-	-	5.81
(Raveendran and Murugan, 2021)	VCRS system 38.28	Organic	1	4	0.16	161	32	1	-	-	-	59	-	64	-	6.7	7.1

2.6.3. Application of PCM in Cabinets

The studies installed PCMs on the interior walls of cabinets and the top and bottom of the racks. Installation of PCMs in the compartments was advantageous in protecting foods and medicines from degradation by sustaining a stable temperature within the cabinets during automatic stopping and power cuts. Using PCMs should not cover a large area of the cabinets because it decreases storage space for storing items. It's also crucial to consider the PCM's orientation (Bista et al., 2018). Several researchers researched in this field, as identified below.

(Gin and Farid, 2010) experimentally employed aluminum panels in the shape of slabs comprised of PCM with a ten-millimeter thickness on the freezer cabinet walls, as illustrated in Figure 2.24. They tested a vertical freezer with a eutectic mixture of water and ammonium chloride PCM (melting point of -15.4°C). The test found that the temperature of products in the freezer with and without PCM changed by 5°C and 13°C , respectively. Likewise, they noted that installing the PCM panels allowed the freezer to keep the cabinet temperature during a power loss, which resulted in lower item and cabinet fluctuation temperatures, as depicted in Figure 2.25.

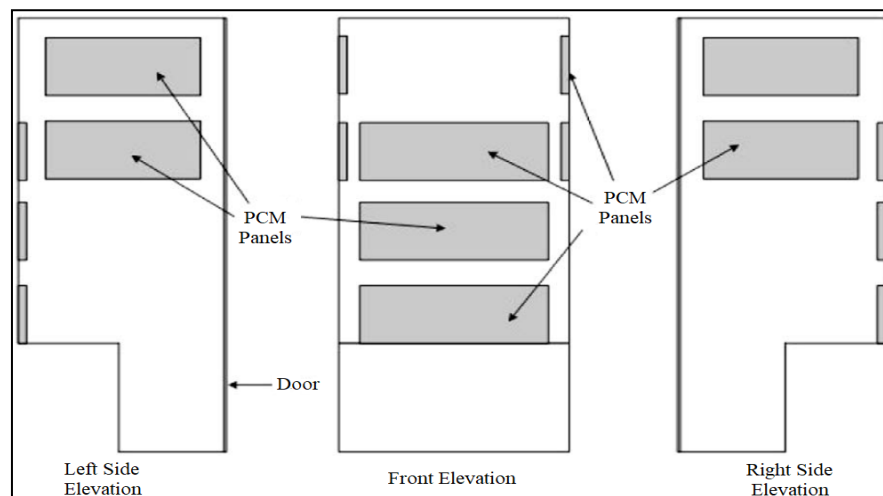


Figure 2.24. Position of PCM panels made by (Gin and Farid, 2010).

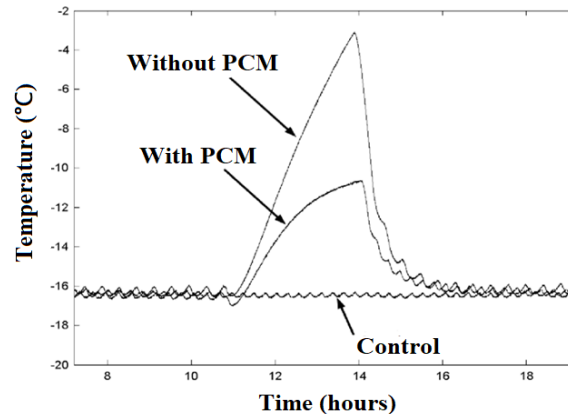


Figure 2.25. PCM's effect on temperature swings during power failures (Gin and Farid, 2010).

In addition, (Gin et al., 2010) did another experiment in which they implemented PCM to the freezer cabinet's walls using the same technique as in the former experiment (Gin and Farid, 2010). However, researchers made a difference from the previous study by evaluating PCM's impact on energy usage. A freezer's energy consumption rose by 11% to 17% and 15% to 21% when its door was opened or when it was defrosted. The application of PCM on the freezer saved energy usage during defrosting and door openings by 8% and 7%, respectively.

Moreover, (Gin et al., 2011) used computational fluid dynamics (CFD) modeling to examine the previous experimental study (Gin and Farid, 2010). The results demonstrated good agreement with the experimental data by (Gin and Farid, 2010). The CFD models also showed that PCM helped keep the temperature in the freezer chamber from rising. Finally, they claimed that this simulation could be expanded for investigating the impacts of utilizing fins, arranging PCM panels, and extending the surface area.

Experimentally (Oró et al., 2012) used PCM to assess temperature fluctuations within a vertical freezer cabinet during door openings and power cuts. The freezer's evaporator was utilized as a food rack and located on the seven racks.

An inorganic salt-hydrate (Climsel C-18) was put inside a stainless-steel panel and then placed horizontally on the shelves, as presented in Figure 2.26. They concluded that a freezer with PCM had a 4°C to 6°C lower interior air temperature variation than a freezer without PCM. Also, the PCM could keep the interior temperature for almost 3 hours in a power failure case.



Figure 2.26. PCM encapsulation container and location by (Oró et al., 2012).

(Marques et al., 2013) utilized (CFD) simulation to compare the household refrigerator's temperature stability with water and eutectic PCMs installed into the refrigerator compartment. Additionally, situations involving the orientation of the PCM and compartment models were studied. The model proposed that a PCM orientation that induced lower compartment temperatures was vertical and horizontal combination with a eutectic PCM had a melting point of around zero in a full height compartment, as explained in Figure 2.27. In addition to that, the study recommended splitting the same compartment into two trays and applying a horizontal PCM in both trays with ice (water) solely.

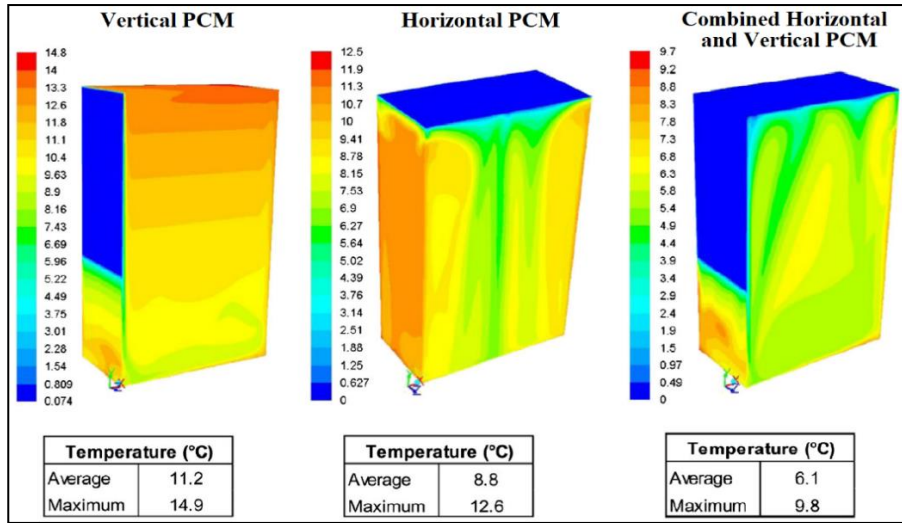


Figure 2.27. Comparison of PCM orientations by (Marques et al., 2013).

(Abdolmaleki et al., 2020) placed a eutectic mixture of polyethylene glycols (PEGs) PCM in the vertical freezer compartments, as can be seen in Figure 2.28. This method reduced freezer's temperature fluctuation by 40.59% and resulted in an 8.37% reduction in power consumption.

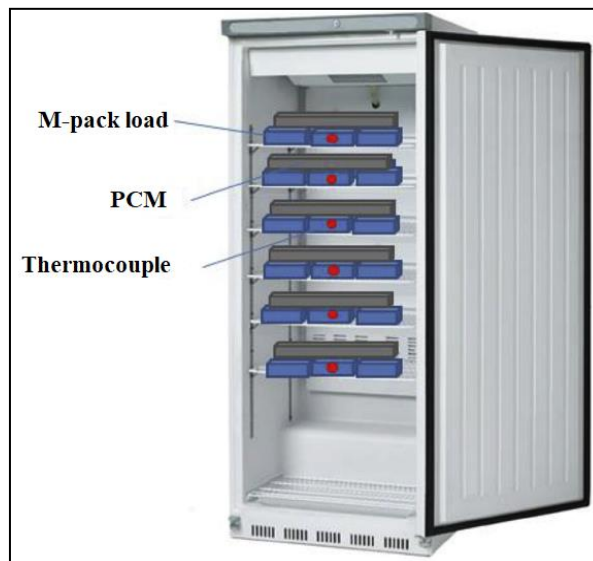


Figure 2.28. PCM position by (Abdolmaleki et al., 2020).

(Pavithran et al., 2021) used a numerical CFD simulation to examine the integration of PCM in refrigerator compartments at various positions. A PCM was

employed that was eutectic and had a melting point of -3°C . There were five compartments in the refrigerator interior (A, B, C, D, and E). The freezer compartment was denoted by E, while the fridge's compartments were represented by A, B, C, and D, as shown in Figure 2.29. They examined five different cases of PCM orientation and configuration. Their results are demonstrated in Table 2.3. The best cases were the horizontal and vertical combination arrangements and more PCM covering areas, which resulted in less temperature fluctuation within the refrigerator compartments concerning time.

Table 2.3 PCM orientations and locations, covering area by PCM, and compartment variation temperatures (Pavithran et al., 2021).

Cases	PCM orientations and locations	Covering area by PCM %	Compartment variation temperatures ($^{\circ}\text{C}$) after 600s.	
			Without PCM	With PCM
1	One horizontal PCM at location D	5	17 - 21	5 - 11
2	Two horizontal PCM at locations C and D	7.5	17 - 21	7 - 9
3	Three horizontal PCM at locations B, C, & D	10	17 - 21	2 - 8
4	Combined of one horizontal PCM at location D and one vertical PCM to the cabinet wall	10	17 - 21	0 - 7
5	Combined of two horizontal PCM at locations C & D and one vertical PCM to the cabinet wall	15	17 - 21	≤ 3

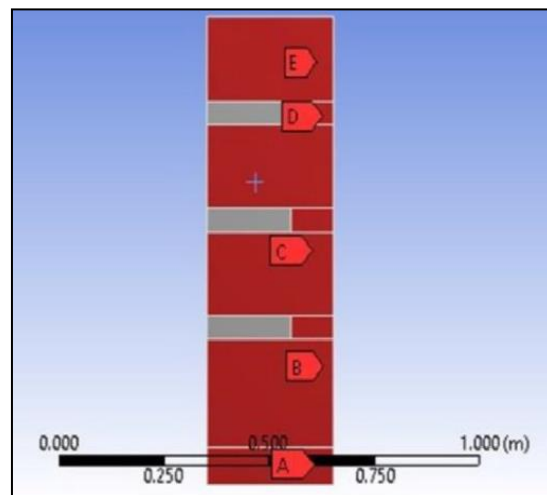


Figure 2.29. Domain modeled by (Pavithran et al., 2021).

(Kasinathan and Kumaresan, 2021) evaluated the refrigerator's energy performance with deionized water containing 3% wt of natural graphite on the evaporator side (inside the freezer compartment). Consequently, the refrigerator saved 7–13% of energy for various thermal loads.

(Karthikeyan et al., 2021) implemented the hydrate salt HS3N and paraffin OM-03 organic commercial PCMs in a slab rectangle layout inside the freezer and fridge cabinets, respectively, as indicated in Figure 2.30. The study reported that freezer and fridge cabinet temperatures fluctuated by 0.4°C and 0.4°C less than the ordinary refrigerator.



Figure 2.30. PCM configuration in the freezer and fridge cabinets (Karthikeyan et al., 2021).

Table 2.4 summarizes the data of the studies explained in this section.

Table 2.4 List of investigations and their outcomes that installed PCM in the cabinets.

Researcher	Household appliance type & volume (L)	PCM types and its location	Mass of PCM (kg)	PCM properties			T _a °C	Fridge cabinet fluctuation temperature °C		Freezer cabinet fluctuation temperature °C		Compressor on and off times (min.)				Improving in %	
				T _{Ph} °C	k $\frac{w}{m \cdot ^\circ C}$	h _f $\frac{kJ}{kg}$		Without PCM	With PCM	Without PCM	With PCM	Without PCM		With PCM		COP	E
												on	off	on	off		
(Gin and Farid, 2010)	Vertical freezer 153	Eutectic (water and ammonium chloride) in freezer	2.2	-15.4	-	-	-	-	-	13	5	-	-	-	-	-	-
(Gin et al., 2010)	Vertical freezer 153	Eutectic (water and ammonium chloride) in freezer	2.2	-15.4	-	620	25 32	-	-	15.3	12.4	-	-	-	-	-	7-8
(Oró et al., 2012)	Vertical freezer 270	Inorganic salt hydrate (Climsel C-18)	7.84	-18	0.5 to 0.7	306	21	-	-	9 to 13	4 to 6	-	-	-	-	-	-
(Abdolmaleki et al., 2020)	Vertical freezer 180	Eutectic solution (70wt.%PE G300+30wt.%PEG200)	1.5	-20	-	-	16 to 43	-	-	-	-	595	844	545	894	-	8.37
(Pirvaram et al., 2019)	Refrigerator -	Eutectic solution in fridge	-	-3	0.21	300	32	17-21	2-8	-	-	-	-	-	-	-	-

Table 2.4 (Continued)

Researcher	Household appliance type & volume (L)	PCM types and its location	Mass of PCM (kg)	PCM properties			T _a °C	Fridge cabinet fluctuation temperature °C		Freezer cabinet fluctuation temperature °C		Compressor on and off times (min.)				Improving in %	
				T _{Ph} °C	k $\frac{w}{m \cdot ^\circ C}$	h _f $\frac{kJ}{kg}$		Without PCM	With PCM	Without PCM	With PCM	Without PCM		With PCM		COP	E
												on	off	on	off		
(Kasinathan and Kumaresan, 2021)	Refrigerator 180	De-ionized water+3% wt natural graphite in freezer	0.300	-15	-	319.3	28	-	-	-	-	310	360	330	360	-	7-13
(Karthikeyan et al., 2021)	Refrigerator 185	HS3N in freezer	1.1	-3	0.35	247	-	1.3	0.9	1.4	1	-	-	-	-	-	-
		OM-03 in fridge	2.2	5	0.146	229											

2.6.4. Application of PCM in Condenser and Evaporator

As explained in previous sections, many studies employed PCMs in both the condenser and evaporator individually. Both installations offered advantages and disadvantages. However, simultaneous application of them could overcome the drawbacks of using PCM on them individually (Mastani Joybari et al., 2015).

Accordingly, a refrigerator with new dual-energy storage (DES) that included a cold storage evaporator (CSE) and a heat storage condenser (HSC) to optimize the heat transfer of evaporator and condenser was developed by (Cheng et al., 2017). For the condenser and evaporator, paraffin and undecane were utilized as SSPCMs. Three refrigerators (HSC, CSE, and DES) were simulated and compared with a conventional refrigerator. The DES refrigerator included the best features of both the CSE and HSC refrigerators. The condenser and evaporator of the DES refrigerator were capable of continuously rejecting heat and cold throughout the whole cycle. The ratio of off-to-on time for DES, CSE, and HSC refrigerators was 4.3, 3.0, and 2.2, respectively. The comparison between COP, electricity consumption, and energy savings for the four refrigerators is tabulated in Table 2.5.

Table 2.5 The results of various parameters by (Cheng et al., 2017).

Variables	Ordinary	HSC	CSE	DES
Electrical consumption (kWh)	0.5	0.44	0.42	0.34
COP	1.34	1.59	1.67	1.86
Energy saving (%)	0	12	16	32

2.6.5. Application of PCM in Condenser and Cabinets

The use of PCMs in refrigerator condensers and cabinets helped to improve energy consumption, minimize temperature variations, and keep food quality. As a result of these contributions, this study has been published, as detailed below.

(Karthikeyan et al., 2021) experimentally employed PCMs in the condenser, freezer cabinet, and fridge cabinet, as presented in Figures 2.11 and 2.30. Besides, the application of PCMs in the condenser and both cabinets was explained in Sections 2.6.2 and 2.6.3, respectively. They also tested the refrigerator with both the aforementioned cases together and named it PCM at all locations. Consequently, PCM design in all locations yielded lower condenser temperatures and a better improvement in the performance of the refrigerator. The temperature in the inlet and outlet condenser was cooled by 6°C and 4.8°C , respectively. The freezer and fridge cabinets' temperatures fluctuated by 1.1°C and 0.8°C , respectively, less than the standard refrigerator, as depicted in Figure 2.31.

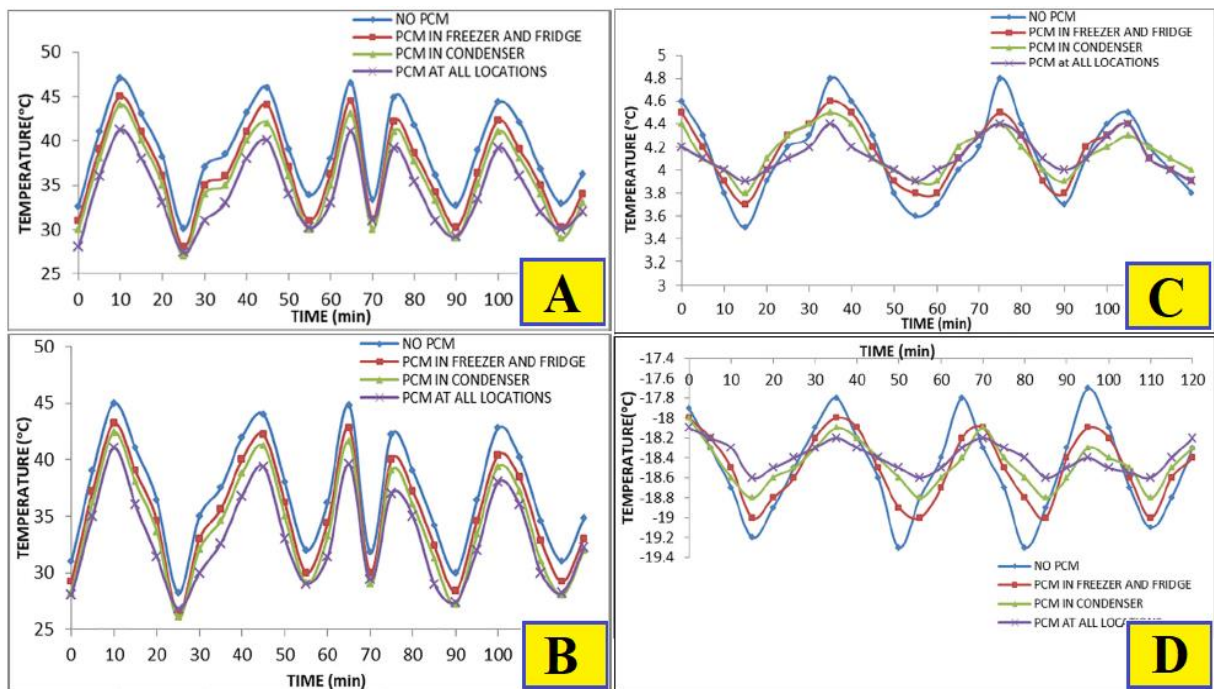


Figure 2.31. Temperature vs. time for (a) condenser upper part, (b) condenser lower part, (c) fridge cabinet, and (d) freezer cabinet by (Karthikeyan et al., 2021).

2.6.6. Application of PCM in Evaporator and Cabinets

Due to the impact of incorporating PCMs in the evaporators and cabinets on saving power usage, stabilizing cabinets temperature, and extending

compressor stopping time. Hence, (Elarem et al., 2017) tested the PCMs in the evaporator and cabinets simultaneously. They ran simulation and modeling tests to discover the optimal condition for immediately regulating the refrigerator compartment temperature. Four different arrangements in the evaporator and the cabinet's walls and racks were made, as shown in Figure 2.32. The case-4 provided superior heat transfer capability and enabled the refrigerator cabinet to attain its stable temperature more efficiently than the other three cases. Additionally, it could extend the compressor's off time and enhance energy consumption.

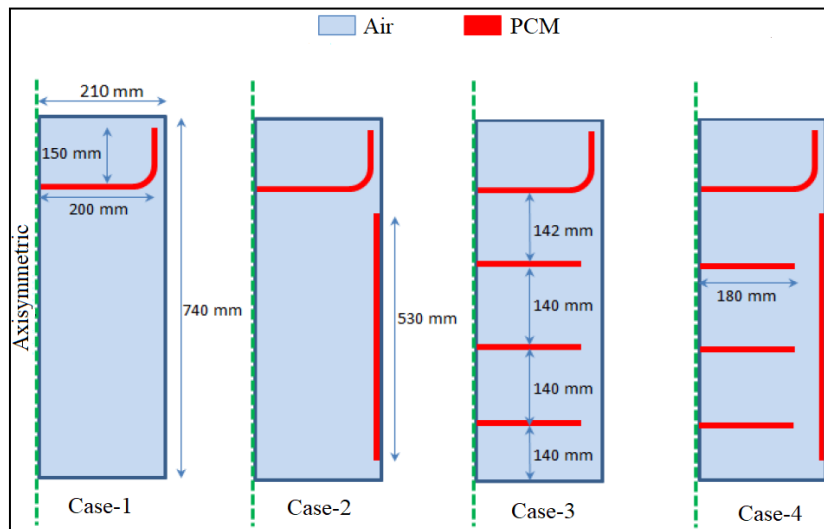


Figure 2.32. PCM arrangements in evaporator (case-1), evaporator and cabinet wall (case-2), evaporator and cabinet racks (case-3), and evaporator and cabinet's wall and racks (case-4) by (Elarem et al., 2017).

2.7. Conclusion

In recent decades, many studies have proposed different techniques to improve the overall performance of household vapor compression refrigeration system appliances, such as refrigerators and freezers. The nature of these solutions was differed according to their implementation and costs. Using PCMs has attracted researchers due to their cost-effective and easy installation. The purpose

of these studies was to improve COP, reduce energy consumption, and minimize temperature fluctuations in the cabinets. Consequently, the performance enhancement of household refrigerators and freezers has been achieved by applying PCMs to the condenser, evaporator, and fridge and freezer cabinets individually and simultaneously. Thus, following a comprehensive survey of the relevant literature, the below conclusions are drawn.

i. Application of PCM individually

1. Application of PCM in condenser: A comprehensive literature review showed that PCM utilization on the condenser could reduce the condenser temperature and increase its heat transfer efficiency. This improvement led to a shorter compressor on-cycle period, less energy use, and a better COP for the system. The enhancement rate depended on the capacity, thermal conductivity, and number of PCMs. The difference between PCM phase change temperature and ambient temperature and between PCM phase change temperature and maximum condenser temperature were also accountable. The studies used a variety of PCM numbers employed, types, arrangements, and methods to improve the thermal conductivity of PCMs in this advancement, as summarized below.

a) Number of PCM employed: Most of studies employed a single PCM, while a few used double PCMs in a cascade design, for instance (Karthikeyan et al., 2021 and Pirvaram et al., 2019). The use of double PCMs was more advantageous in improving the refrigerator's overall efficiency.

b) Type of PCM: Organic PCMs were used mostly, mainly paraffin compounds.

- c) **Arrangement of PCM:** Almost all PCMs were encapsulated in aluminum pouches and installed on the condenser tubes, which completely covered the back face of the condenser area. The exception was (Kumar et al., 2020) encased PCM in aluminum pouches and wrapped around condenser pipes.
- d) **Thermal conductivity enhancer method:** Most studies utilized the encapsulation method because the PCMs leaked in their liquid phase. However, (W.-L. Cheng et al., 2011 and P. M. Kumar et al., 2020) combined encapsulation with the addition of nanoparticles and shape stabilizing mechanisms, respectively.

2. Application of PCM in evaporator: According to an extensive review of published studies, PCM incorporation on the evaporator extended the compressor off-cycle period, resulting in less energy utilization. Additionally, it improved the COP since the constant volumetric rate of the compressor extracted more mass flow from the evaporator. Another gain was a decline in the number of compressor's starts and stops. PCMs with low phase change points increased evaporation and cabin temperatures more than those with higher ones. However, PCMs with higher phase change temperatures and latent heat capacity decreased the total operating time by increasing the compressors' on and off times per cycle. As a result, the overall performance of the refrigerator increased. The following aspects covered the PCM implementation in detail, as previously discussed in the condenser.

- a) **Number of PCM employed:** All the studies reviewed in this design used a single PCM.

- b) **Type of PCM:** Largely eutectic salt solution of inorganics PCMs and distilled water as a PCM have been used.
- c) **Arrangement of PCM:** Mostly PCMs have been encapsulated in metal slab design and positioned between the refrigerator's evaporator coil and the back wall. Except for (Md Imran Hossen & Afroz, 2011 and Rahman et al., 2014), which submerged the evaporator coil in a PCM box.
- d) **Thermal conductivity enhancer method:** Only encapsulation was employed to prevent leaks and improve heat conductivity.

3. Application of PCM in cabinets: Previous studies have shown that the application of PCMs in cabinets was advantageous in preserving food quality by decreasing the temperature fluctuating within the cabinets during automatic stopping and power cuts. Besides that, they concluded that the use of PCMs caused a reduction in energy usage during defrosting and door openings. The primary requirement of this arrangement was not to occupy too much volume in the cabinets. In the following sections, PCM installations are described.

- a) **Number of PCM employed:** A single PCM in the freezer and fridge cabinets was equipped.
- b) **Type of PCM:** Eutectic PCMs have mainly been employed.
- c) **Arrangement of PCM:** PCMs were housed in metal and plastic panels in a slab shape and fitted on cabinet walls and racks. The orientation of PCM panels was also considered. The efficient orientation was the horizontal and vertical combination.

d) Thermal conductivity enhancer method: The sole mechanism employed was encapsulation.

ii. Application of PCM simultaneously

1. Application of PCM in condenser and evaporator: This setup was superior to the PCM in the condenser and evaporator alone. It reduced the drawbacks of PCM implantation on the condenser and evaporator individually. Additionally, it improved COP and energy consumption more than the PCM in the evaporator and condenser separately. The installation of PCMs followed the same technique as aforementioned in the evaporator and condenser alone.

2. Application of PCM in condenser and cabinets: This arrangement helped the refrigerator to operate with less energy consumption, lower temperature swings, better-preserved food quality, and a higher COP than the refrigerator with PCM in the condenser and cabinets individually. PCM placement was similar to the process of placing PCM in condensers and cabinets separately. The PCM setup was the same as in the condenser and cabinets individually.

3. Application of PCM in evaporator and cabinets: This design reduced energy consumption, temperature fluctuations, and food quality degradation more than the PCM application in evaporators and cabinets alone. The PCM arrangement was the same as that employed in the evaporators and cabinets.

In this study, based on the conclusions of the published literature, the implementations of PCMs on the condenser, evaporator, and fridge cabinet have been investigated. The PCMs were arranged in an individual and simultaneous manner as follows:

I. Application of PCM individually

1. Application of PCM in condenser: In this study, triple PCMs with and without nanoparticles were installed. In addition, the setup of double PCMs has been investigated to compare it with triple PCMs. The PCMs were positioned according to the refrigerant's temperature, from high to low. As a PCM, organic paraffin was selected due to its suitable thermal properties for this design. The PCMs were encapsulated in copper tubes and mounted vertically as fins on the condenser tubes.

2. Application of PCM in evaporators: In this design, single PCM, double PCM, and a combination of both were performed. The PCMs have been placed on the non-functional sides of the evaporators. As a PCM, inorganic hydrate salts (ammonium chloride and potassium hydrogen carbonate) (SP-17), (sodium carbonate and potassium hydrogen carbonate) (SP-7), and distilled water were chosen. In aluminum pouches, the PCMs were packed.

II. Application of PCM simultaneously

1- Application of PCM in condenser and evaporators: This configuration was not executed experimentally by researchers. Therefore, it has been investigated experimentally. The application procedure was the same as for the condenser and evaporator individually.

2- Application of PCM in condenser, evaporator, and fridge cabinet:

This setup of PCMs was an important contribution because it has not been performed in previous studies. For the condenser and evaporator, the establishment process of PCMs included similar mechanisms as performed individually. However, in the fridge cabinet, single organic paraffin as a PCM was encapsulated in aluminum panels in slab form and positioned in the location of shelves. Due to the limited volume, the freezer cabinet operated with no PCM.

The following contribution are made in this study:

- 1- Installation of triple PCMs with nanoparticles (CHS-1) and triple PCMs without nanoparticles (CHS-2) on the condenser.
- 2- Implementation of double PCMs (ECS-2) and a combination of single and double PCMs (ECS-3) on the evaporators.
- 3- Utilizing PCMs on both the fridge and freezer evaporators.
- 4- Using copper tubes as a container for PCMs and their arrangement on the condenser.
- 5- Using aluminum pouches on the non-functional sides of the evaporators.
- 6- Experimental investigation of PCMs in the condenser and the evaporator simultaneously.
- 7- The use of PCMs together at all locations (condenser, evaporator, and fridge cabinet).

CHAPTER 3

MATHEMATICAL MODELLING AND SYSTEM DESCRIPTION

3.1. Introduction

This chapter is divided into two parts. In the first part, the description and the thermodynamic processes of the system are explained thoroughly. In the second part, the mathematical modelling of thermodynamic processes in the vapor compression refrigeration system based on the principle of conservation of energy is highlighted.

3.2. System Description

In this study, a household refrigerator that operated on the principle of the vapor compression refrigeration system was investigated. The household refrigerator prototype is shown in Figure 3.1. The schematic of the system is displayed in Figure 3.2, which includes a compressor, condenser, capillary tube, and evaporator. The condenser was an air-cooled wire and tube model, while the evaporator was a plate and tube type. Both the condenser and evaporator heat exchangers utilized natural convection for heat transfer. The compressor was a hermetic reciprocating single-speed type. R600a (Isobutane) was used as the refrigerant in this system. The refrigerator had freezer and fridge cabinets, each with its own evaporator and door. The freezer cabinet included a single tray, while the fridge cabinet contained three racks of the same size and a chamber for fresh

fruit and vegetables. The thermostat was located on the fridge's evaporator. The specifications of the refrigerator are listed in Table 3.1.

Table 3.1 The specifications of the household refrigerator.

Brand name	Cold Universal
Model	UNI-275S
Climate type	ST/T
Total volume (Liter)	260
Freezer Volume (Liter)	55
Fridge Volume (Liter)	205
Rated current (A)	1.0
Rating voltage (VAC)	220 - 240
Energy efficiency class	B
Power consumption with starting (kWh/24h)	1.237
Power consumption at a steady-state (kWh/24h)	1.158
Annual power consumption (kWh)	422.67
Compressor model	Embraco - EMY3118Y
Compressor type	Hermetic reciprocating
Compressor speed mode	Single speed
Refrigerant	R600a
Refrigerant weight (g)	75
Defrost type	No defrost
Condenser material	Copper
Evaporator material	Aluminum
Overall dimension (mm) (Height × Width × Depth)	1700 × 550 × 570
Condenser dimension (mm) (Length×Width)	1000 × 500
Evaporator-freezer dimension (mm) (Length×Width)	950 × 35
Evaporator-fridge dimension (mm) (Length×Width)	380 × 400
Freezer cabinet tray dimension (mm) (Length×Width)	390 × 320
Fridge cabinet trays dimension (mm) (Length×Width)	450 × 300

The compressor was the starting and ending point of the system process. The superheated vapor refrigerant ran into the compressor, in which it was pressurized from low evaporator pressure to high condenser pressure. Then, the refrigerant was moved to the condenser, where it became a liquid due to heat transfer with the environment (ambient temperature). After that, the refrigerant loses pressure and temperature by the capillary tube. Due to the pressure loss, the refrigerant moved more slowly and became colder as it came out of the capillary

tube. The refrigerant was entered into the evaporators in liquid and vapor form. The heat transfer occurs; thereby, the refrigerant has consumed the heat from the load inside the refrigerator cabinets. This heat extraction caused the refrigerant to be a superheated vapor, which turned into the compressor, and then the process begins again (Arora, 2014).



Figure 3.1. Household refrigerator prototype.

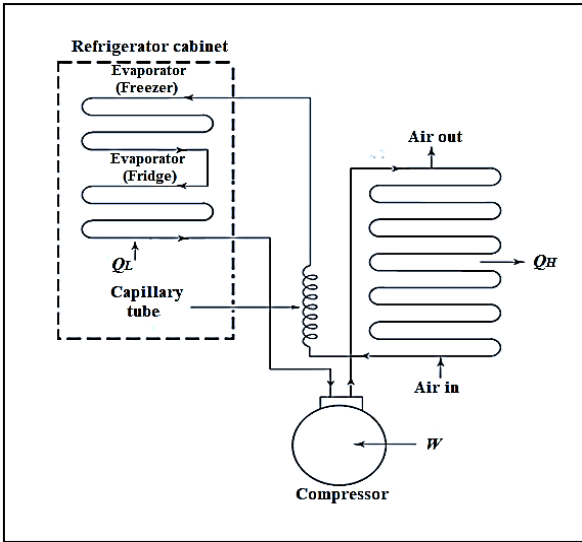


Figure 3.2. A scheme of the household refrigerator system.

3.3. Mathematical Modelling

The vapor compression refrigeration cycle was the most common system utilized in household refrigerators. There were four thermodynamic processes involved in this cycle, as highlighted in Figure 3.4 and outlined below.

1-2 Isentropic compression in the compressor.

2-3 Constant pressure (isobaric) heat rejection in the condenser.

3-4 Isenthalpic expansion (throttling) in a capillary tube.

4-1 Constant pressure (isobaric) heat absorption in the evaporator.

Notably, two of the processes were defined by constant pressure, while the third was described by constant enthalpy. Thus, although the fourth process was characterized by isentropic, the P-h diagram represented in Figure 3.5 is still convenient because the work done was measured by the change in enthalpy.

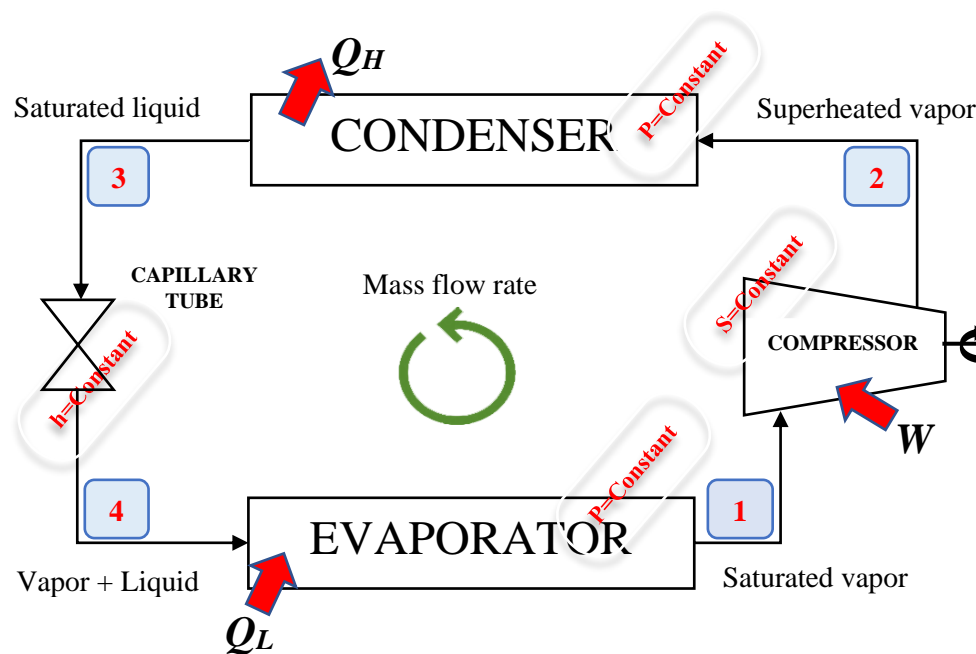


Figure 3.4. Standard vapor compression refrigeration cycle.

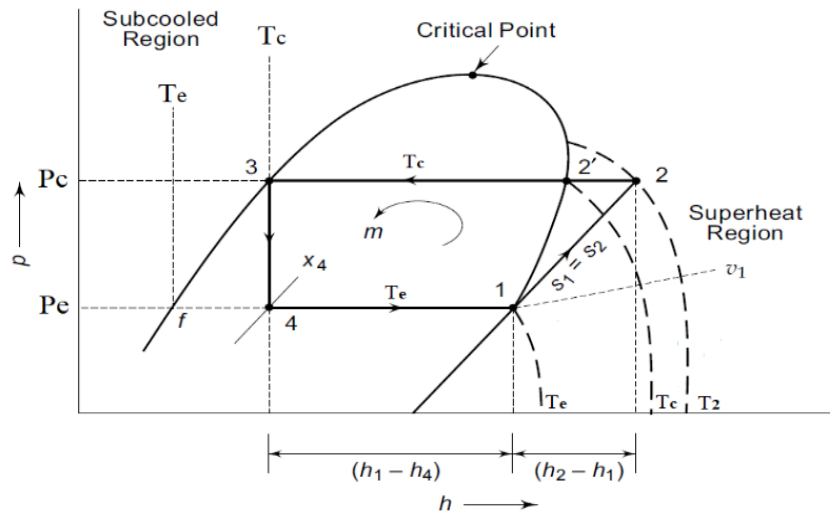


Figure 3.5. Standard vapor compression refrigeration cycle on P-h diagram (Arora, 2000).

The components of the system, along with their thermodynamic processes and heat transfer correlations based on the principle of energy conservation, are described in the following sections.

The following statement expresses the theory of conservation of energy.

$$q - w = \Delta h + \Delta KE + \Delta PE \quad (3.1)$$

Where q and w are the amount of heat transferred into the system and work done by the component, respectively. Δh is the change in specific enthalpy. ΔKE and ΔPE are the change in kinetic and potential energies, respectively.

3.3.1. Compressor Analysis

For the compressor, $Q = 0$, $\Delta KE = 0$, and $\Delta PE = 0$.

The refrigerant is compressed adiabatically from low evaporator pressure to high condenser pressure. This adiabatic compression required work to be performed under the condition of constant entropy.

Hence, this work is done by the compressor w and can be defined as:

$$w = - (h_2 - h_1) \quad (3.2)$$

Where w is the compressor work done (kJ/kg) and h_1 and h_2 are the suction and discharge specific enthalpies (kJ/kg) of the compressor, respectively.

In addition, the compressor consumes power for its work, so the power transfer to the compressor or the energy consumption by the compressor E is expressed as follows:

$$E = \dot{M}_{ref} \times \Delta h = \dot{M}_{ref} \times (h_2 - h_1) \quad (3.3)$$

Where E is compressor energy consumption (kJ/s) or (kW) and \dot{M}_{ref} is the mass flow rate of the refrigerant (kg/s).

Thereby, the refrigerant discharged from the compressor and continuously circulated in the system during the on-cycle time has a mass flow rate (\dot{M}_{ref}), which can be calculated as follows:

$$\dot{M}_{ref} = \frac{\text{Compressor energy consumption}}{\text{Compressor work done}} = \frac{E}{w} \quad (3.4)$$

3.3.2. Condenser Analysis

The refrigerator's condenser functions as a heat exchanger by converting superheated vapor refrigerant into saturated liquid through thermodynamic contact with air. It continually rejects heat, which is extracted by refrigerant within the cabinets. As a result, no changes in potential or kinetic energies occur, and the condenser does not perform any work, according to energy conservation theory. Hence, in the condenser, $w = 0$, $\Delta KE = 0$, and $\Delta PE = 0$.

Thus, heat rejection in the condenser, Q_H can be expressed as:

$$Q_H = \dot{M}_{ref} \times \Delta h = \dot{M}_{ref} \times (h_2 - h_3) \quad (3.5)$$

Where h_2 and h_3 are the inlet and outlet specific enthalpies (kJ/kg) of condenser, respectively.

3.3.3. Capillary Tube Analysis

For the capillary tube (adiabatic expansion (throttling)), $q = 0$, $w = 0$, $\Delta KE = 0$, and $\Delta PE = 0$.

Therefore, change in enthalpy in throttling $\Delta h = 0$

$$h_3 = h_4 \quad (3.6)$$

3.3.4. Evaporator Analysis

The refrigerator's evaporator serves as a heat exchanger by changing a mixture of mostly saturated liquid with some vapor into saturated vapor via thermodynamic contact with cabinet air. Consequentially, based on the energy conservation concept, no changes in potential or kinetic energies happen, and the evaporator accomplishes no work. Therefore, in the evaporator, $w = 0$, $\Delta KE = 0$, and $\Delta PE = 0$.

Thereby, heat extraction by the evaporator, Q_L can be stated as:

$$Q_L = \dot{M}_{ref} \times \Delta h = \dot{M}_{ref} \times (h_1 - h_4) \quad (3.7)$$

Where h_1 and h_4 are the evaporator output and input specific enthalpies (kJ/kg), respectively.

3.3.5. Freezer and Fridge Cabinets Analysis

The refrigerator cabinets can extract heat from the ambient through their walls and doors, although they are insulated. In addition to that, the heat is made by storing products inside them. So, the following equation can be used to calculate the heat gain from cabinets across their doors and walls:

$$Q_c = UA\Delta T \quad (3.8)$$

Where Q_c is the amount of heat gain through cabinet' wall and door (Watt), U is the overall heat transfer coefficient of wall and door ($\text{W}/\text{m}^2\cdot^\circ\text{C}$), A is the area of wall and door (m^2), and ΔT is the temperature difference between inside and outside of the cabinet ($^\circ\text{C}$).

To find the (U) of each wall and door, it is required to determine the thermal resistance (R_T) of each wall and door. This is because the correlation for calculating (U) includes the (R_T), as stated below.

$$U = \frac{1}{R_T} \quad (3.9)$$

Each cabinet's walls are composed of roughly 1 mm of galvanized sheet steel on the exterior, a 37 mm-thick polyurethane (PUR) foam core, and 2 mm of high-impact polystyrene (HIPS) on the interior. Also, the doors are made of 1 mm galvanized sheet steel, 67 mm PUR foam, and 2 mm HIPS on the outside, core, and inside, respectively, as showed in Figure 3.6. However, in this study, all wall and door thicknesses were assumed to be PUR foam alone due to the thinness of HIPS and galvanized sheet steel. As a result, the total thermal resistance of each wall and door is shown in Figure 3.7.

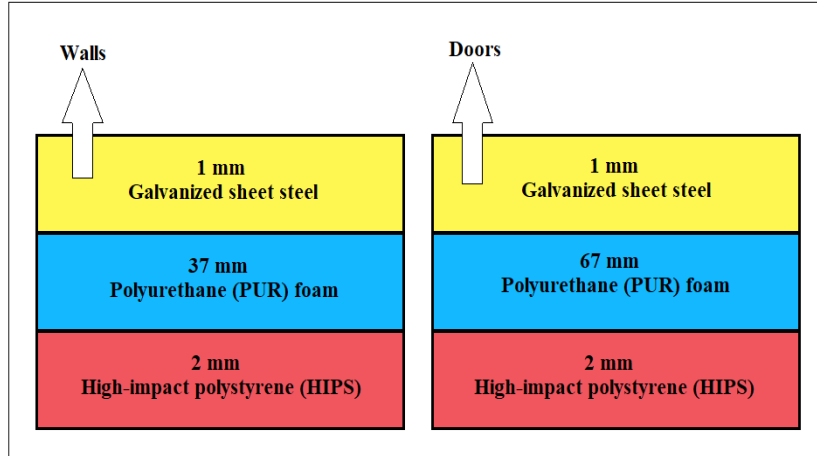


Figure 3.6. The components of walls and doors.

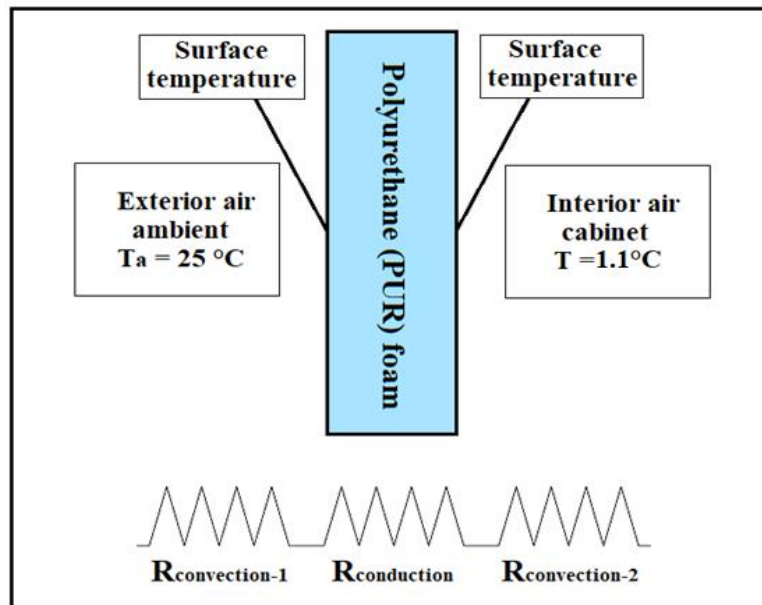


Figure 3.7. One dimensional thermal resistance circuit.

Thereby, the total thermal resistance (R_T) can be expressed as follows:

$$R_T = R_{convection-1} + R_{conduction} + R_{convection-2} \quad (3.10)$$

$$R_T = \frac{1}{h_i A} + \frac{L}{KA} + \frac{1}{h_e A} \quad (3.11)$$

The inside and outside surface temperatures were assumed for estimating the internal (h_i) and external (h_e) heat transfer coefficients. Then, the

thermophysical properties of the air inside and outside the cabinet are determined using the mean temperature. The mean temperature (T_m) can be written as:

$$T_m = \frac{T_s + T_\infty}{2} \quad (3.12)$$

The mathematical correlations of the Nusselt number (Nu) utilized to determine the convection coefficient (h) depend on the Rayleigh number (Ra) and Prandtl number (Pr). Also, Rayleigh number is the product of Grashof number (Gr) and Prandtl number. Thus, it can be determined by the following correlation (Holman, 1986):

$$Ra = GrPr = \frac{g\beta(T_s - T_\infty)L_c^3}{\nu^2} Pr \quad (3.13)$$

Where the thermal expansion coefficient (β) is determined as follows:

$$\beta = \frac{1}{T_m} \quad (3.14)$$

Nevertheless, in vertical walls, the characteristic length (L_c) is equal to the height, while in horizontal walls, it is computed as follows:

$$L_c = \frac{A_s}{P_s} \quad (3.15)$$

Where (A_s) and (P_s) can be calculated from:

$$A_s = length \times width \quad (3.16)$$

$$P_s = 2(length + width) \quad (3.17)$$

Due to the vertical and horizontal walls of refrigerator cabinets, different Nusselt number correlations are employed. Thus, the Eq. (3.18), which was valid for the entire range of the Rayleigh number, was applied to the vertical walls and

doors. Additionally, for horizontal walls with hot bottoms and cold tops, Eq. (3.19), available for a range of (10^5 – 10^{11}) of the Rayleigh number, was used.

$$Nu = \left[0.825 + \frac{0.387Ra^{\frac{1}{6}}}{\left[1 + \left(\frac{0.492}{Pr} \right)^{\frac{9}{16}} \right]^{8/27}} \right]^2 \quad (3.18)$$

$$Nu = 0.27 Ra^{\frac{1}{4}} \quad (3.19)$$

Eventually, the heat transfer coefficients are obtained by the following equation:

$$h_{i,e} = \frac{Nu k}{L} \quad (3.20)$$

3.3.6. Coefficient of Performance (COP)

The performance of refrigeration systems is evaluated by the coefficient of performance (COP). The refrigerator COP is the ratio of evaporator heat extraction (refrigeration effect) to compressor work done, as expressed below:

$$COP = \frac{\text{Refrigeration effect}}{\text{Compressor work done}} = \frac{h_1 - h_4}{h_2 - h_1} \quad (3.21)$$

3.3.7. Phase Change Material

The storing energy in the PCMs was based on their latent heat of fusion. Thus, the following formula can be used to calculate the amount of latent energy stored.

$$Q_{pcm} = M \times h_f \quad (3.22)$$

Where Q_{pcm} is the amount of stored latent energy (kJ), M is the mass of PCM (kg), and h_f is the PCM latent heat of fusion (kJ/kg).

3.3.8. Estimation of Required Mass

In this section, the final forms of the equations developed for calculating the proper masses of PCMs are described. For the condenser, by substituting Eq. (3.5) into Eq. (3.22) and multiplying by a compressor on time (T_{on}) cycle, Eq. (3.23) was derived and applied to compute the required mass of PCM as follows:

$$M = \frac{Q_H \times T_{on}}{h_f} \quad (3.23)$$

Similarly, the same condenser method was used for the evaporators by substituting Eq. (3.7) into Eq. (3.22) and multiplying by a compressor on time (T_{on}) cycle, Eq. (3.24) was developed and used to calculate the required mass of PCM as follows:

$$M = \frac{Q_L \times T_{on}}{h_f} \quad (3.24)$$

However, the mass of PCM was determined for the fridge cabinet by substituting Eq. (3.8) into Eq. (3.22). Then, multiplying it by a compressor off time (T_{off}) cycle, Eq. (3.25) was developed as follows:

$$M = \frac{Q_c \times T_{off}}{h_f} \quad (3.25)$$

In the abovementioned correlations (Q_H , Q_L , and Q_c) should be in kilowatts to estimate masses in kilograms. Additionally, (T_{on}) and (T_{off}) times should be expressed in seconds.

3.3.9. Percentage of Improvement

The improvement percentage was calculated using the following correlation:

$$\text{Percentage improvement (\%)} = \frac{\text{New value} - \text{Original value}}{\text{Original value}} \times 100 \quad (3.26)$$

CHAPTER 4

EXPERIMENTAL WORK

4.1. Introduction

In this chapter, the experimental works are performed and thoroughly described. Initially, it covered the installation of data loggers for energy, pressure, and temperature. Then, the employment, positioning, and distribution of temperature sensors on the system's components are emphasized. Finally, the PCM selection, PCM preparation, PCM nanoparticle inclusion, experimental procedures for installing PCMs, experiments, data acquisition, and uncertainty analysis are explained.

4.2. Energy Data Logger

A Zhurui power recorder (PR10), purchased from Shenzhen Zhurui technology company, was utilized for recording energy consumption. Its specification was listed in Table 4.1. It had an easy setup form, as shown in Figure 4.1. The refrigerator wire plug was directly plugged into the PR10's socket. It measured the voltage, current, power, power factor, and frequency. It also measured accumulated electricity consumption, electricity bills, and electricity time of a variety of electrical appliances. It was daily recorded as a chart or list form. According to the company's PR10 description, it was suitable for measuring, screening, and recording power usage in household appliances. The calibration was done against a high accuracy Universal digital multimeter (UNI-T UT89X), and the results are in Appendix A.



Figure 4.1. Zhurui power recorder (PR10) and its setup.

Table 4.1 Specifications of Zhurui (PR10) power recorder.

Parameters	Specifications
Accuracy	$\pm 0.5\%$ FS
Rated voltage	85 - 265 VAC
Rated power	≤ 2.5 Watt
Current range	0.005 - 15 A
Power range	0.1 - 3750 Watt
Energy range	0 - 999999 kWh
Bill range	0 - 999999
Time range	0 - 999 days
Power factor range	0 - 1
Outline size	125×79×39 mm

4.3. Pressure Gauge Data Recorder

Recording the compressor's pressures were performed by Elitech PGW-500 wireless digital pressure gauge and analog Hongsen pressure gauges, as depicted in Figure 4.2. They were acquired from Elitech technology company and Zhejiang Hongsen machinery company. The PGW-500 and Hongsen gauges specifications are presented in Table 4.2. The PGW-500 calibration results against Hongsen pressure gauges are presented in Appendix B. The PGW-500 was programmed to

record pressure every 30 seconds. It was used and swapped with the Hongsen pressure gauges on the suction and discharge lines of the compressor during the 48 hours of each experiment, which can be seen in Figure 4.3.



Figure 4.2. The Elitech PGW-500 and Hongsen gauges.

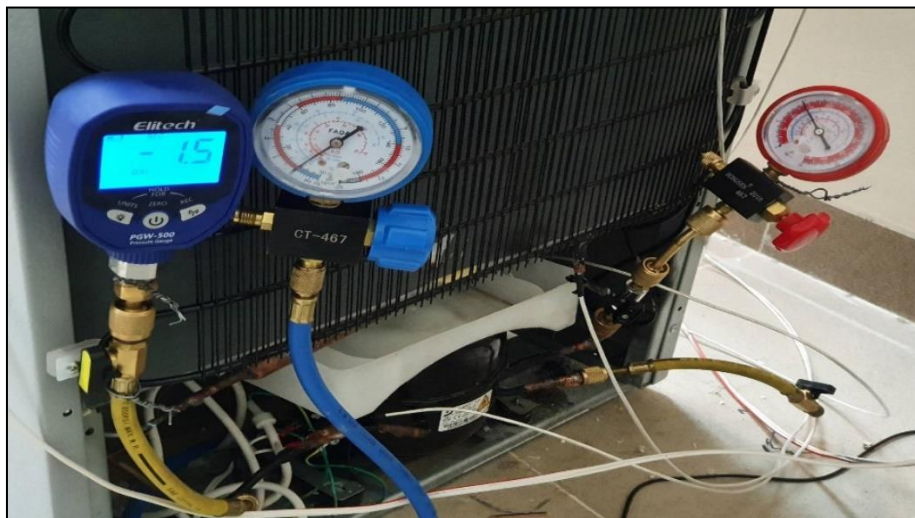


Figure 4.3. Set up of Elitech PGW-500 and Hongsen pressure gauges.

Table 4.2 The specifications of the Elitech PGW-500 and the Hongsen gauges.

Specification	Elitech PGW-500	Hongsen	
		Low side	High side
Accuracy	$\pm 0.5\%$ FS	$\pm 1\%$ FS	$\pm 1\%$ FS
Refrigerant	87 types	4 types	4 types
Units	psi, cmHg, inHg, bar, kPa, MPa, kg/cm ²	psi, kg/cm ²	psi, kg/cm ²
Range	-14.5–500 psi	-30 – 250 psi	0 – 500 psi
Offline records	9943 readings	-	-

4.4. Temperature Sensors and Data Logger

For measuring and recording temperatures, high-quality resistance temperature detector (RTD PT100) sensors and a 16-channel temperature data logger (KCM-LCD16) were ordered from Yuyao Kingcreate Instruments Company, as demonstrated in Figure 4.4. Their specifications are provided in Table 4.3. The sensors were calibrated using a J-type thermocouple, and the calibration data are given in Appendix C. The data logger recorded data each second through a memory card.

Table 4.3 Specification of temperature sensors and temperature data logger.

Temperature sensors		Temperature data logger	
Parameters	Specifications	Parameters	Specifications
Name	RTD	Brand name	Kingcreate
Type	PT 100	Model number	KCM-LCD162WDATA
Accuracy	$\pm 0.5\%$	Measured input	Thermocouple & RTD
Temperature range	-200 – 250 °C	Record storage	Micro memory SD card
Probe diameter	4 mm	Record interval	1 second – 1 hour
Probe length	30 mm	Accuracy	$\pm 0.5\%$
Probe material	Stainless steel	Channel	16
Cable length	2000 mm	Display range	-1999 - 1999

4.5. Implementation and Positioning of Temperature Sensors

In this section, the implementation and location of temperature sensors on the refrigerator's components are demonstrated and described. As shown in Figure

4.5, fifteen sensors were mounted on the components to detect their temperatures. The location of the sensors is displayed in Table 4.4. The mechanism of implementing sensors on each component is explained in the following subsections.

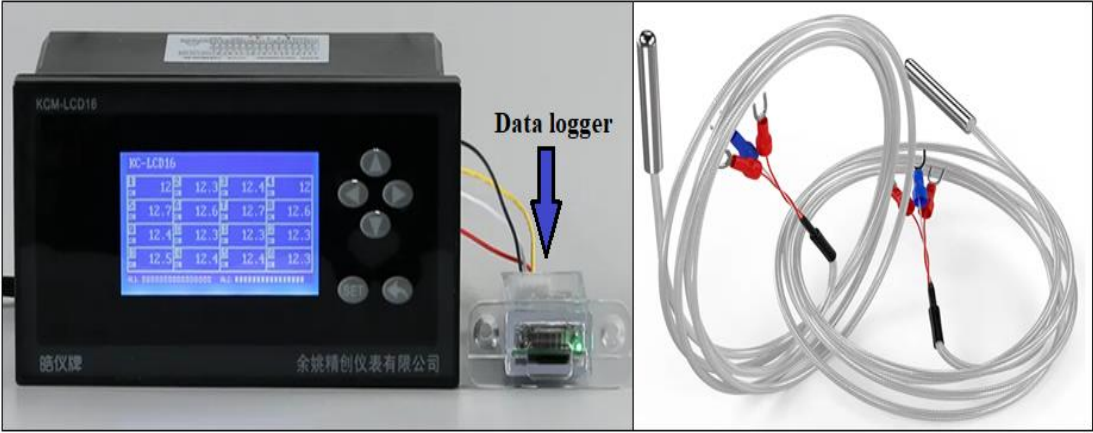


Figure 4.4. Temperature sensor and data logger.

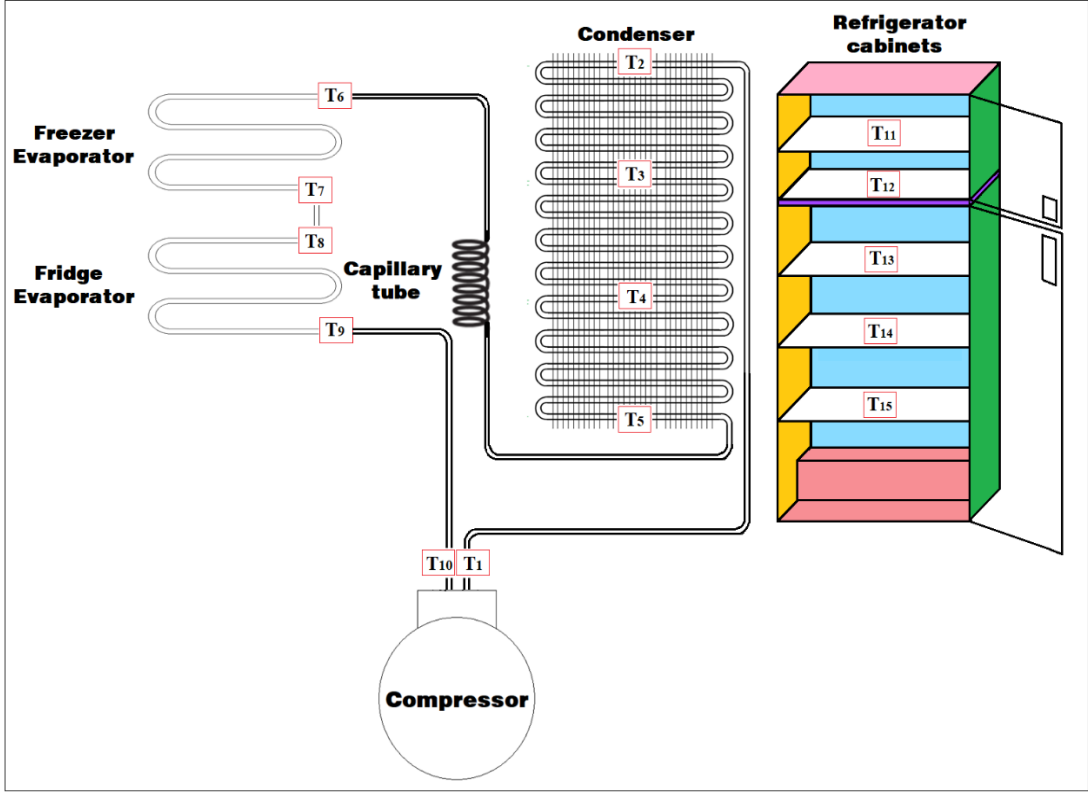


Figure 4.5. Location of temperature sensors.

Table 4.4 Location of temperature sensors.

Name	Location
T ₁	Discharge of compressor
T ₂	Top of condenser
T ₃	Middle one of condenser
T ₄	Middle two of condenser
T ₅	Bottom of condenser
T ₆	Inlet of evaporator (freezer)
T ₇	Outlet of evaporator (freezer)
T ₈	Inlet of evaporator (fridge)
T ₉	Outlet of evaporator (fridge)
T ₁₀	Suction of compressor
T ₁₁	Top compartment freezer cabinet
T ₁₂	Bottom compartment freezer cabinet
T ₁₃	Top compartment fridge cabinet
T ₁₄	Middle compartment fridge cabinet
T ₁₅	Bottom compartment fridge cabinet
T ₁₆	Room (ambient)

4.5.1. Sensor Installation on the Condenser

Four temperature sensors (T₂, T₃, T₄, and T₅) were placed on the condenser surface tubes, as displayed in Figure 4.6. The procedure and technique of implementing sensors on the condenser are seen in Figure 4.7. The process was commenced by preparing a copper tube. It had the same length as the sensor probe. Also, the inside diameter of the copper tube was matched to the diameter of the sensor probe to make sure the copper tube and the sensor were in good thermal contact. Next, the copper tube's end was wrapped around the condenser tube and welded in the wrapping area. Then, the welding area and copper tube were painted to match the condenser tubes in color. Finally, the probe sensor was inserted into the copper tube.

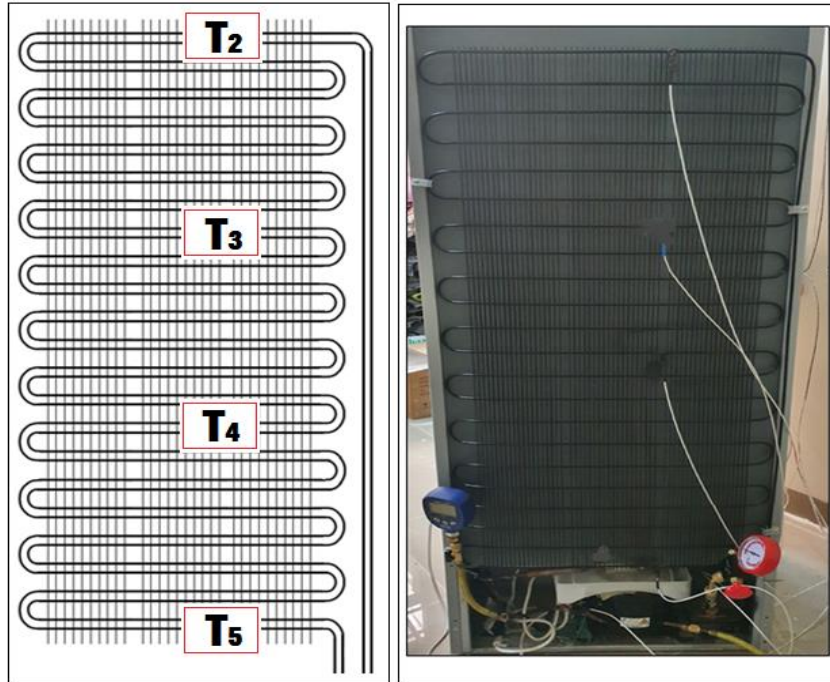


Figure 4.6. Location of temperature sensors on condenser.

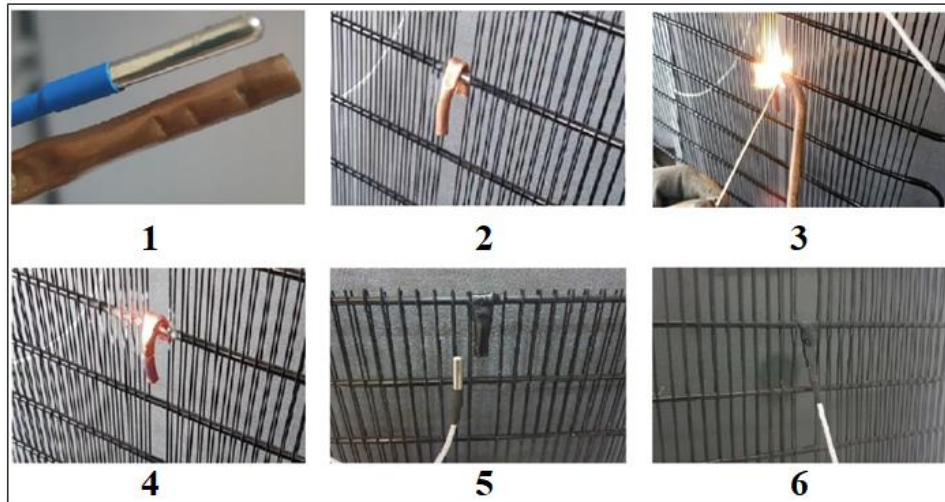


Figure 4.7. The installation processes of temperature sensors on the condenser.

4.5.2. Sensor Installation on the Compressor

An increase or decrease in compressor temperatures can affect the compressor's lifespan and efficiency. Accordingly, to evaluate PCM's impact on compressor temperatures, two sensors were mounted on the compressor's suction

and discharge surface tubes, as displayed in Figure 4.8. The sensors' setup method was comparable to that of the condenser.

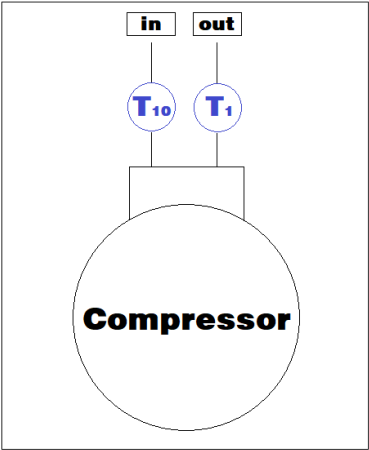


Figure 4.8. Location of temperature sensors on compressor.

4.5.3. Sensor Installation on the Evaporator

As described in the previous chapter, the refrigerator consisted of two cabinets, each with an evaporator. The evaporators were connected in a series. Thus, four temperature sensors were attached to the surfaces of the tubes at the inlet and exit of each evaporator. The sensors were implemented using the same concept and technique as in the condenser. The location and configuration of temperature sensors are depicted in Figure 4.9.

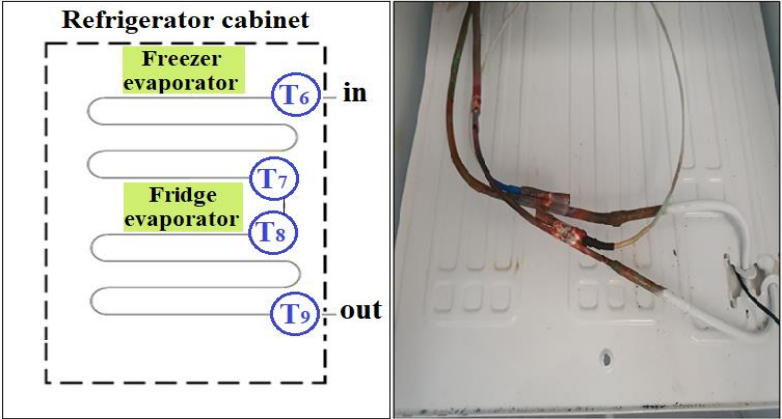


Figure 4.9. Location and arrangement of temperature sensors on evaporators.

4.5.4. Sensor Installation in the Cabinets

As shown in Figure 4.10, five temperature sensors were embedded in the middle of each tray in the cabinets to measure the average temperatures. Two sensors were in the freezer and three in the fridge. A cone-shaped piece of plastic was used and cut at the sharp end to support the sensors. A small area of the sensor probe was inserted into the hollow cutting area. The cutting area had the same diameter as the sensor probe to completely capture the sensor. Lastly, the plastic cone was put on the cabinet tray with silicon, as can be seen in Figure 4.11.

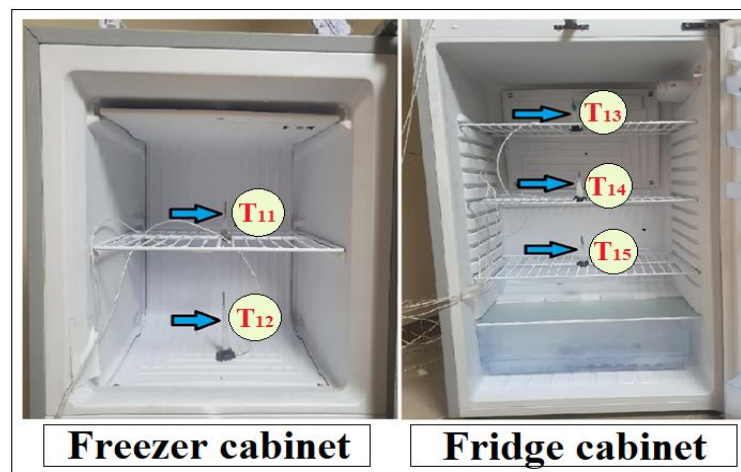


Figure 4.10. Location of temperature sensors in the cabinets.

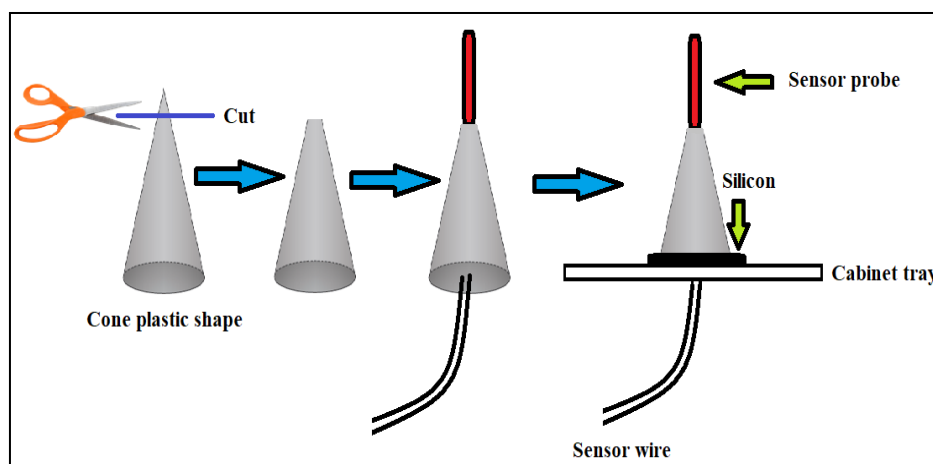


Figure 4.11. Steps of preparing and installing sensors in the cabinets.

4.6. Selection of PCMs

Although PCMs had low thermal conductivity, they were effective in improving the overall heat transfer requirements of a condenser or an evaporator using air as the exterior fluid and natural convection as the heat transfer method. The potential of PCMs to store energy is based on their latent heat of fusion. Therefore, any changes in it will cause the phase change temperature of PCMs to change. So, for refrigerators, the thermal and chemical composition of PCMs should not undergo any changes in their melting and solidification phases because it acts on their latent heat and phase change point. Hence, the two most important properties of the PCM were the phase change temperature and the latent heat of fusion (Azzouz et al., 2005).

Thereby, to choose an effective PCM for a specific application, the melting point of the PCM must be taken into account. Accordingly, PCMs have been selected mainly based on their phase change temperature. In addition, it was crucial to account for a temperature difference of 5°C to 10°C between the PCM phase change temperature and the maximum working temperature of the application. Furthermore, the temperature interval of 5°C to 10°C of PCMs in the melting to solidification and vice versa should be considered to overcome the supercooling problem of PCMs, particularly salt hydrate inorganic PCMs (Lane and Lane, 1983). The phenomenon of supercooling describes the situation in which a liquid does not solidify or crystallize despite being cooled below its freezing point (Hu et al., 2017).

In this study, the proper PCMs have been selected using the data collected from the temperature sensors mounted on the refrigerator's components. At first, to choose PCMs for the condenser, four sensors were attached to the condenser, as seen in Figure 4.12. Thereafter, the condenser area was divided into four

sections based on the temperatures measured by the sensors from T_1 - T_5 , as shown in Figure 4.12. The line between the condenser and the compressor was considered a condenser section because it contributed to the condenser cooling. Next, based on the aforementioned suggestion by (Lane and Lane, 1983), the PCMs for the condenser parts have been selected.

However, for evaporators, (Berdja et al., 2020) recommended selecting PCMs with phase change temperatures between the maximum and minimum surface temperatures of the evaporator for charging the PCM. Thus, four temperature sensors were installed on the inlet and outlet tubes of the freezer and fridge evaporators to determine suitable PCMs, as seen in Figure 4.9. Alongside this, the phase change temperature of the selected PCM must be lower than or between the maximum and minimum temperatures of the cabinet to support the cabinet's temperature. Additionally, the solution proposed by (Lane and Lane, 1983) to solve the subcooling problem has been considered. Moreover, the PCM was selected for the fridge cabinet in which they melted and solidified between the maximum and minimum temperatures of the cabinet. The selected PCMs and their properties are tabulated in Table 4.5.

The PCMs were purchased from Rubitherm, Germany, except for distilled water. The DSC graphs between latent heat of fusion and temperature of RT44HC, RT35HC, RT28HC, RT4, SP-7, and SP-17 are provided in Appendices D, E, F, G, H, and I. The RT44HC, RT35HC, RT28HC, and RT4 are organic paraffin PCMs. However, SP-17 and SP-7 are mixture of inorganic hydrate salts (ammonium chloride + potassium hydrogen carbonate + distilled water) and (sodium carbonate + potassium hydrogen carbonate + distilled water), respectively. The application of each PCM in each experiment for the evaporators, fridge cabinet, and each condenser part is explained in detail in the section 4.11.

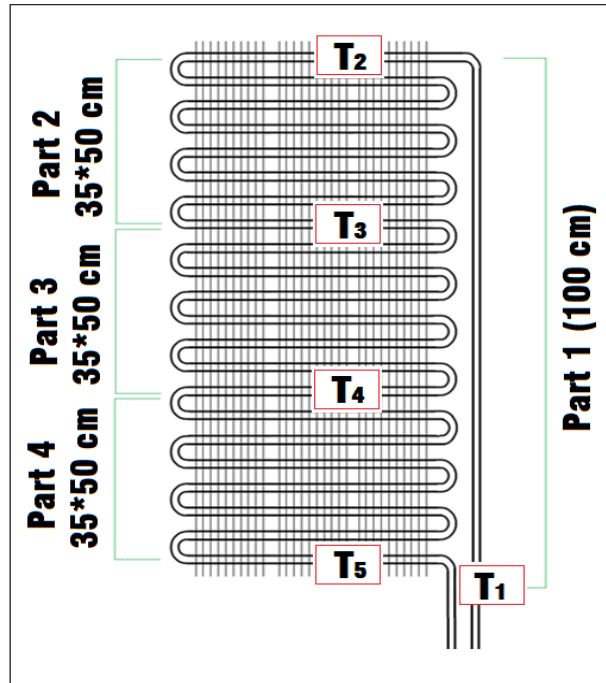


Figure 4.12. The parts of the condenser.

Table 4.5. Specifications of selected PCMs.

Name	Type of PCM	h_f	Cp	ρ_{solid}	ρ_{liquid}	k	T _{ph}	T _{interval.ph.}
RT44HC	Organic	250±7.5%	2	800	700	0.2	44	41 to 44
RT35HC	Organic	240±7.5%	2	880	770	0.2	35	34 to 36
RT28HC	Organic	250±7.5%	2	880	770	0.2	28	27 to 29
RT4	Organic	175±7.5%	2	870	770	0.2	4	2 to 4
SP-17	Inorganic	300±7.5%	2	1200	1100	0.6	-17	-17 to -22
SP-7	Inorganic	290±7.5%	2	1125	1115	0.6	-7	-6 to -8
Water	Distilled water	330±7.5%	4.186	920	1000	0.6	0	0

4.7. Required Mass of PCMs

Determining the proper mass for PCMs was a crucial challenge, as their excess or insufficiency can impact the refrigerator's performance. The masses are determined using the correlations from the previous chapters. Based on Eq. (3.23), the minimum mass required was about 0.813 kg for the condenser if each RT44HC, RT35HC, or RT28HC was utilized. Nevertheless, utilizing this mass will have a minimal influence on the refrigerator's energy consumption and

functionality because the compressor's off-cycle time was shorter than the time required to solidify the PCM. This was based on a study by (Gao et al., 2020) that used paraffin as a PCM to determine its melting and solidification times. As a result, the total solidification time was longer than the total melting time. The longer solidification phase was due to the fact that it included two main heat transfer steps. At the commence of solidification, the PCM was a liquid. The primary mechanism of heat transfer was free convection, and the level of PCM solidification was optimum during this stage. Once the solidification cycle proceeded, the amount of solid PCM rose, the natural convection method slowed, and heat conduction became the primary method of heat transfer. Since free convection was no longer the primary heat transfer method, the solidification process slowed down because organic PCMs exhibit low thermal conductivity. Hence, excess PCM mass was necessary for keeping a sufficient quantity of PCM in the solid state during the compressor's on-cycle time. The quantity of additional PCM mass should not exceed twice the calculated amount because (Gao et al., 2020) found that the solidification time of paraffin was about 2-3 times larger than the melting time. Accordingly, 1.5kg of PCM have been applied to the condenser.

Nevertheless, the estimated masses for freezer and fridge evaporators were 0.439kg and 0.037kg, respectively, according to the Eq. (3.24). Similarly to the condenser, these masses, if employed, will have a minimal effect on the overall performance of the refrigerator. Thus, extra mass is needed. However, the amount of PCM employed should not raise the freezer and fridge cabinet temperatures above the standards. As in this study, the freezer and fridge cabinets should not exceed -18°C and 5°C , respectively, according to ISO standards (ISO 15502:2005). Besides this, the maximum PCM mass deployed for the freezer and fridge evaporators was 0.8kg and 0.8kg, respectively.

The primary criterion for installing PCMs in cabinets is that they do not reduce the cabinet volume significantly. Therefore, only the PCM was installed in the fridge cabinet due to the limited space in the freezer cabinet. The first step in computing the PCM mass of the fridge cabinet was finding the overall heat transfer coefficient for each wall and door, as represented in Figure 4.13. The procedure for finding the overall heat transfer coefficient includes the steps described below. At first, the interior and exterior surface temperatures of the walls and door of the fridge cabinet are assumed. In addition, using Eq. (3.12), the mean temperature has been calculated to obtain the Prandtl number and Kinematic viscosity of air at 1 atmospheric pressure. Further, in Eq. (3.13), the Rayleigh number is calculated. The thermal expansion coefficient and characteristic length are calculated using Eqs. (3.14) and (3.15). Furthermore, the Nusselt number was found by applying Eqs. (3.18) and (3.19) for vertical and horizontal walls, respectively. Moreover, through the empirical correlation of the heat transfer coefficient in Eq. (3.20), its value has been determined and inserted in Eq. (3.11) to compute the total thermal resistance. Lastly, the total heat transfer coefficient is calculated using Eq. (3.9).

Later, depending on Eq. (3.8), the heat transfer gain to the fridge cabinet through the walls, door, and gasket is estimated, as reported in Table 4.6. Afterward, the total heat gain is inserted into Eq. (3.25), and the minimum mass required is 0.175 kg. However, this mass is the minimum needed for regulating temperature fluctuations within the cabinet. Hence, the additional mass could reduce temperature fluctuations significantly. As such, 1kg was applied in this study. A sample of calculations for the condenser and evaporator are presented in Appendices J and K, respectively.

Table 4.6. Overall heat transfer gain of fridge cabinet.

Component	U (W/m ² .°C)	A (m ²)	T _a . (°C)	T _{int} . (°C)	ΔT (°C)	Q _c (Watt)
Right wall	0.430	0.541	25	1.10	23.90	5.553
Left wall	0.430	0.541	25	1.10	23.90	5.553
Back wall	0.428	0.621	38	1.10	36.90	9.799
Top wall	0.936	0.254	-22	1.10	-23.10	-5.490
Bottom wall	0.677	0.254	37	1.10	35.90	6.168
Door	0.303	0.621	25	1.10	23.90	4.500
Gasket	9.073	0.034	25	1.10	23.90	7.330
Total heat gain						33.411

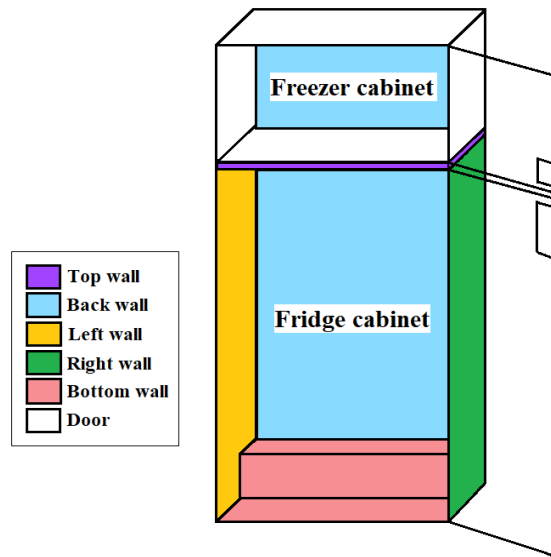


Figure 4.13. Cabinets of refrigerator.

4.8. Preparation of PCMs

This section addresses the preparation process of PCMs for use in the condenser, evaporator, and cabinets.

4.8.1. Preparation of PCM for the Fridge Cabinet

The PCM was encapsulated in an aluminum panel of the same size as the cabinet trays. A Rubitherm company-manufactured aluminum panel had a

dimension of (450*30*10 mm) and was filled with 0.333 kg of organic RT4 PCM used for the fridge cabinet, as viewed in Figure 4.14.

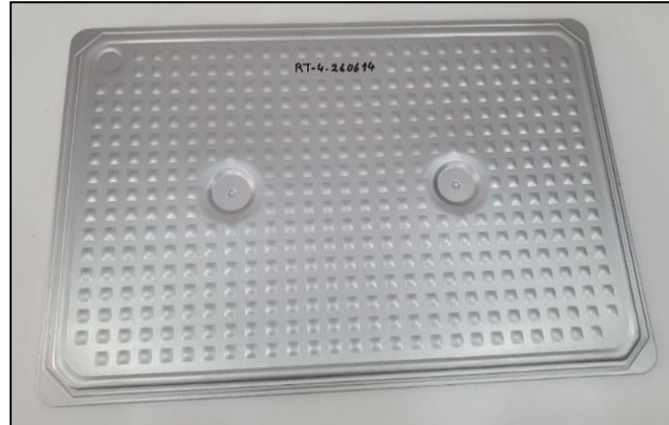


Figure 4.14. Rubitherm-manufactured aluminum PCM panel.

4.8.2. Preparation of PCM for the Evaporator

As seen in Figure 4.15, PCMs were encapsulated in aluminum pouches. The dimensions of the aluminum pouches mirrored the dimensions of the evaporator faces. The thickness of the pouches was 1 mm. The pouches are ordered from Rubitherm. The purpose of using aluminum pouches was to achieve good thermal contact with the evaporators.



Figure 4.15. Rubitherm-manufactured aluminum pouches.

4.8.3. Preparation of PCM for the Condenser

For the condenser, PCMs were encased in copper tubes. The thirty copper tubes were fabricated for condenser parts 2 and 3, as indicated in Figure 4.16. For each part, 15 tubes with a 30 cm length, 1.6 cm diameter, and 0.2 cm thickness, each carrying 0.045kg of PCM, were manufactured. Whereas, for condenser part 1, a copper tube with a length of 95 cm, a diameter of 1.6 cm, and a thickness of 0.2 cm that can hold 0.150 kg of PCM was created using the same technique as in Figure 4.16. The goal of employing copper tubing was to achieve proper thermal contact with the condenser tubes.

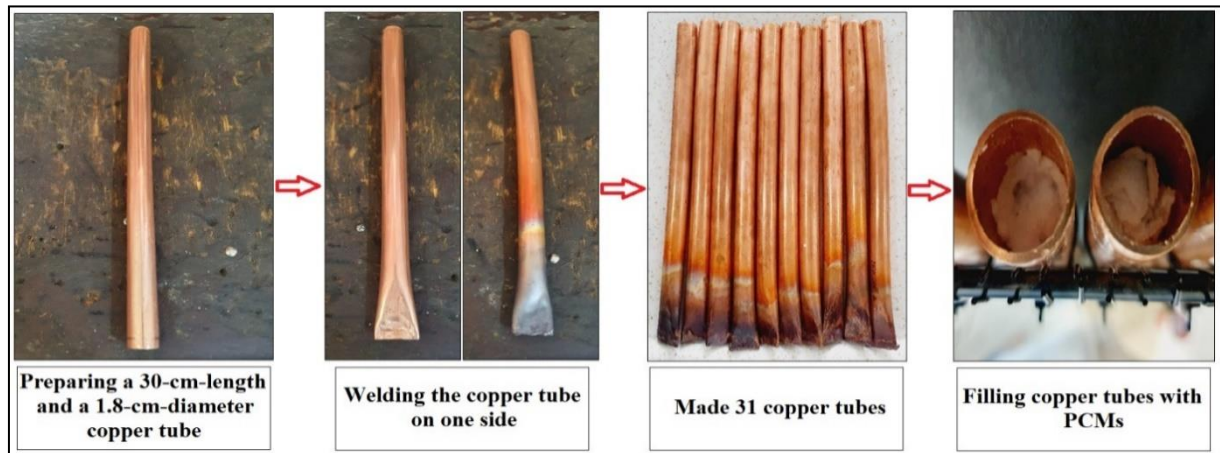


Figure 4.16. Copper tube fabrication process.

4.9. PCM Nanoparticle Inclusion

PCMs, especially organics, exhibit weak thermal conductivity. Hence, several studies improved the thermal conductivity of PCMs by adding metal oxide nanoparticles (Arshad et al., 2020), metal nanoparticles (Kumar et al., 2020), and expanding graphite (Cheng et al., 2010) into them. So, in this study, copper oxide (CuO) nanoparticles were added to the RT35HC PCM. The addition of nanoparticles was accomplished using the same technique and procedure as (Arshad et al., 2020) experimentally added CuO nanoparticles to RT35HC. This

study also utilized the same nanoparticle percentage, type, and specifications used by (Arshad et al., 2020).

The nanoparticle inclusion procedure was practiced firstly by melting RT35HC in a hot water bath at a constant temperature of 70 °C. Then, sodium dodecylbenzene sulfonate (SDBS) was incorporated as a surfactant into RT35HC at a weight percentage ratio of 4:1 of the nanoparticles to improve the dispersion stability. SDBS is a high-concentration anionic surfactant with dispersing, detergency, foaming, emulsification, and moistening capabilities. It was acknowledged as a nontoxic chemical. The properties of CuO and SDBS are presented in Table 4.7, which they purchased from Baoji GuoKang Bio-Technology company. Thereafter, for 30 minutes at 70°C, RT35HC and SDBS were stirred continuously at 450 rpm.

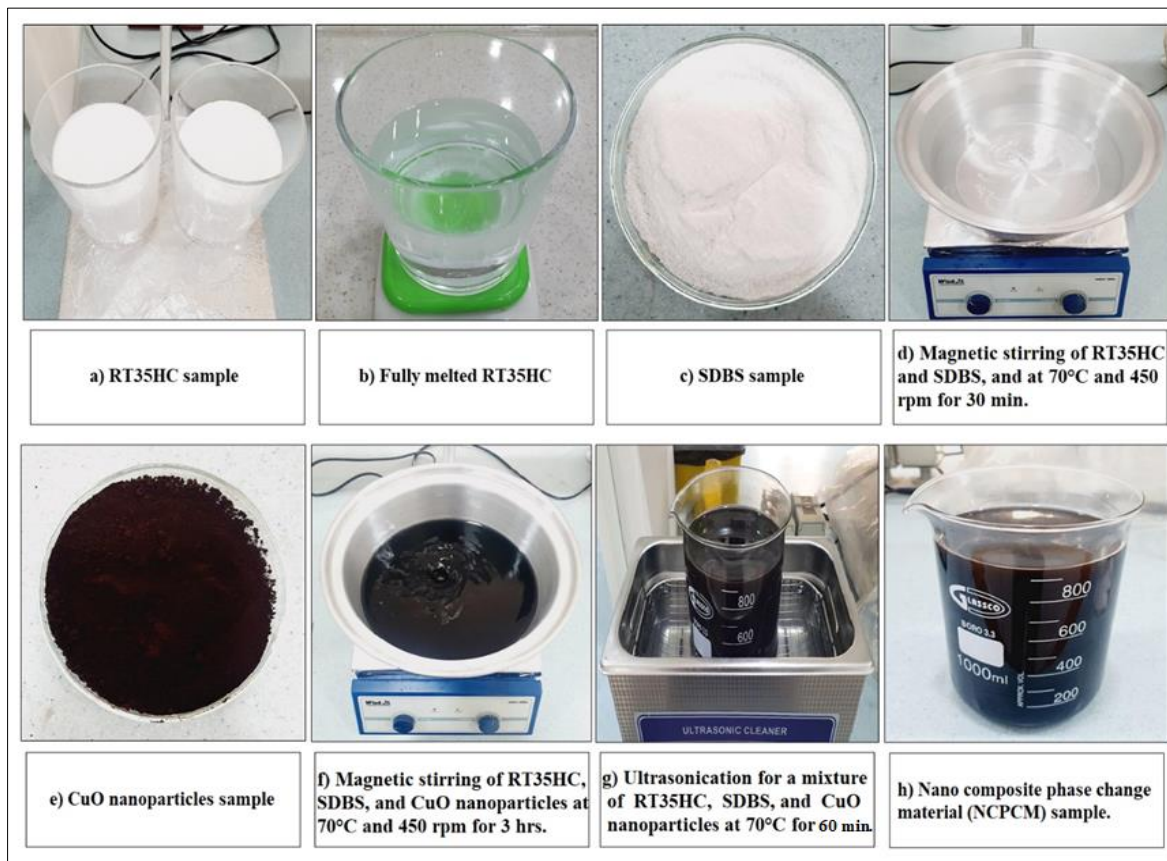


Figure 4.17. PCM Nanoparticle inclusion procedures.

Later, 1.0 wt.% CuO nanoparticles were introduced to RT35HC and stirred for an additional 3 hours to establish a stable and homogeneous nanoparticle dispersion. Further, a mixture of RT35HC and CuO nanoparticles was subjected to an ultrasonication procedure at 40 kHz for 60 minutes to disperse nanoparticles more effectively and reduce agglomeration and sedimentation. Eventually, the PCM nanoparticle inclusion sample was cooled to room temperature and named nanocomposite phase change material (NCPCM). The processes of producing NCPCM are viewed in Figure 4.17. The results of the nanoparticle addition on PCM's properties reported by (Arshad et al., 2020) are listed in Table 4.8. Nanoparticle dispersion in RT35HC did not change the chemical structure of RT35HC. Additionally, the percentage increase in thermal conductivity was 55 and 38 for solid and liquid phases, respectively.

Table 4.7 Properties of CuO nanoparticles and SDBS.

CuO		SDBS	
Property	Value	Property	Value
Particle size	40 nm	Chemical name	SDBS
Surface area	29 m ² /g	Molecular formula	C ₁₈ H ₂₉ NaO ₃ S
Density	3.9 g/mL	Color	White
Form	Nano powder	Form	Powder
Purity	99.5 %	Purity	98 %
Particle shape	Spherical	Stability	Stable
Molecular weight	79.55 g/mol	Molecular weight	348.48 g/mol

Table 4.8. Thermophysical experimental properties of RT35HC and NCPCM.

Properties	RT35HC	NCPCM
Melting temperature (°C)	34.06 - 36.06	34.70 - 36.44
Solidification temperature (°C)	31.47 - 31.71	31.13 - 31.71
Specific heat (liquid) (J/g. °C)	1.77	2.13
Specific heat (solid) (J/g. °C)	1.88	2.32
Thermal conductivity (liquid) (W/m. K)	0.34	0.469
Thermal conductivity (solid) (W/m. K)	0.214	0.331
Latent heat of fusion (melting) (kJ/kg)	250.88	233.91
Latent heat of fusion (solidification) (kJ/kg)	260.79	235.42

4.10. Experimental Procedures

In this section, implementation forms of PCMs on the condenser, evaporator, and inside the cabinets are explained as follows.

4.10.1. PCM Implementation in the Fridge Cabinet

Aluminum PCM panels were inserted into the locations of trays within the cabinet. The PCM-containing aluminum panels were positioned horizontally, as explained in Figure 4.18. Even though (Pavithran et al., 2021) shown that the combination of horizontal and vertical positioning yields superior results, the restricted volume posed a challenge.



Figure 4.18. The position of aluminum PCM panels in the fridge cabinet.

4.10.2. PCM Implementation on the Evaporator (Freezer)

The plate-and-tube evaporator inside the freezer cabinet had three sides, which can be seen in Figure 4.19. The experimental tests were accomplished by applying PCM on these three non-functional faces in a separate case, as presented in Figure 4.19. PCMs were encapsulated in aluminum pouches and attached to the

faces to provide good thermal contact. The dimension of the aluminum pouches was 35 by 30 mm. The dimension was the same for all aluminum bags that contain different PCMs. However, the mass of the PCMs within the pouches varied depending on the experiments.

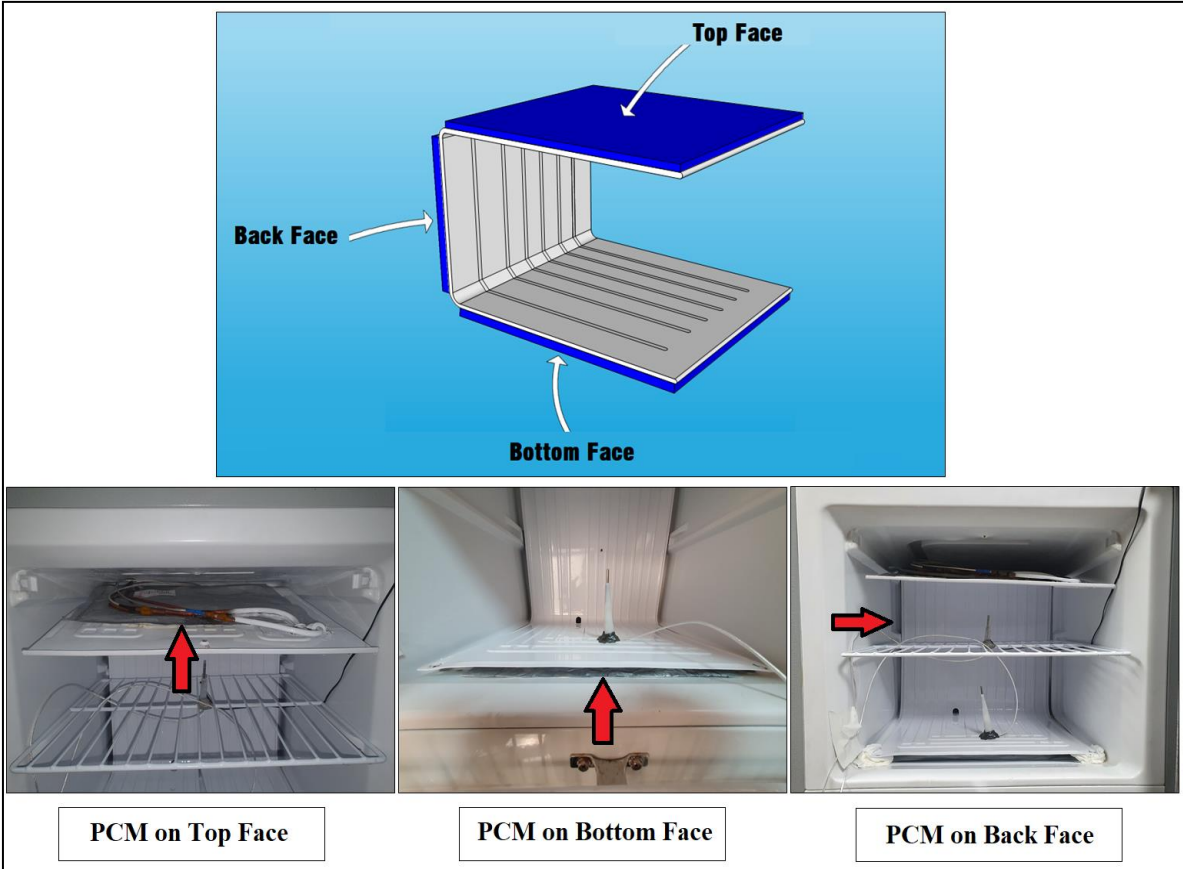


Figure 4.19. PCM configuration on the evaporator (Freezer).

4.10.3. PCM Implementation on the Evaporator (Fridge)

A plate and tube evaporator within the fridge cabinet was rectangular with only one face, as shown in Figure 4.20. According to Figure 4.20, the PCMs were mounted on the non-operational top and bottom parts of the backside. PCM implementation was the same as achieved in the evaporator (freezer). However, the PCMs differed in mass.

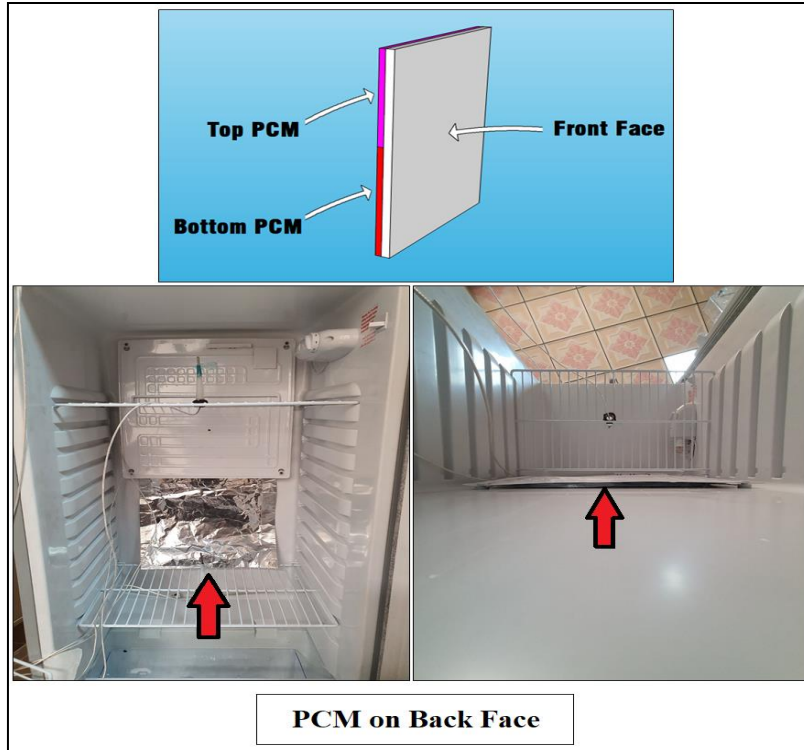


Figure 4.20. PCM setup on the evaporator (Fridge).

4.10.4. PCM Implementation on the Condenser

A wire and tube condenser was divided into four parts. As a part, the distance between any two temperature sensors was specified, as described in Figure 4.21. This partition aimed to select a suitable PCM and its phase change temperature. Therefore, depending on these partitions, the commercial organic paraffins (RT44HC, RT35HC, and RT28) were chosen. The copper tubes containing PCMs were attached to the condenser tubes in parts 2 and 3, as given in Figure 4.21. Their location was between the refrigerator's back wall and the rear surface of the condenser tubes. While, for condenser part 1, it connected with the condenser tube. The area of thermal contact between the PCM tubes and condenser tubes was small. However, this was done to minimize the amount of heat absorbed by the PCMs, which is passed to the condenser tubes and then to the refrigerant

during the compressor off-cycle period. This phenomenon has been confirmed in the studies that applied PCMs to the condenser, which reduced the refrigerator's overall functionality.

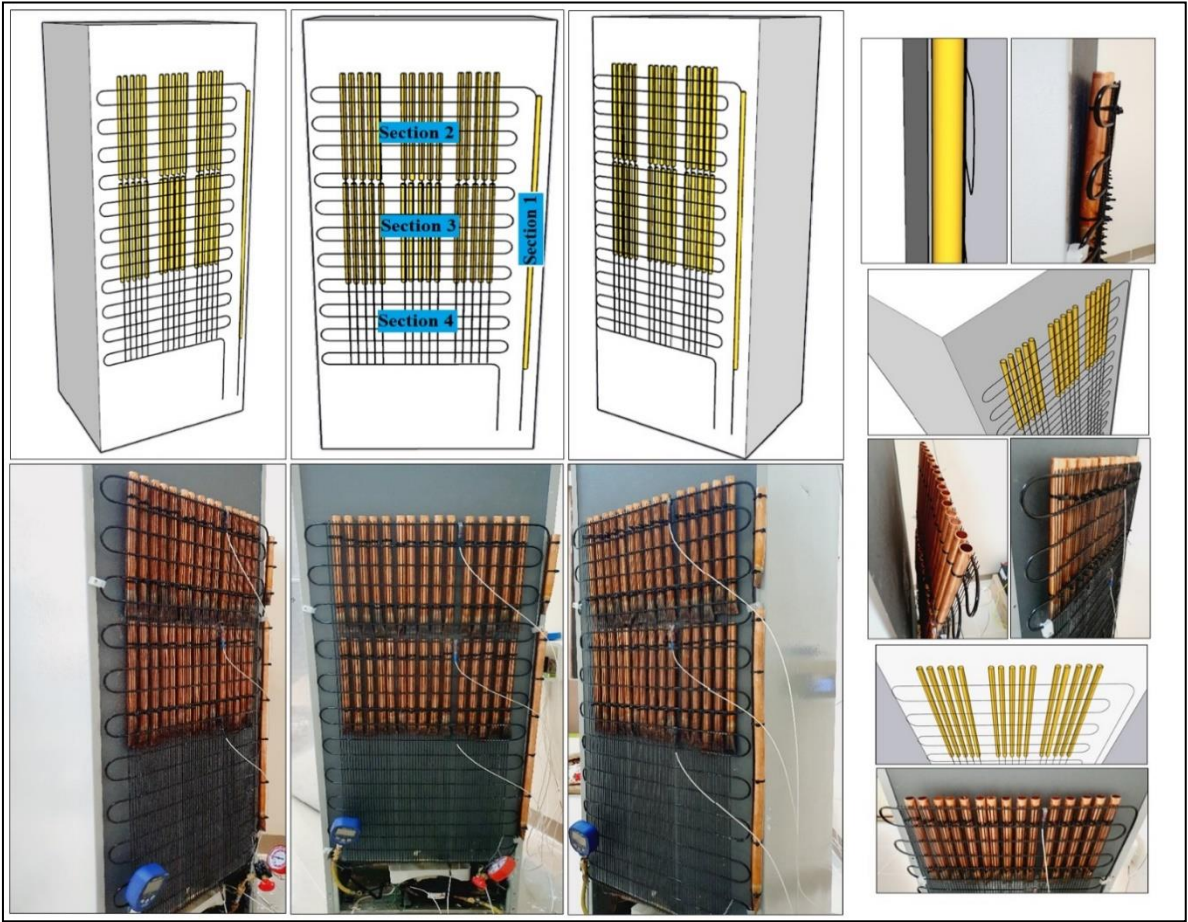


Figure 4.21. Copper tube arrangement on the condenser sections.

4.11. Experiments

In this section, the type and amount of PCMs used in each experiment including PCMs are thoroughly explained. The ISO guidelines (ISO 15502:2005) for testing the energy consumption of household refrigerators were followed in the experiments. The ISO standards proposed testing a refrigerator with empty cabinets and closed doors in an environment with a temperature of $25 \pm 0.5^\circ\text{C}$ and a relative humidity between 45% and 55%. Additionally, the freezer and fridge

cabinets should be kept at temperatures below -18°C and 5°C , respectively. Accordingly, a split air conditioner and humidifier were used to maintain the test room's temperature at $25 \pm 0.5^{\circ}\text{C}$ and the relative humidity between 45% and 55%. Initially, the first experiment was conducted on a household refrigerator without a PCM. The name and label of this experiment were household refrigerator (HR). The measured temperatures for this test are displayed in Table 4.9. Thereafter, the experiments with PCMs have been conducted as described below.

Table 4.9. The observed temperatures for the first experiment (HR).

Name	Measured value ($^{\circ}\text{C}$)		Location
	On cycle	Off cycle	
T ₁	73.49	33.01	Discharge of compressor
T ₂	48.96	28.51	Top of condenser
T ₃	48.08	26.94	Middle one of condenser
T ₄	43.48	24.92	Middle two of condenser
T ₅	27.70	24.68	Bottom of condenser
T ₆	-30.77	-5.65	Inlet of evaporator (freezer)
T ₇	-30.76	-14.33	Outlet of evaporator (freezer)
T ₈	-29.44	-1.39	Inlet of evaporator (fridge)
T ₉	-15.17	-0.92	Outlet of evaporator (fridge)
T ₁₀	20.64	30.65	Suction of compressor
T ₁₁	-22.03	-18.32	Top compartment freezer cabinet
T ₁₂	-25.01	-19.62	Bottom compartment freezer cabinet
T ₁₃	0.48	2.46	Top compartment fridge cabinet
T ₁₄	0.34	1.38	Middle compartment fridge cabinet
T ₁₅	0.16	1.76	Bottom compartment fridge cabinet
T ₁₆	25 ± 0.5	25 ± 0.5	Room (ambient)

4.11.1. Application of PCM in Condenser

On the condenser side, three experiments were considered, as listed in Table 4.10. The experiments are named condenser heat storage (CHS) and linked with an experiment number. The average temperature of each section was decisive in the choice of PCM for it. Thus, for section 1, the maximum average temperature between sensors T₁ and T₂, which was 61.23°C , was taken into account.

Additionally, the maximum average temperature between sensors T_2 and T_3 was 48.52°C for section 2. Furthermore, the maximum temperature between sensors T_3 and T_4 in section 3 averaged 45.78°C . Section 4 was not coated with PCM in any experiment since its average maximum temperature (35.59°C) was close to the ambient temperature.

For section 1, RT44HC was implemented in all three cases because this section provided a higher temperature. The difference between the PCM melting temperature and the room temperature was higher than the discrepancy between the PCM melting temperature and the maximum average section temperature, allowing the PCM to solidify significantly. Consequently, sections 2 and 3 represented the difference between experiments.

In CHS-1, NCPCM and RT35HC were adopted for parts 2 and 3, respectively. The difference between the melting point of the PCMs used in this case and the maximum average part temperature and the room temperature was about more than 10°C . Nonetheless, the difference between CHS-1 and CHS-2 was in the PCMs for sections 2 and 3. The RT35HC and RT28HC were installed in sections 2 and 3, respectively. In section 3, the gap between the PCM phase change point and the room temperature was about 5°C . Triple PCMs were applied in both of the abovementioned experiments. Nevertheless, CHS-3 included double PCMs. Parts 1 and 2 had RT44HC, whereas part 3 had RT35HC. The maximum average temperature of section 2 was around 5°C higher than the PCM phase change temperature.

Table 4.10. Experiments on the condenser.

Experiments	Name	Section-1	Section-2	Section-3	Section-4
Experiment 1	CHS-1	RT44HC	NCPCM	RT35HC	-
Experiment 2	CHS-2	RT44HC	RT35HC	RT28HC	-
Experiment 3	CHS-3	RT44HC	RT44HC	RT35HC	-

4.11.2. Application of PCM in Evaporator

On the evaporator side, three experiments have been conducted, as given in Table 4.11. The experiments are termed evaporator cold storage (ECS) and assigned a number. In all cases, the same amount of PCM was utilized to compare the efficiency of PCMs in improving the refrigerator's overall performance. For both evaporators in the ECS-1, a single PCM has been used. According to Table 4.9, the average inlet and outlet temperatures of the freezer evaporator during the off and on cycles were between -9.99°C and -30.77°C , respectively. Also, the freezer cabinet fluctuated between -18.97°C and -23.52°C . Thus, SP-17 was chosen, as its interval phase change temperature ranges from -17 to -22 . Moreover, the average input and output temperatures of the fridge evaporator for the off and on cycles were -1.16°C and -22.30°C , respectively. In addition, the average temperature in the fridge cabinet was 1.10°C . Hence, SP-7 was applied to the entire back side of this evaporator since it could charge at the evaporator temperature and melt at the cabinet temperature.

Nevertheless, in the ECS-2, double PCMs with different freezing points were deployed on both evaporators. PCMs were arranged toward the surface temperatures of the evaporators. In other words, PCMs with low-freezing temperatures were fitted on the sides of the evaporators where the temperature within the cabinet was higher than elsewhere. As such, SP-17 was used for the top and back surfaces, while SP-7 was for the bottom surface of the freezer evaporator. Also, for the fridge evaporator, SP-7 and distilled water were applied to the top and bottom parts, respectively. The SP-7 was outside the operating temperature range of the freezer evaporator. It was chosen because it could remain frozen and support the second evaporator in keeping the temperature of the fridge cabinet within ISO guidelines. In addition, as distilled water has a higher latent heat of

fusion than SP-7, the fridge cabinet might become warmer than when using SP-7 alone. The higher latent heat of fusion required more refrigeration capacity to reach complete freezing. In ECS-3, the same PCM as in ECS-1 and ECS-2 was used for the freezer and fridge evaporators, respectively.

Table 4.11. Experiments on the evaporator.

Experiments	Name	Freezer evaporator			Fridge evaporator	
		Top	Back	Bottom	Top part	Bottom part
Experiment 1	ECS-1	0.250kg SP-17	0.250kg SP-17	0.300kg SP-17	0.5kg SP-7	0.300kg SP-7
Experiment 2	ECS-2	0.250kg SP-17	0.250kg SP-17	0.300kg SP-7	0.5kg SP-7	0.300kg distilled water
Experiment 3	ECS-3	0.250kg SP-17	0.250kg SP-17	0.300kg SP-17	0.5kg SP-7	0.300kg distilled water

4.11.3. Application of PCM in Condenser and Evaporator

In this case, PCMs were tested on both the condenser and evaporator simultaneously to overcome the drawbacks of using them individually. The most efficient experiments on the condenser and evaporator were combined. This experiment is titled dual energy storage (DES).

4.11.4. Application of PCM in Condenser, Evaporator, and Fridge Cabinet

The goal of this experiment was to improve the fridge cabinet's temperature variations and the refrigerator's overall efficiency. This experiment included (DES) and three aluminum PCM panels on the upper, middle, and lower partitions of the fridge cabinet. Thus, the title of this test was combined energy storage (CES). Each PCM panel contained 0.333kg of RT4. The RT4 was selected for this test since its interval temperature ranges from 2°C to 4°C, and the fridge cabinet temperature fluctuates between 0.33°C and 1.87°C.

4.12. Data Acquisitions

After installing data recorders, sensors, and PCMs, experiments were initiated at the room temperature maintained at $25 \pm 0.5^\circ\text{C}$ by a split unit air conditioner. The data was collected over two days, the first 24 hours including starting operation and the second 24 hours comprising only steady-state operation. Data recording intervals of one second for temperature and thirty seconds for pressure have been established. Nonetheless, the energy consumption has been recorded for an entire day. After the data gathering, the data analysis was performed, which involved the distinguishing data for each refrigerator cycle of a 24 hours operation. The total number of cycles varied according to the experiments. The cycle consisted of an automatic on and off time. Maximum and minimum temperatures and pressures were determined for each cycle. The maximum and minimum temperatures and pressures of all cycles during 24 hours were averaged to determine the correct values. Then, the averaged values are used to determine the enthalpies of four points, which are shown in Figure 3.5. The enthalpies were determined using the Danfoss Coolselector®2 software version 4.8.2, which calculated the refrigerant properties given in Figure 4.22.

The screenshot shows the 'Refrigerant Calculator' window. At the top, there is a table with columns for various refrigerant properties: Input, T, p, v, d, h, s, x, Cp, Cv, Viscosity, Conductivity, and Speed of sound. The units for these properties are listed below the table: °C, bar, m³/kg, kg/m³, kJ/kg, kJ/(kg·K), kJ/kg, kJ/kg, Pa·s, W/(m·K), and m/s. Below the table, the 'Refrigerant' is set to R134a. The 'Saturated gas' section has 'Known value:' with buttons for T, p, d, h, s. The 'Saturated liquid' section has 'Known value:' with buttons for T, p, d, h, s. The 'Enter known value(s):' section has input fields for T (0 °C), h (0 kJ/kg), p (0 bar), s (0 kJ/(kg·K)), d (0 kg/m³), and x (0.5). At the bottom, there are radio buttons for 'Density input' (selected) and 'Specific volume input'. There are also buttons for 'Show refrigerant information', 'Clear grid', and 'Close'.

Figure 4.22. Danfoss Coolselector®2 software version 4.8.2. refrigerant calculator.

Moreover, the refrigerant mass flow rate was computed by dividing the compressor's power consumption by its work done. Finally, the COP, Q_H , and Q_L are calculated and discussed thoroughly in the following chapter through tabulations and graphs.

4.13. Uncertainty Analysis

Due to the existence of systematic, bias, and random errors during the measurement, uncertainty is required for the instruments, apparatus, and sensors. Therefore, the following correlation provided by (Holman, 2021) has been used to estimate the uncertainty of RTD temperature sensors and Elitech PGW-500 pressure gauge in this study. A sample of calculations for each one is presented in Appendix L, and the results are listed in Table 4.12.

$$U = \sqrt{\frac{\sum_{i=1}^n (x_i - \bar{x})^2}{N \times (N-1)}} \quad (4.1)$$

where U is the uncertainty, N is the number of readings, \bar{x} is the average value of all the readings taken for the X variable, and the result of the i^{th} measurement is represented by x_i .

Table 4.12. Results of uncertainty.

Instrument	Uncertainty
Temperature sensor	± 0.044
Pressure gauge (Elitech PGW-500)	± 0.006

CHAPTER 5

RESULTS AND DISCUSSION

5.1. Introduction

This chapter explained and discussed the results of all experiments conducted on the household refrigerator with and without PCM. The findings are divided into two 24-hour periods. The first 24 hours included the startup operation, while the second 24 hours covered the steady-state operation. In this study, the first 24 hours of operation were not taken into account because it included the startup operation. The startup operation was not required in testing the energy consumption of household refrigerators according to the ISO standard (ISO 15502:2005). Therefore, the other characteristics of refrigerators were also ignored during this period. In steady-state operation, the energy consumption, COP, temperatures of the refrigerator's components, and the pressure and temperature of evaporation and condensation in a home refrigerator with and without PCM have been compared. Tables 5.1 and 5.2 show the results of experiments for different parameters. Also, the refrigeration cycle for all the experiments on the P-h diagram is presented in Figures 5.1, 5.2, and 5.3. Thereby, the following sections covered the discussion and explanation of the results of the steady-state operation.

Table 5.1. The results of experiments for different parameters.

Tests	Temperatures (°C)										Compressor on/off periods (min)			
	Condenser						Evaporators				Per cycle		Per 24h	
	Top	Bottom	Sections				Freezer		Fridge		on	off	on	off
			1	2	3	4	in	out	in	out				
HR	48.96	27.70	61.23	48.52	45.78	35.59	-30.77	-30.76	-29.44	-15.17	8.80	13.38	572.50	867.50
CHS-1	45.31	25.15	55.55	43.96	37.41	28.69	-32.02	-31.37	-30.16	-16.23	8.00	15.50	490.00	949.79
CHS-2	46.69	25.80	57.34	45.48	39.82	30.58	-31.77	-30.95	-30.01	-15.51	8.15	15.00	506.95	933.05
CHS-3	48.66	27.04	59.97	47.95	43.04	32.93	-30.98	-30.82	-29.78	-15.17	8.33	14.70	520.85	919.15
ECS-1	52.71	28.10	63.83	51.78	47.73	36.36	-27.40	-27.38	-25.76	-14.16	9.70	20.85	460.07	979.93
ECS-2	51.10	27.79	62.32	50.21	46.41	35.65	-28.35	-28.23	-27.35	-14.33	9.30	21.72	431.63	1008.37
ECS-3	51.36	28.03	62.62	50.63	46.76	35.83	-28.23	-27.89	-26.68	-14.23	11.50	27.38	425.93	1014.07
DES	47.11	25.90	57.46	45.81	38.77	29.46	-31.72	-31.31	-30.14	-15.48	11.38	23.57	468.92	971.08
CES	46.42	25.50	56.70	45.35	38.41	29.02	-31.87	-31.33	-30.13	-15.87	12.10	26.05	456.68	983.32

Table 5.2. The results of experiments for different parameters.

Tests	T_{sub} (°C)	Q_H (kW)	Q_L (kW)	ρ_{suc} (kg/m ³)	w (kJ/kg)	M_{ref} (kg/s)	R_E (kJ/kg)	h_1 (kJ/kg)	h_2 (kJ/kg)	h_3 (kJ/kg)	h_4 (kJ/kg)	ΔP (bar)	Cycles per 24h	T_1 (°C)	T_{10} (°C)
HR	0	0.385	0.262	1.097	124.7	0.000973	270.7	536.6	661.3	265.9	265.9	8.51	65	73.49	20.64
CHS-1	2.55	0.374	0.261	0.989	117.4	0.000951	275.7	535.2	652.6	259.5	259.5	6.52	61	65.79	19.72
CHS-2	1.9	0.377	0.261	1.020	119.5	0.000955	275.1	536.2	655.7	261.1	261.1	6.88	62	67.99	20.14
CHS-3	0.66	0.381	0.261	1.074	123.5	0.000963	272.4	536.6	657.3	264.2	264.2	7.55	62.5	71.28	20.37
ECS-1	-0.4	0.418	0.288	1.381	120	0.001072	270.7	537.6	657.1	266.9	266.9	10.29	47	74.95	21.19
ECS-2	-0.09	0.403	0.278	1.323	118.5	0.001034	271.2	537.4	655.9	266.2	266.2	9.84	46.5	73.55	21.02
ECS-3	-0.33	0.411	0.284	1.367	117.7	0.001056	270.7	537.5	655.7	266.8	266.8	10.06	37	73.88	21.11
DES	1.8	0.377	0.263	1.090	116.3	0.000965	274.7	536.1	652.4	261.4	261.4	7.68	41	67.82	20.51
CES	2.2	0.377	0.264	1.072	116.2	0.000964	275.2	535.6	651.8	260.4	260.4	7.38	38	66.98	19.75

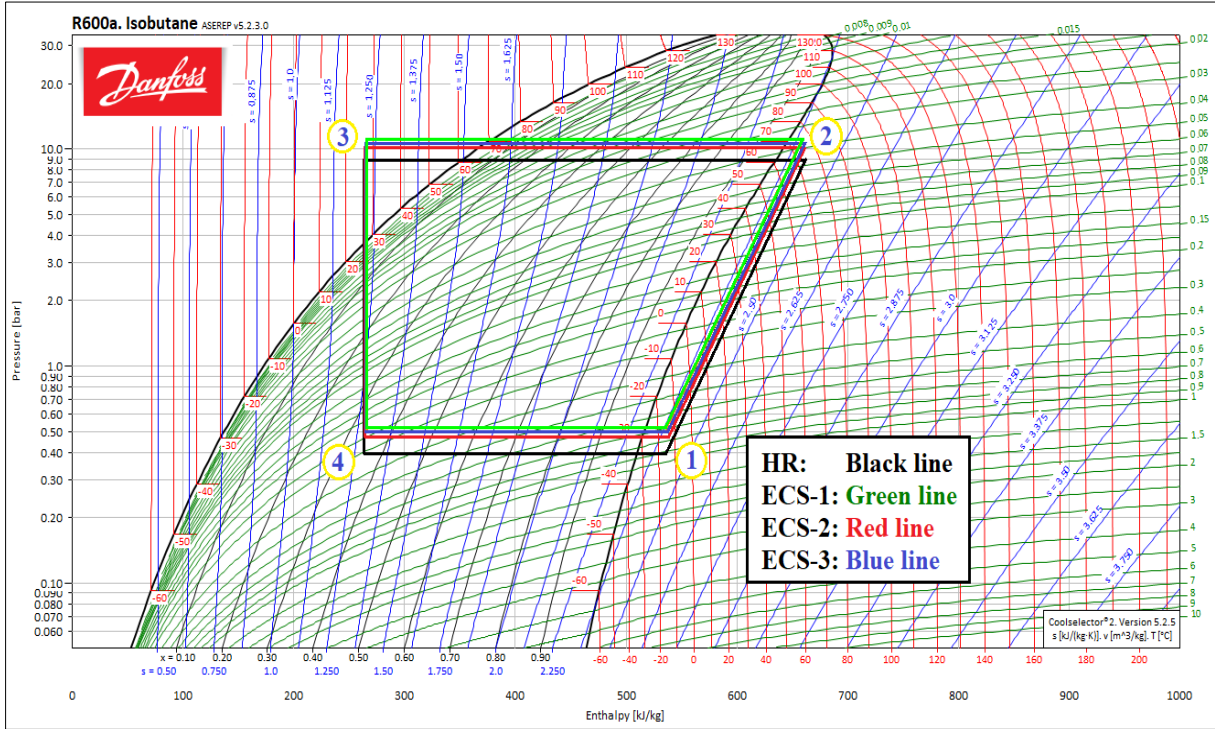


Figure 5.1. Refrigeration cycle for ECS-1, ECS-2, and ECS-3 vs. HR.

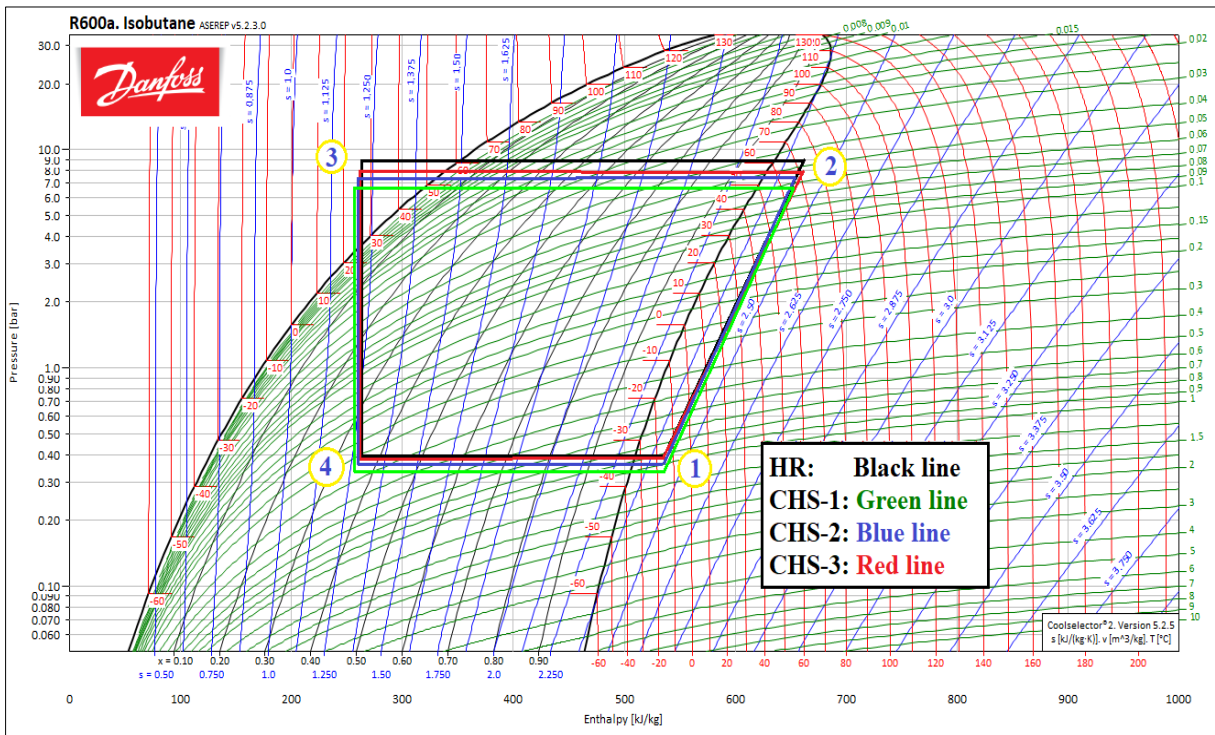


Figure 5.1. Refrigeration cycle for CHS-1, CHS-2, and CHS-3 vs. HR.

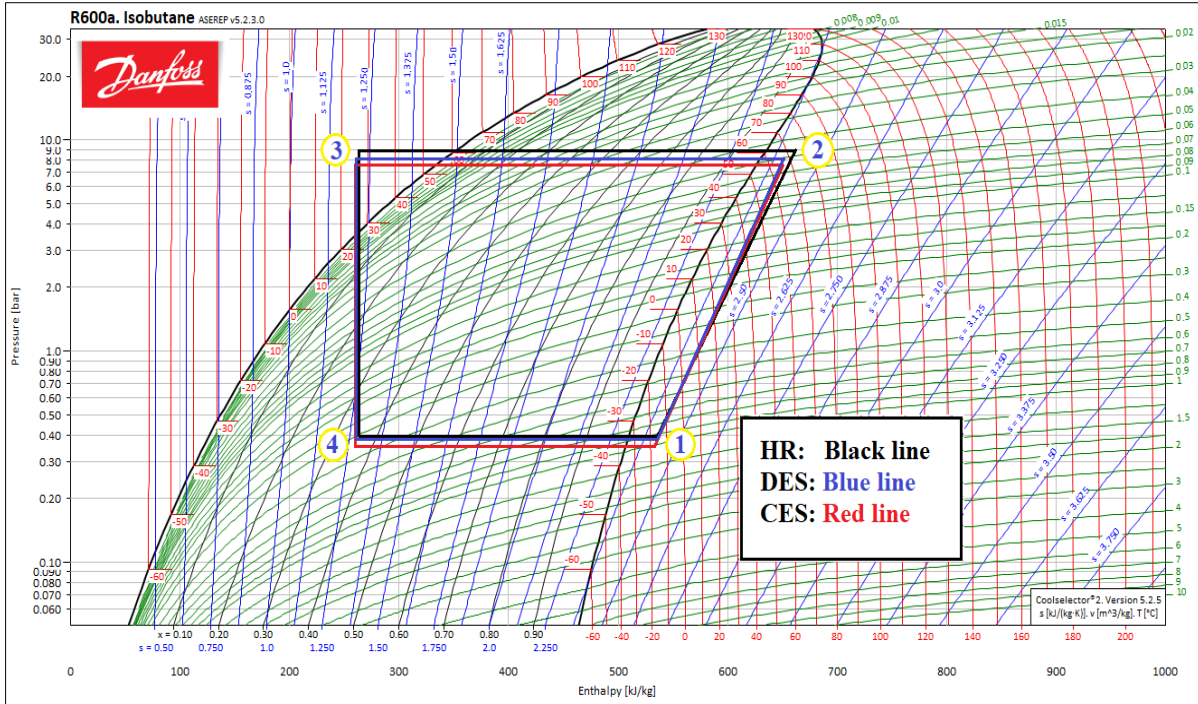


Figure 5.3. Refrigeration cycle for DES and CES vs. HR.

5.2. Compressor Pressures and Temperatures

In refrigeration systems, the suction and discharge pressures of the compressor represent the evaporator and condenser pressures, respectively. Any changes in these pressures will affect the overall performance of the refrigerator. Therefore, due to the application of PCMs to the evaporator and condenser in this study, both pressures changed significantly. As shown in Figure 5.4, there was a spike in evaporation and condensation pressures in ECS experiments over other experiments because PCMs absorbed the cabinet's heat in the off-cycle period and then transferred it to the evaporator in the on-cycle period. As a result, the evaporator's heat dissipation load dramatically lowered in the on-cycle time. Nevertheless, PCMs optimized the condenser's heat transfer rate due to their higher thermal conductivity than air and superior capacity for absorbing heat energy in CHS experiments. Consequently, the condensation and evaporation pressures declined to a level below HR.

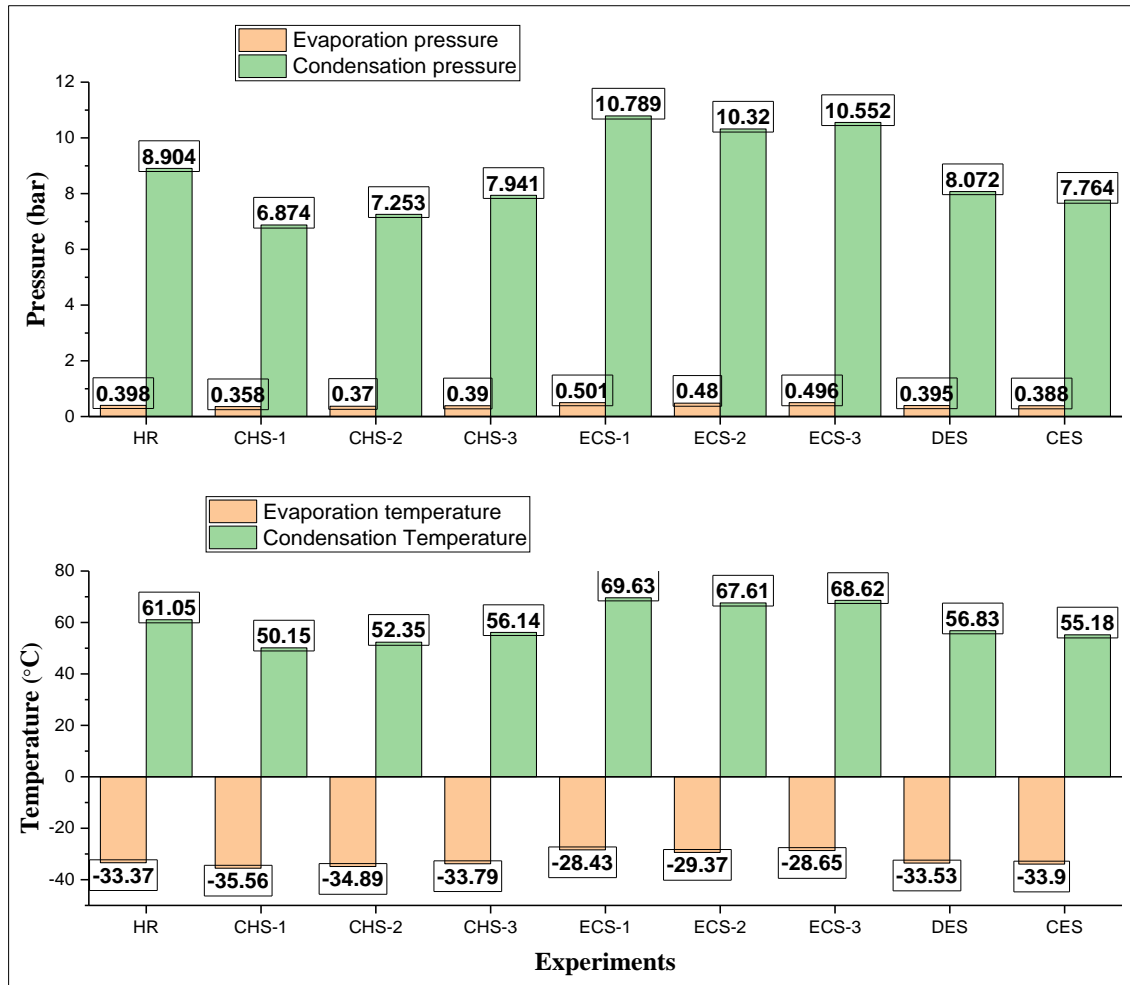


Figure 5.4. Evaporation and condensation pressures and temperatures.

The CHS-1 and ECS-3 were chosen for the DES and CES experiments due to their outstanding performance in optimizing refrigerator performance. However, merging the CHS-1 and ECS-3 was advantageous in minimizing the evaporation and condensation pressures that rose because of the PCMs on the evaporators. The increase in on/off cycle times due to the evaporator PCMs, as provided in Table 5.1, made melting and solidification times increase for the condenser PCMs. Accordingly, the performance of condenser PCMs was enhanced, leading to a fall in compressor pressures to a level between CHS-1 and HR. The further drop in compressor pressures at the CES test was due to the PCM

panels within the fridge cabinet. Since the panels supplied additional cooling during the compressor's shutoff cycle, the fluctuating temperature inside the cabinet decreased dramatically. The relation between compressor pressures and temperatures is directly proportional. In turn, the condensation and evaporation temperatures shifted with the same behavior as pressure shifts when PCMs were present, as depicted in Figure 5.4. Lastly, condensation and evaporation temperatures directly affected compressor inlet and outlet surface temperatures, as illustrated in Table 5.2.

5.3. Evaporation and Evaporator Surface Temperatures

5.3.1. ECS Experiments

As is evident in Figure 5.4, a refrigerator with ECSs operated at a higher evaporation temperature than a household refrigerator (HR) and a refrigerator with other arrangements of energy storage. The PCMs made this increase because they absorbed the heat in the cabinets during the off-cycle time and transferred it to the evaporator and then to the refrigerant during the on-cycle time. In this process, PCMs accumulated significant amounts of heat due to their energy absorption capacity and thermal conductivity. Consequently, PCMs improved the heat transfer rate of the evaporators. This improvement was between cabinet air and evaporators by installing PCMs on the faces of the evaporators. Therefore, the evaporator's heat dispersion load could be dramatically lowered during on-cycle time. Also, the relationship between evaporation and evaporator surface temperatures is directly proportional. Thus, all ECS experiments showed the warmest evaporator surface temperatures, as seen in Figures 5.5a and 5.6a.

As per the results, ECS-1 had higher temperatures than other ECSs because its PCMs froze at lower temperatures. Nonetheless, the lowest temperatures in

ECS-2 were due to the high freezing point of the SP-7 on the freezer evaporator, as it remained frozen during the experiment. Accordingly, as ECS-3 was a mixture of ECS-1 and ECS-2 in applying PCMs, its results were between them. The temperature increase existed from all the cases that implemented PCMs on the evaporators. But the ranges were different because of the phase change point of PCMs.

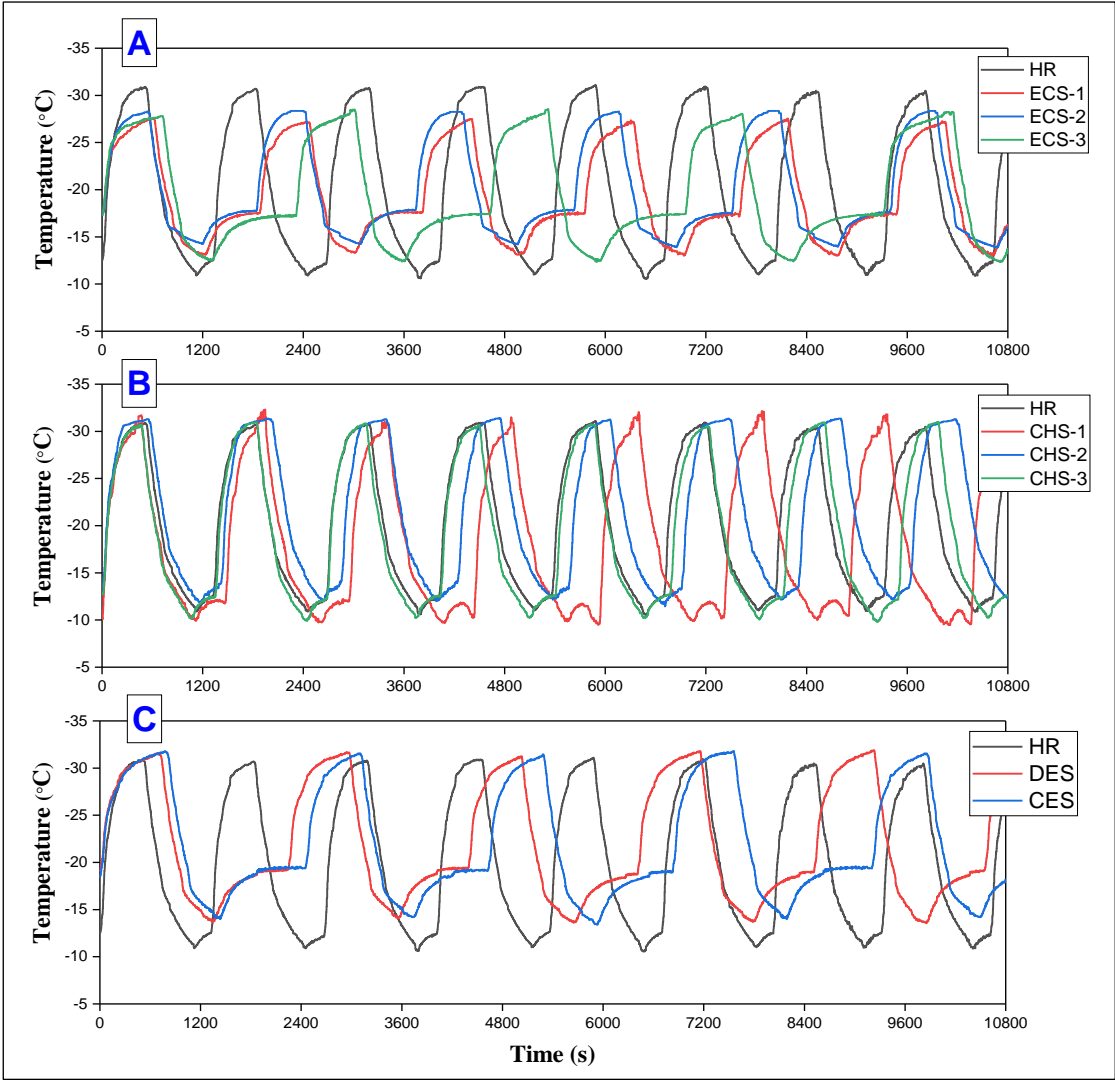


Figure 5.5. Average inlet (T_6) and outlet (T_7) temperatures vs. time for freezer evaporator.

5.3.2. CHS Experiments

Unlike the ECSs, the CHSs presented the minimum condensation and evaporation temperature, as shown in Figure 5.4. The improved heat transfer rate of the condenser by PCMs and NCPCM caused this drop. Since PCMs and NCPCM had superior thermal conductivity to air, and due to their capacity for absorbing substantial amounts of heat, the refrigerant exchanged more heat with them than with air at a faster rate. During this process, the temperature of the refrigerant decreased, and it entered the evaporators. Thus, evaporators operated at a lower evaporation temperature. In addition, as demonstrated in Figures 5.5b, and 5.6b, the surface temperatures of the evaporator dropped as the evaporation temperatures decreased.

Within the findings of CHSs, CHS-1 had the best performance in lowering the temperatures. The NCPCM and the arrangement of a 10°C interval between the maximum average temperatures of parts 2 and 3 and the surrounding temperature with PCMs were accountable for this improvement. The PCM for segment 3 was the weak point of the CHS-2 because it did not change phase to solid significantly during compressor shutdown. Therefore, it was not superior to CHS-1, although triple PCMs were employed. However, compared to other CHS tests, the deficiency of CHS-3 was the use of double PCMs and the PCM for section 2, which did not considerably shift its phase to liquid throughout the compressor operation. Although some PCMs exhibited deficiencies in their function, the CHS tests substantially reduced the temperatures.

5.3.3. DES and CES Experiments

These experiments included the ECS-3 and CHS-1 due to their outperforming results in optimizing the overall refrigerator's efficiency. Since the

on/off cycle time rose with the PCMs on the evaporator, the melting and solidification periods for condenser PCMs and NCPCM extended significantly. As a result, they functioned better in switching their phases. Hence, the DES and CES had lower evaporation temperature than the HR, as displayed in Figure 5.4. Nonetheless, the temperature reduction was not less than the CHS-1 but rather somewhat higher. As the PCM panels in the CES provided extra cooling in off-cycle time, the CES showed a lower evaporation temperature than the DES. In conclusion, the evaporator surface temperatures were also between HR and CHS-1 due to their relationship with the evaporation temperature, as presented in Figures 5.5c, and 5.6c.

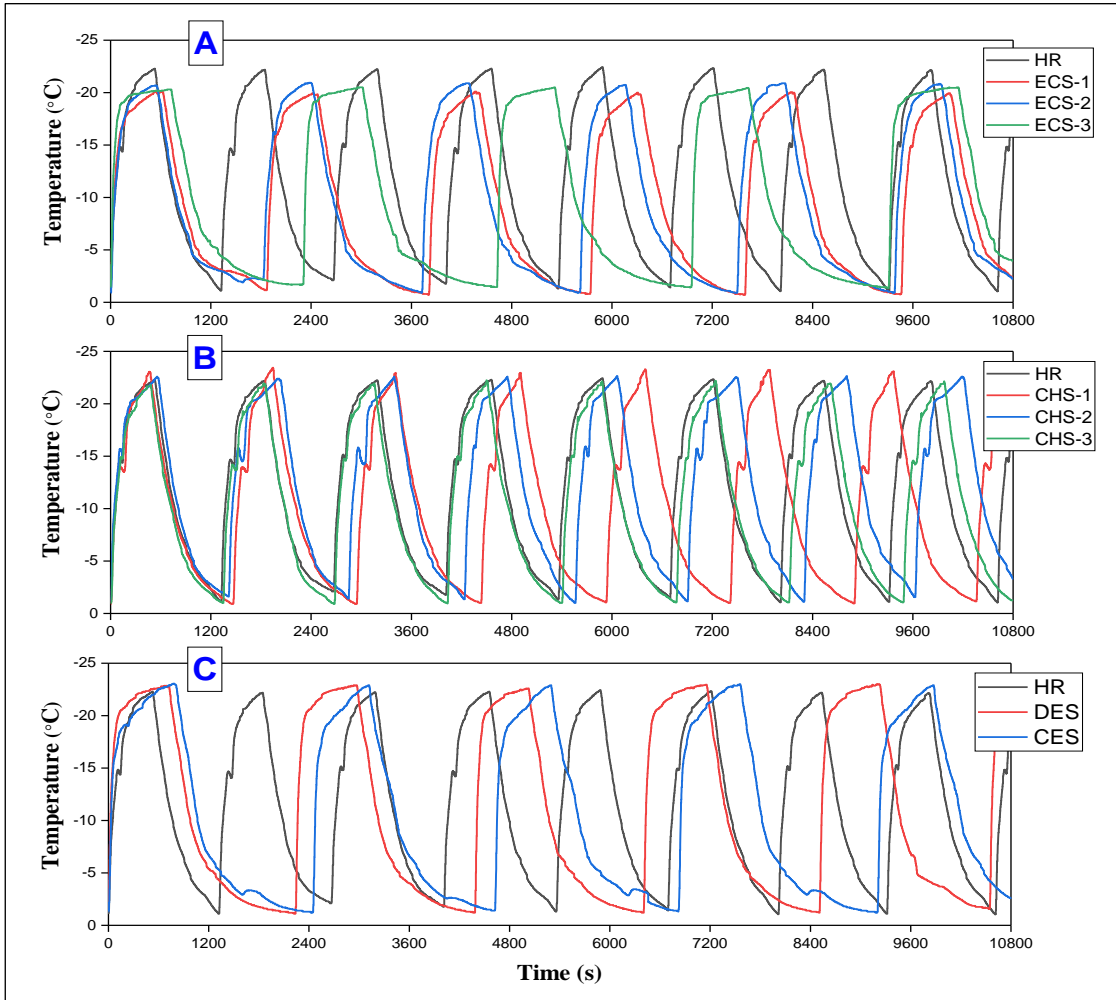


Figure 5.6. Average inlet (T_8) and outlet (T_9) temperatures vs. time for fridge evaporator.

5.4. Condensation and Condenser Surface Temperatures

5.4.1. ECS Experiments

The ECSs exhibited the highest condensation temperatures, according to Figure 5.4. This increase commenced in the evaporator, where the PCMs raised the evaporation's temperature. As a result of the transfer of heat from the PCMs to the refrigerant in the evaporators, the refrigerant entered and discharged the compressor at a higher temperature. Hence, the condensation temperature was higher. Based on their relation, condensation temperature directly affected the condenser surface temperatures. For this reason, the surface temperatures of the condenser sections were also higher, as depicted in Figures 5.7a, 5.8a, 5.9a, and 5.10a.

A comparison of the data from the ECS experiments showed that the ECS-1 warmed the condenser parts more than the other experiments because of the low phase change temperature of the PCMs. Also, in ECS-2, the remaining SP-7 in the frozen state on the freezer evaporator caused minimal temperature rise on the condenser parts during the test period. As the ECS-3 was a combination of the two, its condenser segments performed an intermediate temperature.

5.4.2. CHS Experiments

Based on the data in Figure 5.4, the lowest condensation temperatures were in CHS's experiments. This improvement was a reflection of the condenser's enhanced heat transfer rate, which was facilitated by PCMs and NCPCM. The high thermal conductivity and capacity to collect heat at narrow phase temperatures were the strengths of PCMs and NCPCM in cooling the condenser. The condenser surface temperatures fell as they correlated with the condensation temperature, as can be seen in Figures 5.7b, 5.8b, 5.9b, and 5.10b.

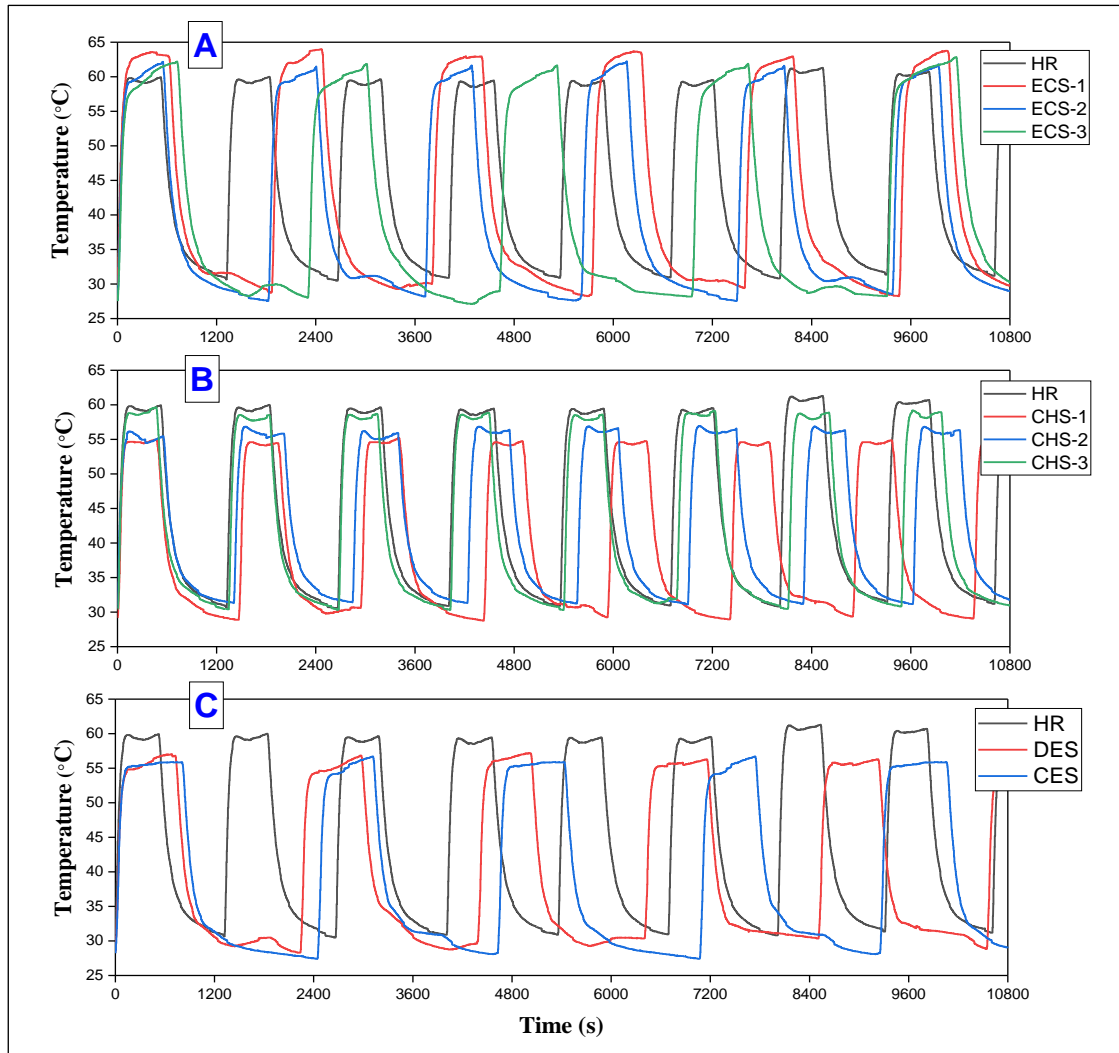


Figure 5.7. Average temperature of (T_1 and T_2) vs. time of section 1 of the condenser.

For all CHS tests in section 1, RT44HC was used, whose performance in cooling the section was related to the PCMs of the other sections. However, the most efficient part of the condenser was 2, as condensation process primarily commenced there. Therefore, in CHS-1, section 2 showed a greater temperature drop than other CHS tests compared to the HR test due to the excellent performance of NCPCM. The NCPCM had 38% and 55% better liquid and solid thermal conductivity than the same PCM without nanoparticles. The decrease in temperature was 4.56°C , while in CHS-2 and CHS-3 it was 2.8°C and 0.57°C ,

respectively. The lesser drop in temperature for CHS-2 resulted from using the same PCM as CHS-1, excluding nanoparticles. Nevertheless, in CHS-3, it was related to the difference between the PCM phase change temperature and maximum segment temperature, which was insufficient for melting the PCM completely. The temperature in the succeeding sections was strongly impacted by the temperature decline in the section 2. Consequently, part 3 revealed the minimum temperature in CHS-1. This segment temperature was colder than the HR by 8.37°C, 5.3°C, and 4.48°C for CHS-1, CHS-2, and CHS-3, respectively. In addition, the PCM employed in this segment efficiently shifted its phase from solid to liquid and vice versa.

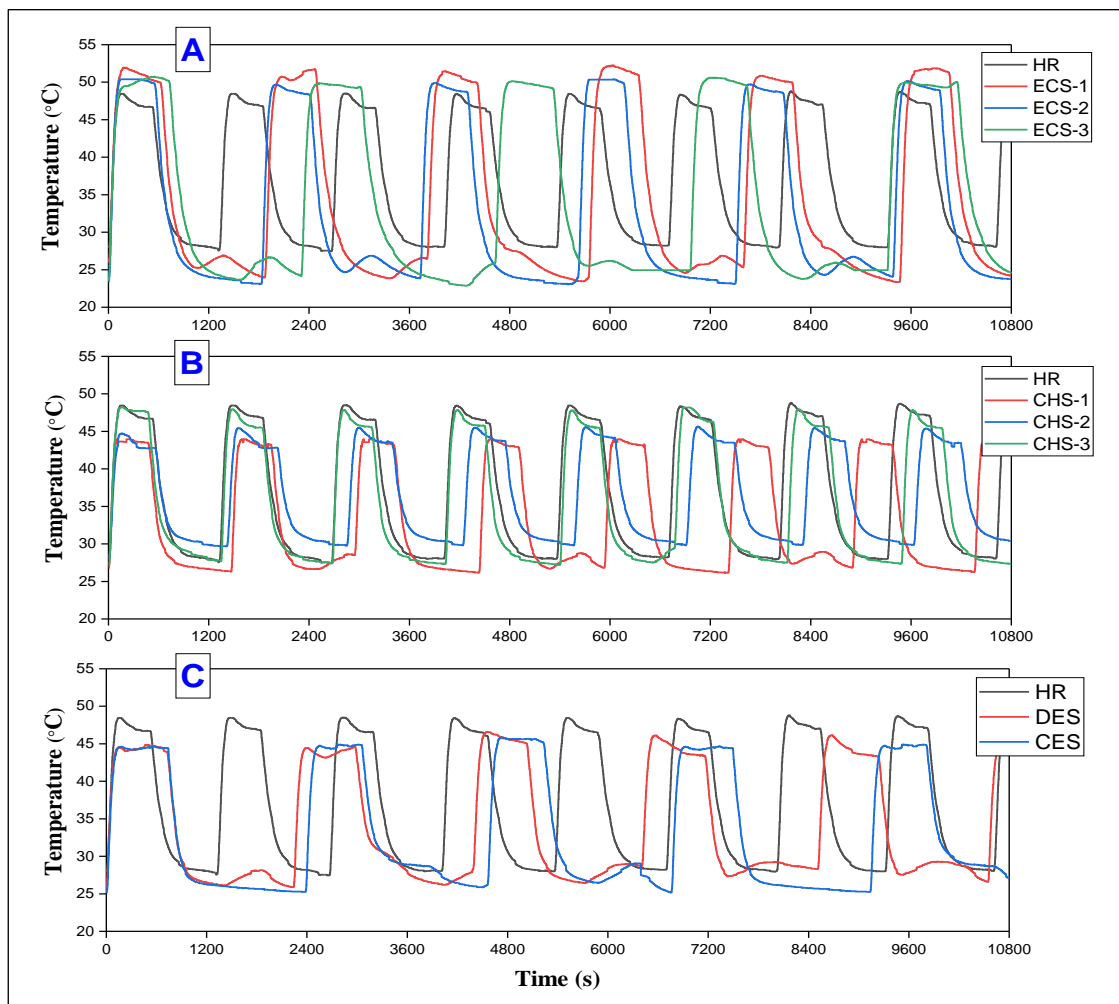


Figure 5.8. Average temperature of $(T_2 \text{ and } T_3)$ vs. time of section 2 of the condenser.

Nonetheless, the PCM in CHS-2 did not significantly transform from liquid to solid because of the insufficient difference between room temperature and the PCM phase change temperature. In this part, although the PCM for CHS-1 and CHS-3 was the same, the high temperature of section 2 in CHS-3 prevented it from cooling that part in the same manner as in CHS-1. Similarly, section 4 was impacted by section 3. Accordingly, section 1 displayed a lower temperature with CHS-1 because the refrigerant circulated through the system at lower temperature. In the published studies, the cooling of condenser temperatures has been achieved with a different amount. However, the ranges depended on the difference between the PCM phase change point and room temperature, as well as the maximum average temperature of the condenser and the PCM phase change point.

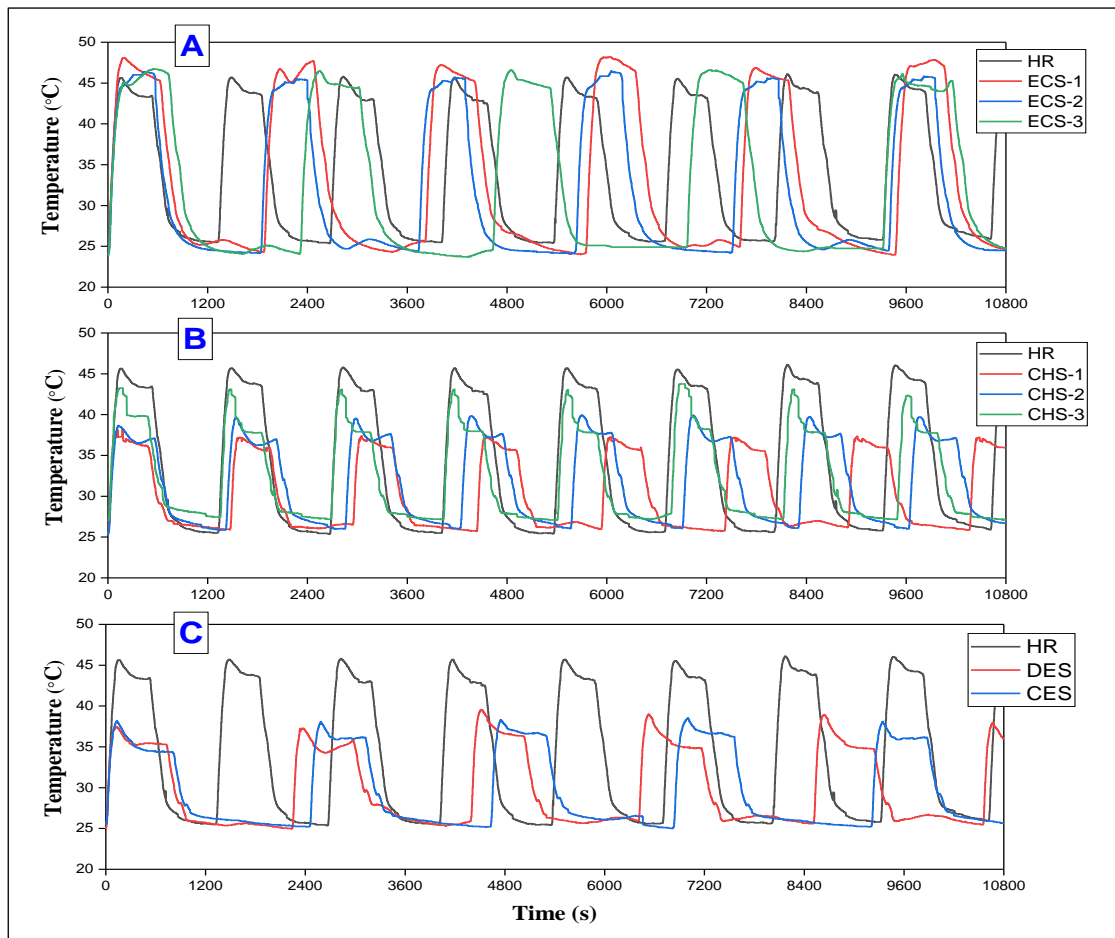


Figure 5.9. Average temperature of (T_3 and T_4) vs. time of section 3 of the condenser.

5.4.3. DES and CES Experiments

In these cases, since the evaporator PCMs lengthened the compressor's on-off cycle period, the melting and solidification periods for condenser PCMs and NCPCMs climbed considerably. In turn, they completed their functions more effectively in absorbing heat than in CHS-1. Thus, they controlled the condensation temperature between the HR and CHS-1 tests, as illustrated in Figure 5.4. Depending on their relationship, the surface temperatures of the condenser parts decreased comparably to the condensation temperature, as demonstrated in Figures 5.7c, 5.8c, 5.9c, and 5.10c.

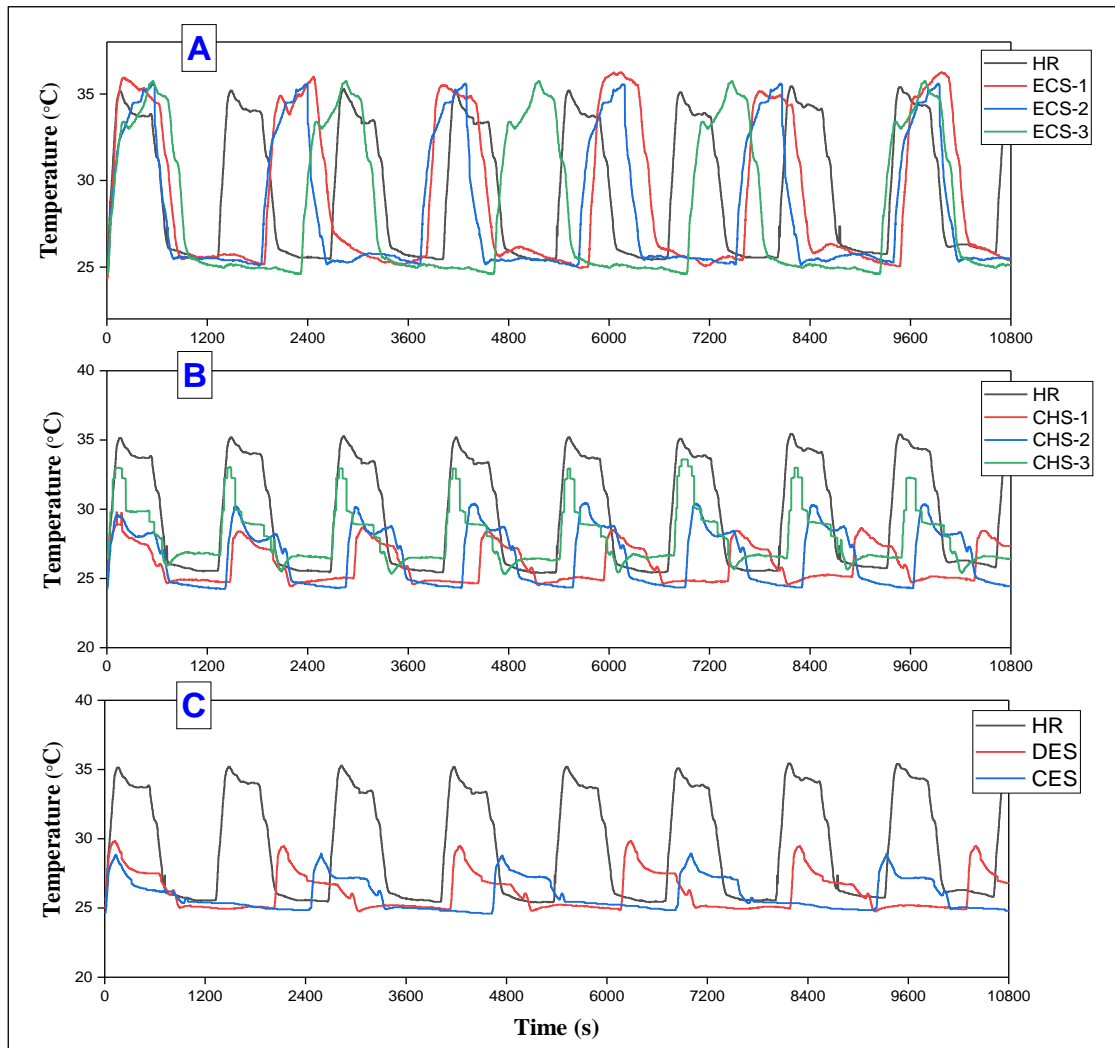


Figure 5.10. Average temperature of (T_4 and T_5) vs. time of section 4 of the condenser.

In comparison to HR, the temperatures of the condenser parts were reduced by roughly the same amount as in CHS-1. Thus, the results confirmed that the PCMs and NCPCMs cooled the condenser excellently despite the elevated temperature of the condenser sections by evaporator PCMs. The presence of the PSM panels in the fridge cabinet in CES provided more cooling to the cabinet, thus reducing the cabinet temperature changes and resulting in lower condenser surface temperatures than DES. So, using PCMs on condensers and evaporators concurrently diminished the shortcomings of employing them separately. In a similar manner, (Cheng et al., 2017) found that the DES test could compensate for the disadvantages of the evaporator PCM with the advantages of the condenser PCM and vice versa.

5.5. Temperature of the Cabinets

The most sensitive temperature is the cabinets' temperature in the refrigerator with the application of PCMs. Therefore, they should not decrease under the standards, as it impacts the quality of the stored products. Consequently, the temperature of the fridge and freezer cabinets remained within the standards of ISO during the experiments, as provided in Figures 5.11, 5.12, 5.13 and 5.14. The reasons for the decrease or increase in the temperature of the fridge and freezer cabinets and the temperature changes in them for each experiment are explained in the following sections.

5.5.1. ECS Experiments

As apparent in Figures, the ECS tests displayed the highest fridge and freezer cabinet temperatures compared to the other PCM experiments and HR. The primary cause of the rise was a transfer of some refrigeration capacity to PCMs for freezing purposes in the on-time cycle. But, for the fridge cabinet, a slight

amount of heat transfer from the condenser to the cabinet that made by PCMs on the evaporator in the on-cycle period was the second cause. A comparison between all cases of ECS revealed that the ECS-3 had a lower average temperature and higher fluctuation in the fridge and freezer cabinets. The lower average temperature was due to the longer on-time cycle to charge PCMs. A larger capacity of the distilled water than the SP-7 for absorbing cold energy was responsible. During the charging process, the temperature of the cabinets fell because of excess cooling provided by the functional faces of the evaporators. However, PCMs provided excess cooling during the off-cycle period, resulting in a higher off-time cycle and temperature fluctuations. Thus, the difference in cabinets' temperatures between ECS-2 and ECS-3 was caused by distilled water.

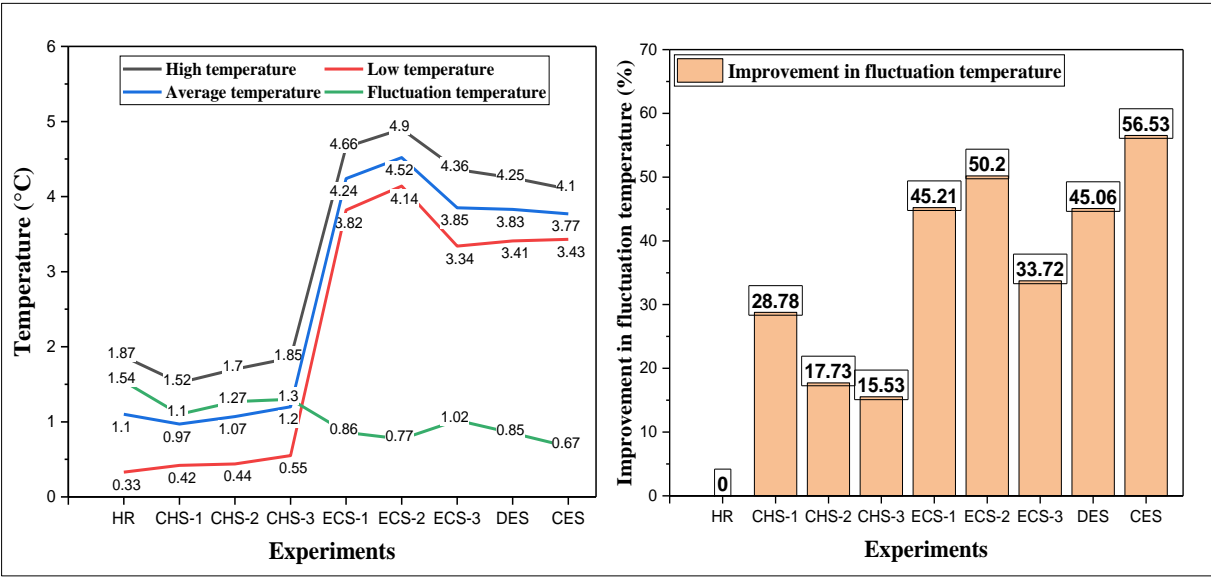


Figure 5.11. Fridge cabinet temperatures and their improvements in fluctuation.

Nevertheless, the difference between ECS-1 and ECS-2 was in the SP-7 on the freezer evaporator and distilled water on the fridge evaporator. As such, in ECS-2, SP-7 did not undergo a phase change, resulting in less refrigeration capacity transfer to the PCMs and a shorter on-cycle duration. Thus, it presented

a slightly lower average temperature in the freezer cabinet with a larger temperature variation than ESC-1. However, higher fridge cabinet temperature with its fluctuation than ESC-1 was related to the latent heat capacity of distilled water as it requires more refrigeration capacity for freezing. Although ECS-2 and ECS-3 had the same PCM on the fridge evaporator, ECS-2 exhibited a higher fridge cabinet temperature. The reason for this was due to the SP-7 on the freezer evaporator remaining frozen throughout the test. So, it needed less runtime to charge the PCMs and achieve the set temperature. Accordingly, the PCMs on the fridge evaporator froze faster, and the cabinet temperature increased. Similarly, both studies (Azzouz et al., 2009) and (Yusufoglu et al., 2015), reported that the refrigerator with an evaporator PCM increased the average fridge cabinet temperature by 4.2°C and 2.1°C, respectively.

5.5.2. CHS Experiments

The mechanism of improving cabinet temperature and fluctuation temperature by CHS test was in the cooling rate of the condenser. As the condenser cooled, its pressure declined, which resulted in a lower temperature in the evaporators. As a result, the average temperature in the cabinets and their swings decreased. Thus, as the CHS-1 efficiently cooled the condenser, the evaporators and cabinets possessed a lower average temperature and variation in temperature than the CHS-2 and CHS-3, as shown in Figures 5.11 and 5.12.

However, from the results of CHS cases, the temperature of the fridge cabinet heated somewhat in the on-time cycle as a result of transferring the PCMs' heat accumulation to the cabinet during the off-time, as presented in Figure 5.11. Notwithstanding, compared to HR, the average fridge cabinet temperatures and temperature swings dropped noticeably in the CHS-1 and CHS-2. Nonetheless, in

CHS-3, even though the fluctuation has improved, the average cabinet temperature rose. The reason for that was the PCMs could not decrease the temperatures of the fridge evaporator significantly.

On the other hand, the results related to the temperature of the freezer cabinet indicated that the CHS tests enhanced average cabinet temperature. Regarding this, the fluctuation of temperatures has improved slightly. Overall, the CHS-1 was the best case, as the condensation and evaporation pressures substantially declined. Though the CHS tests were superior to the ECS tests at keeping cabinets' temperature, they did not improve cabinets' fluctuation temperature as much as the ECS tests, as depicted in Figure 5.12. The location and functioning mechanism of PCMs caused this discrepancy.

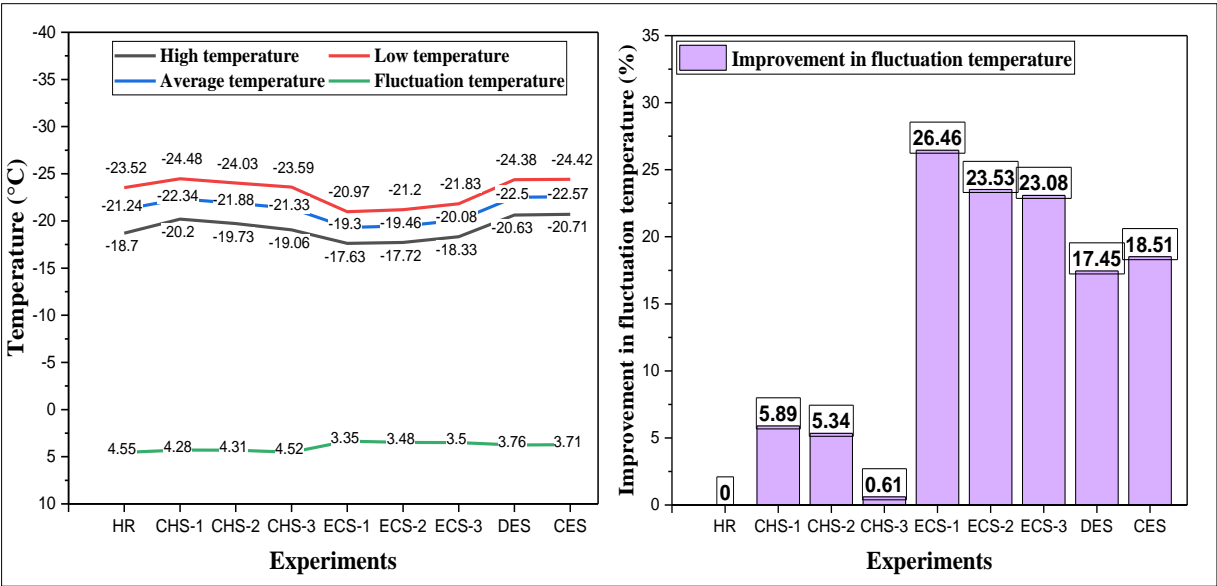


Figure 5.12. Freezer cabinet temperatures and their improvements in fluctuation.

5.5.3. DES and CES Experiments

The DES and CES tests cooled the average freezer cabinet temperature to a level below CHS-1, according to the results shown in Figures. The primary factors

that participated in this enhancement were the decrease in the condensation and evaporation pressures and the increase in the running time cycle. The former is related to the PCMs and NCPCM in the condenser, while the latter is related to the PCMs in the evaporators. Both factors together pushed the evaporators to provide extra cooling to the cabinets. In addition, the average temperature of the fridge cabinet dropped slightly below ECS-3. Evaporator PCMs caused the fridge cabinet temperature to remain high in two ways. In the first, the evaporators extracted a part of refrigeration for charging purposes. In the second, they heated the condenser more. Thus, the heat accumulation by the condenser PCMs and NCPCM rose, leading to a rise in condenser-to-cabinet heat transfer.

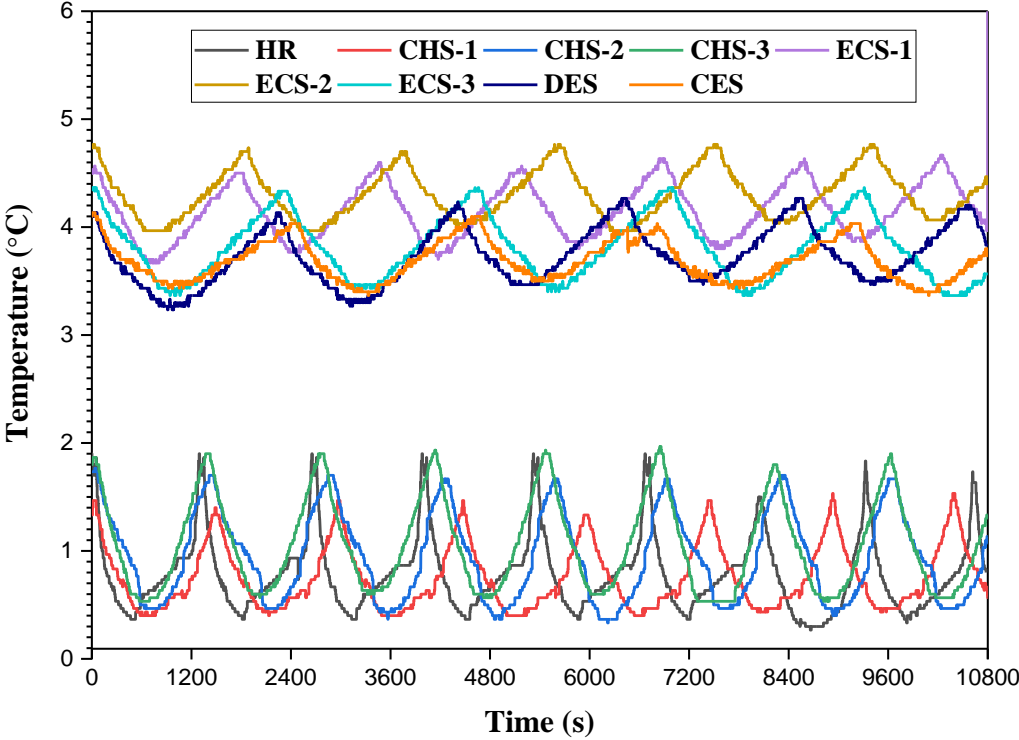


Figure 5.13. Average of fridge cabinet temperatures (T_{13} , T_{14} , and T_{15}) vs. time.

From the graphs, it may be noted that the CES has demonstrated a lesser temperature fluctuation of 0.67°C in the fridge cabinet. Providing additional

cooling by the PCM panels during the shutdown cycle created this improvement. Even though the freezer cabinet temperature was better, the temperature change was slightly higher in DES and CES than ECS-3. However, it maintained between CHS-1 and ECS-3. Thus, implementing PCMs simultaneously on condensers and evaporators would minimize the limitations of applying them separately.

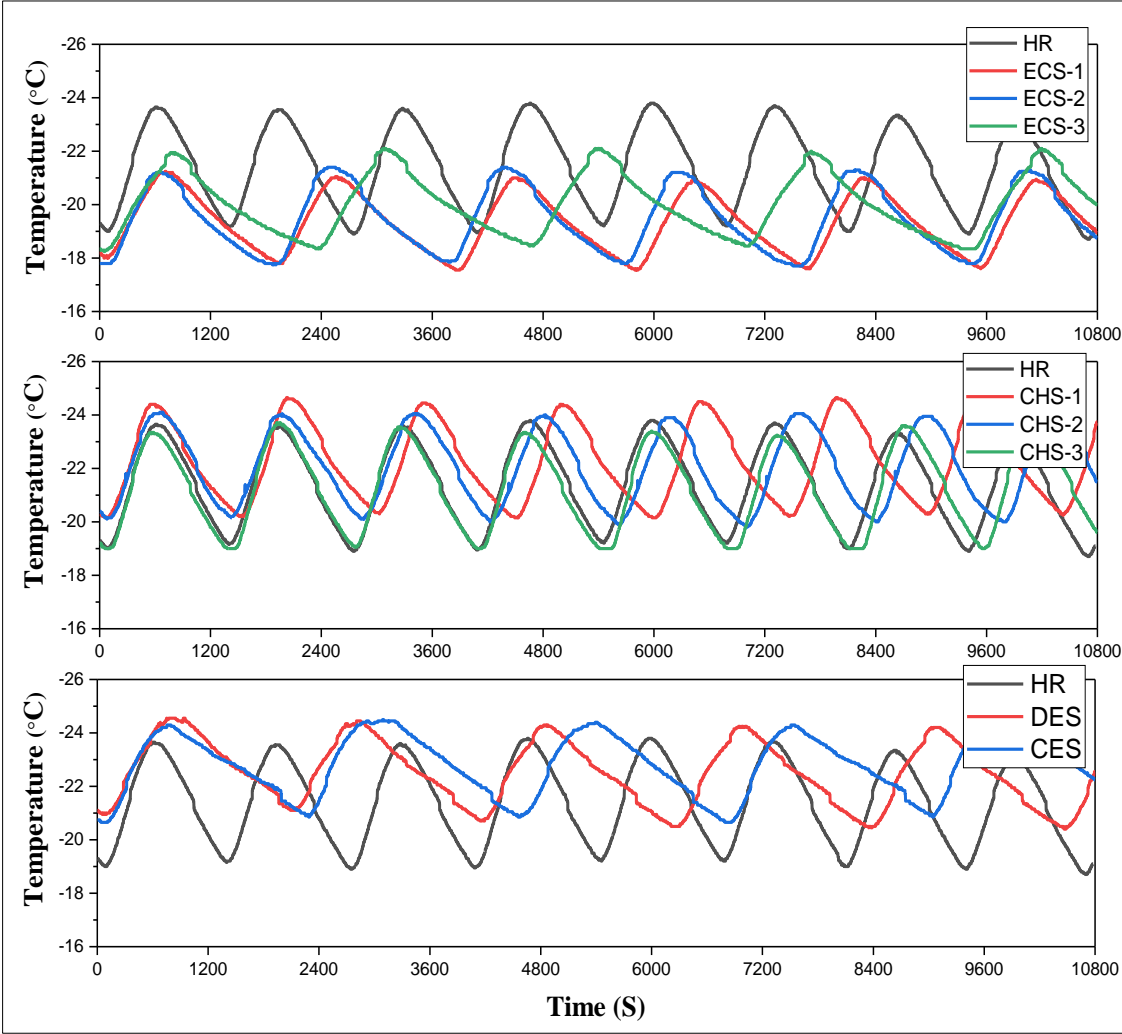


Figure 5.14. Average of freezer cabinet temperatures (T_{11} and T_{12}) vs. time.

5.6. Energy Consumption

The energy consumption of refrigerators is affected by four variables. The variables are the operating time of the compressor, the amount of work the

compressor performed, the sum of the refrigerant mass flow rate that the compressor discharged at its fixed volumetric rate, and number of compressor on/off cycles. The number of compressor cycles plays a significant role because when a compressor initially turns on, it consumes a substantial quantity of energy until it reaches a steady state. It could also have an effect on the lifespan of the compressor. These parameters for all the tests are displayed in Tables 5.1 and 5.2. The PCMs were accountable for controlling the evaporation and condensation pressures, which could influence the aforementioned variables. Therefore, energy savings were obtained in experiments involving PCMs when compared to HR, as illustrated in Figures 5.15 and 5.16. In the following sections, the comparison between experiments is discussed and explained.

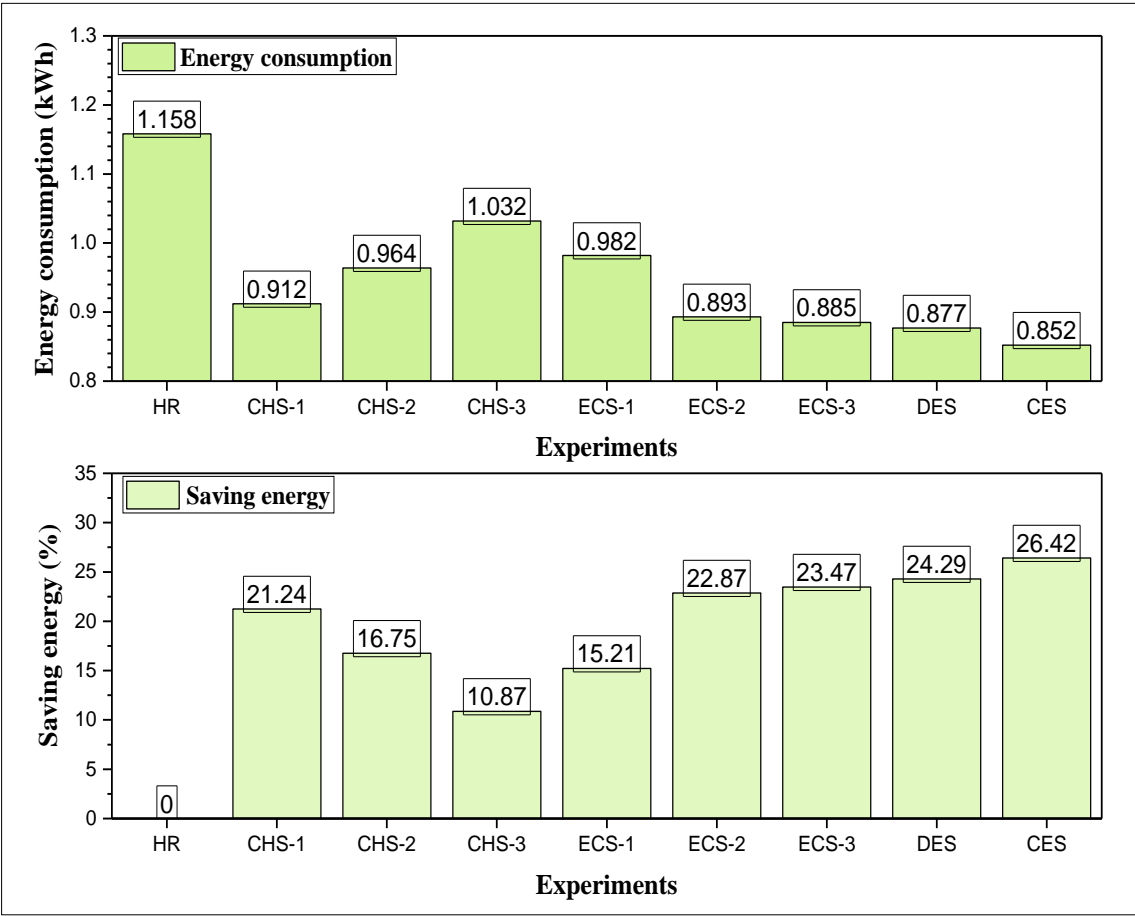


Figure 5.15. The energy consumptions per 24h and their savings.

5.6.1. ECS Experiments

In the ECS experiments, as the PCMs increased the evaporation pressure, the refrigerant entered the compressor with a greater density than HR. As a result, evaporators extracted more refrigerant mass flow rate at the compressor's fixed volumetric rate. Additionally, since PCMs were recognized as a thermal load by the refrigerator, additional time was required for the refrigerator to reach the desired temperature and charge the PCMs. Therefore, the compressor worked longer per cycle. However, the off-cycle time was considerably extended as a consequence of melting PCMs. Consequently, the total operating time and the number of the compressor's cycles decreased dramatically. Further, the work done by the compressor decreased due to the decline in the difference between compressor pressures, as depicted in Table 5.2. In conclusion, even though the mass flow rate increased, total working time, number of cycles, and compressor work declined substantially, resulting in significant energy savings.

In comparison to HR, the results demonstrated that single PCMs on evaporators (ESC-1) conserved less energy than double PCMs (ECS-2). The low freezing temperature of PCMs was the cause behind this. The low temperature of the PCMs forced the compressor to work longer and the evaporators to extract a higher mass flow rate of the refrigerant at their higher temperature and pressure. Thus, double PCMs were more efficient in saving energy compared to single PCMs, as (Yusufoglu et al., 2015), (Elarem et al., 2017), and (Cofré-Toledo et al., 2018) each showed 8.8%, 12%, and 5.81% energy reductions with a single PCM, respectively. Nevertheless, in ECS-3, which was a mixture of single and double PCMs, the PCMs prolonged the compressor run time per cycle more than in ECS-1 and ECS-2 to charge the PCMs. Likewise, they extended the off-cycle time compared to the ECS-1 and ECS-2. Accordingly, the total operating time and

number of cycles decreased greatly, resulting in better energy savings than in the single and double PCMs. The distilled water on the fridge evaporator enabled this improvement because it has a greater capacity for saving energy at a higher temperature than SP-7.

5.6.2. CHS Experiments

The CHSs showed lower evaporation temperatures and pressures than the HR, as presented in Figure 5.4. Thus, the refrigerant had a lower density at the suction line of the compressor, leading to a lower mass flow rate extracted by evaporators. In addition, due to the lower evaporation and condensation temperatures, the evaporators' temperatures decreased to a level below HR. Accordingly, the evaporators cooled the cabinets faster than the HR, resulting in a decrease in the on-time cycle of the compressor. Meanwhile, the compressor's off-time cycle increased as the evaporators and cabinets cooled more. Finally, the total running time declined markedly, but the number of cycles slightly decreased. Furthermore, the compressor's work decreased because of the reduction in the range between compressor pressures. Yet, this reduction was higher than in the ECS experiments. Though the mass flow rate and compressor's work decreased more than in the ECS cases, the total working time and number of cycles decreased less than in the ECS cases. Overall, the energy savings were less than the ECS tests compared to HR.

The performance of PCMs and NCPCM in the melting and solidifying processes, their proper selection for condenser parts, and the thermal conductivity of NCPCM were related to the difference in overall operating time between CHS scenarios. Consequently, the CHS-1 exhibited the lowest energy consumption among the CHS trials as it cooled the condenser at a higher rate. Besides, the triple

PCMs were more energy-efficient than the single and double PCMs according to Figure 5.15. For instance, (Pirvaram et al., 2019) with double PCMs as well as (Sonnenrein et al., 2015) and (Cheng and Yuan, 2013) with a single PCM, saved energy by 13.3%, 10%, and 12.2%, respectively. In comparison with the result of this study, these improvements were lower because triple PCMs with and without nanoparticles reduced energy consumption by 21.24% and 16.75%, respectively. Lastly, the triple PCMs with nanoparticles showed a higher energy saving than a single PCM with polymers (12.2%) and with multi-walled carbon nanotubes (18%), as conducted by (Cheng and Yuan, 2013) and (Kumar et al., 2020), respectively.

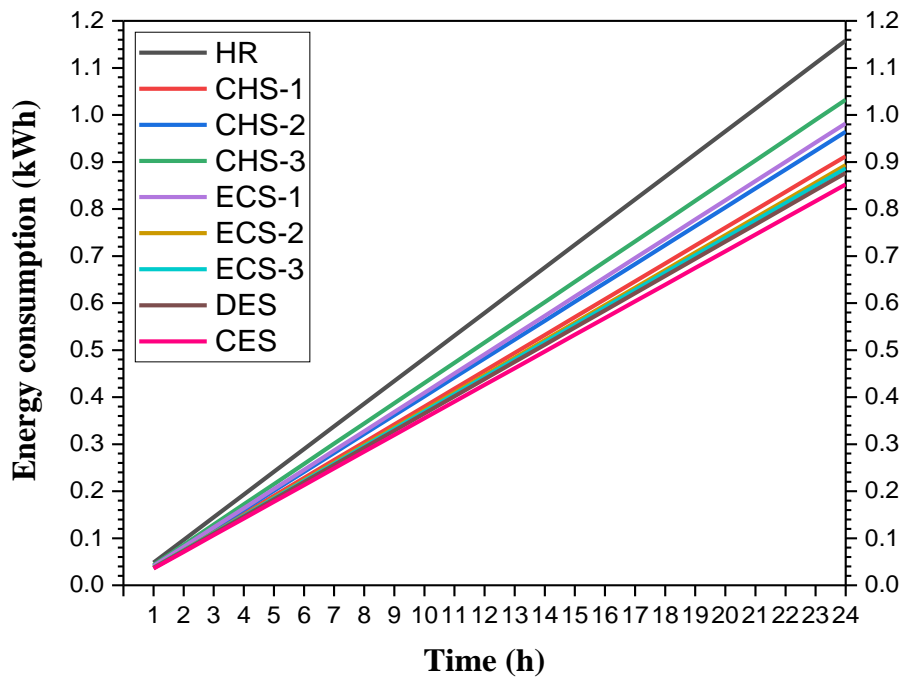


Figure 5.16. Energy consumptions vs. time.

5.6.3. DES and CES Experiments

Due to the effect of PCMs and NCPCM in cooling the condenser, these experiments operated at evaporation and condensation pressures between the

CHS-1 and HR experiments, as illustrated in Figure 5.4. An intermediate pressure indicated an intermediate mass flow rate but not compressor work and total operating time. The compressor's work and total operating time fall between CHS-1 and ECS-3. Therefore, these experiments provided the highest reduction in energy consumption. The main factors that helped in better energy savings were the mass flow rate between CHS-1 and HR tests, a shorter total work time than CHS-1, and the number of compressor cycles.

The decrease in temperature fluctuation in fridge cabinets caused by PCM panels was the difference between DES and CES. Consequently, the condensation and evaporation pressures in CES decreased more than in the DES because the panels served as the additional source of cooling during the off-time cycle of the compressor. As a result, evaporators removed less mass flow rate, the compressor performed less work, and there were fewer cycles than DES. Therefore, the reduction in energy consumption with CES was higher than with DES. Similarly, through simulation, (Cheng et al., 2017) demonstrated that DES saved 32% of energy, which was higher than the DES case in this study. Nevertheless, they used PCMs with higher thermal conductivities and lower latent heat of fusions than this study.

5.7. Coefficient of Performance (COP)

The COP of a refrigerator is the ratio of refrigeration capacity to energy consumption or refrigeration effect to compressor work done. The refrigerator with PCMs exhibited substantial enhancements in COPs, as seen in Figure 5.17. The refrigeration effect for all experiments is given in Table 5.2. The refrigeration effect is the difference between the inlet of the freezer evaporator and the outlet of the fridge evaporator's specific enthalpies. Here, the PCMs and NCPCM were also responsible for the change in refrigeration effect and compressor work.

According to the outcomes of the CHS tests, both the refrigeration effect and compressor work were enhanced compared to HR. As previously described in the energy consumption section, compressor work declined due to the fall in difference between compressor pressures. However, a growth in the refrigeration effects was due to the increase in the subcooling degree of the condenser. The higher subcooling degree than HR means the refrigerant entered the freezer evaporator at a lower temperature and enthalpy. So, the refrigerant left the fridge evaporator at a lower temperature and enthalpy. The relationship between condensation pressure and temperature with the degree of subcooling is inversely proportional. Despite the drop in both enthalpies, the amount of enthalpy decreased by subcooling was higher than by the outlet of the fridge evaporator. Thereby, the refrigeration effect rose significantly. Hence, the CHSs were superior to the ECSs in increasing COP.

Based on the relationship between condensation pressure and subcooling degree, the CHS-1 experiment gained the largest COP among all CHS experiments. The COP enhancement was higher than (Dandotiya and Banker, 2017) and lower than (Cheng et al., 2011) by 4.56% and 10.44%, respectively. The thermal conductivity of the PCM used by (Cheng et al., 2011) was about 4.5 times higher than the PCMs in this study.

On the other hand, for the ECS cases, the change in subcooling degree was opposite to the CHS experiments. As a result of the evaporators' removing heat from PCMs, the evaporator pressure climbed, which increased the condensation pressure. In turn, the subcooling degree decreased to below HR. This means the temperature and enthalpy of the inlet freezer evaporator were higher than the HR. Despite this, the refrigerant departed the fridge evaporator with a higher temperature and enthalpy. The fridge evaporator outlet raised enthalpy more than

subcooling. Thus, the refrigeration effect grew, but not more than in the CHS trials. It turned out that the ECSs were weaker than the CHSs in raising COP. The ECS-3 showed the highest COP in the ECS tests as the distilled water in the fridge cabinet had a higher capacity for absorbing energy. As well, a considerable decline in the compressor's work was another crucial point. For the same mass of PCM used, it optimized approximately the same amount of COP compared to published studies. The increase and decrease in the subcooling temperature of all tests compared to HR are shown in Table 5.2.

Due to the location of the condensation pressure between CHS-1 and HR, the experiments with the highest COP among the experiments were the DES and CES. The condensation pressure between CHS-1 and HR indicated that the increasing rate of subcooling degree was closer to that of the CHS-1. That is why the refrigeration effect was considerably nearer to that of CHS-1. In addition to that, the work performed by the compressor was minimal because they executed a minimal difference between compressor pressures among tests. Thus, they raised the COP at the highest rate. Since its pressures were lower than the DES, the CES improved COP better. A sample of calculation for COP is provided in Appendix M.

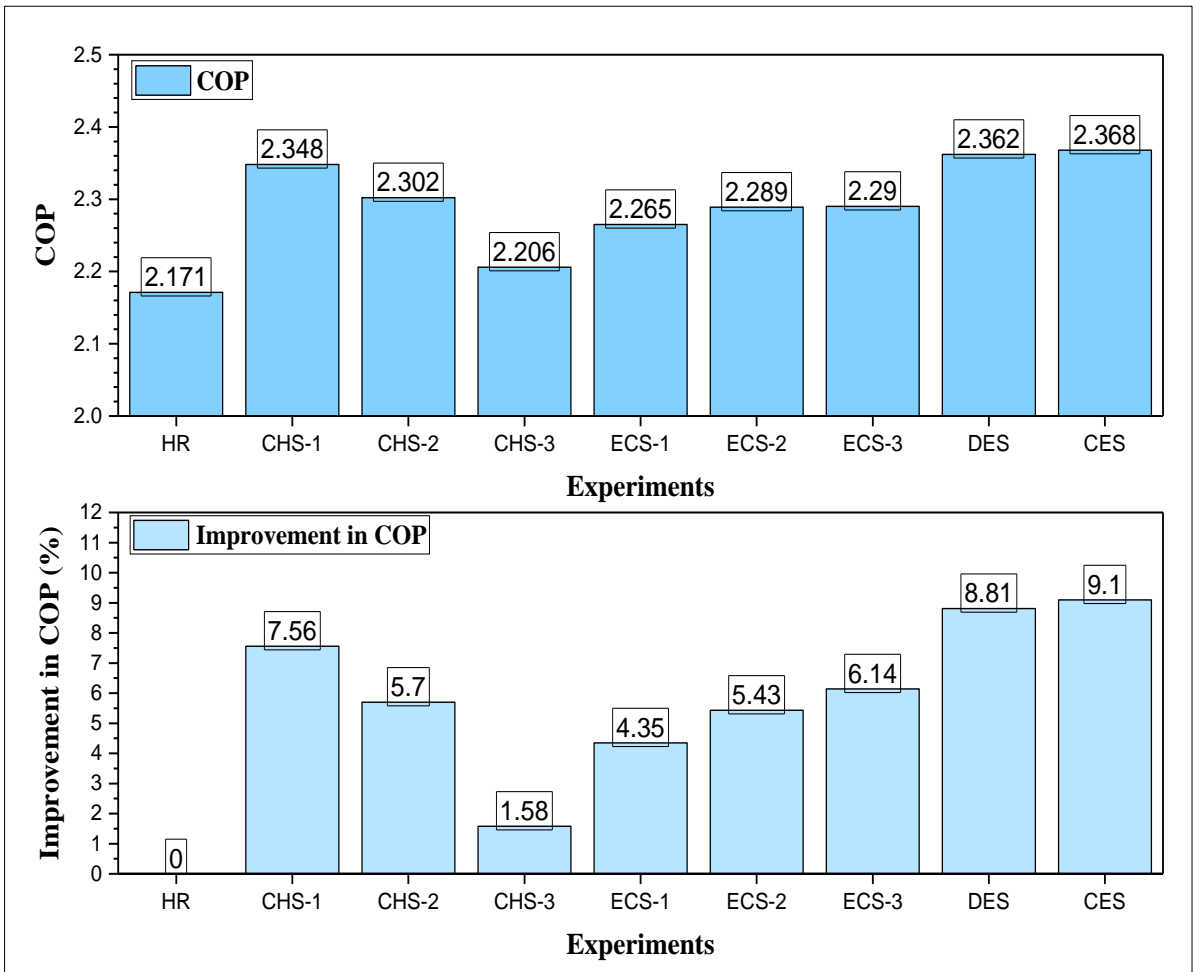


Figure 5.17. The COPs and their improvements.

CHAPTER 6

CONCLUSION AND FUTURE WORK

5.1. Conclusion

Refrigerators, directly and indirectly, contribute to the emission of greenhouse gases through refrigerant leakage and energy consumption, respectively. Alongside this, the desire to preserve the quality of foods and medicines is growing. Thus, this study aimed to optimize the overall performance of a household refrigerator using PCMs and nanoparticles experimentally. A refrigerator with (condenser heat storage, CHS), (evaporator cold storage, ECS), (dual energy storage, DES), and (combined energy storage, CES) is investigated and evaluated. As a result, the overall functionality of the refrigerator with PCM arrangements was enhanced through comprehensive analysis and experimental testing. Based on the experimental results, the following conclusions were drawn:

1. In improving the COP, the refrigerator with CHS designs was superior to ECS designs because of the substantial increase in subcooling degree and drop in compressor pressures. However, the DES design outperformed the CHS designs by achieving a refrigeration effect close to that of the CHS designs and the minimum difference between compressor pressures. Also, the CES showed better performance than the DES due to the efficiency of PCM panels in reducing compressor pressures and their difference as well as increasing the refrigeration effect further. The enhancements in COP were 4.35-6.14%, 1.58-

- 7.56%, 8.81%, and 9.1% for the ECSs, CHSs, DES, and CES, respectively, compared to HR.
2. In energy savings, the ECS setups were better than the CHS setups due to the lower total operating time and the number of compressor cycles. Nevertheless, DES setup provided a greater reduction in energy consumption than ECS setups, due to the lower mass flowrate removal by evaporators and less compressor work. The two factors that made the DES perform better energy savings improved with the PCM panel for CES. Also, the number of compressor cycles was reduced, so it used less energy to operate than DES. The savings in energy were 10.87-21.24%, 15.21-23.47%, 24.29%, and 26.42% for CHSs, ECSs, DES, and CES, respectively, compared to HR.
 3. For the average temperature of the fridge cabinet, the CHS layouts exhibited better temperature control as the fridge evaporator provided additional cooling to the cabinet. The DES and CES layouts outperformed the ECS layouts due to the condenser PCMs' capacity for cooling the fridge evaporator. The average temperature was 1.1°C, 0.97-1.2°C, 3.85-4.52°C, 3.83°C, and 3.77°C for HR, CHSs, ECSs, DES, and CES, respectively.
 4. For the average temperature of the freezer cabinet, the CES was the optimal case due to the decline in condensation and evaporation pressures and the increase in the operating time cycle. Together, the two factors prompted the evaporator to provide additional cooling to the cabinet. The CHS cases were better than the ECS cases as related to the decrease in evaporator temperatures. The average temperature was -21.24°C, -21.33 – -22.34°C, -19.3 – -20.08°C, -22.5°C, and -22.57°C for HR, CHSs, ECSs, DES, and CES, respectively.
 5. For the fluctuation temperature in both cabinets, the DES and CES tests exhibited a medium range between the CHS and ECS tests in the freezer

cabinet and the highest level in the fridge cabinet among the experiments. Also, due to the location of PCMs in the cabinets, ECS experiments performed better than CHS experiments. Although some experiments showed a spike in the average temperature of the cabinets, the temperature swings were considerably limited. Fortunately, both cabinets kept their average temperature under the ISO guidelines for the household refrigerator in a $25\pm 0.5^{\circ}\text{C}$ environment. The fluctuation improvements ranged between 15.53-56.53% and 0.61-26.46% for the fridge and freezer cabinets, respectively, compared to HR. This modification could preserve the quality of foods.

6. Overall, based on the aforementioned conclusions, the CES was the most efficient case in optimizing the overall refrigerator's performance due to the combination of the pros and cons of the CHS, ECS, and PCM panels.

5.2. Recommendations for Further Work

This study inspires further investigation. The following suggestions are areas that could benefit from further research:

- ❖ Using PCMs on the interior cabinet walls and placing the thermostat sensor within the cabinet rather than behind evaporators.
- ❖ Increasing the heat transfer rate of PCMs by enhancing their thermal properties with the addition of the suitable additives.
- ❖ Installing the PCMs between components of the refrigerator and PCM panels in the cabinets simultaneously.
- ❖ Inserting PCM panels with multiple PCM types into both cabinets.

REFERENCES

- Abdolmaleki, L., Sadrameli, S.M., Pirvaram, A., 2020. Application of environmental friendly and eutectic phase change materials for the efficiency enhancement of household freezers. *Renew. Energy* 145, 233–241.
- Abhat, A., 1983. Low temperature latent heat thermal energy storage: Heat storage materials. *Sol. Energy* 30, 313–332.
- American Society of Heating, R. and A.-C.E. (ASHRAE), 2018. 2018 ASHRAE Handbook, Ashrae.
- Apra, C., de Rossi, F., Greco, A., Renno, C., 2003. Refrigeration plant exergetic analysis varying the compressor capacity. *Int. J. Energy Res.* 27, 653–669.
- Arora, C.P., 2014. Refrigeration Air Conditioning, Nineteenth.
- Arshad, A., Jabbal, M., Yan, Y., 2020. Thermophysical characteristics and application of metallic-oxide based mono and hybrid nanocomposite phase change materials for thermal management systems. *Appl. Therm. Eng.* 181, 115999.
- Azzouz, K., Leducq, D., Gobin, D., 2008. Performance enhancement of a household refrigerator by addition of latent heat storage. *Int. J. Refrig.* 31, 892–901.
- Azzouz, K., Leducq, D., Gobin, D., 2009. Enhancing the performance of household refrigerators with latent heat storage: An experimental investigation. *Int. J. Refrig.* 32, 1634–1644.
- Azzouz, K., Leducq, D., Guilpart, J., Gobin, D., 2005. Improving the energy efficiency of a vapor compression system using a phase change material. In: *Second Conference on Phase Change Material and Slurry: Scientific Conference and Business Forum*. pp. 15–17.
- Baetens, R., Jelle, B.P., Gustavsen, A., 2010. Phase change materials for building applications: A state-of-the-art review. *Energy Build.* 42, 1361–1368.
- Bansal, P., Vineyard, E., Abdelaziz, O., 2011. Advances in household appliances- A review. *Appl. Therm. Eng.* 31, 3748–3760.

- Berdja, M., Yahi, F., Tetbirt, A., Ouali, M., Djebiret, M.A., Mokrane, M., 2020. Theoretical analysis of two evaporator configurations for a conventional refrigerator coupled to a phase change material. In: IOP Conference Series: Materials Science and Engineering. IOP Publishing, p. 12014.
- Bista, S., Hosseini, S.E., Owens, E., Phillips, G., 2018. Performance improvement and energy consumption reduction in refrigeration systems using phase change material (PCM). *Appl. Therm. Eng.* 142, 723–735.
- Cabeza, L.F., Martorell, I., Miró, L., Fernández, A.I., Barreneche, C., Cabeza, L.F., Fernández, A.I., Barreneche, C., 2021. 1 - Introduction to thermal energy storage systems. In: Cabeza, L.F. (Ed.), *Advances in Thermal Energy Storage Systems (Second Edition)*, Woodhead Publishing Series in Energy. Woodhead Publishing, pp. 1–33.
- Cerri, G., Palmieri, A., Monticelli, E., Pezzoli, D., 2003. Identification of domestic refrigerator models including cool storage. In: *International Congress of Refrigeration*. Washington DC.
- Cheng, W.-L., Mei, B.-J., Liu, Y.-N., Huang, Y.-H., Yuan, X.-D., 2011. A novel household refrigerator with shape-stabilized PCM (Phase Change Material) heat storage condensers: An experimental investigation. *Energy* 36, 5797–5804.
- Cheng, W.-L., Yuan, X.-D., 2013. Numerical analysis of a novel household refrigerator with shape-stabilized PCM (phase change material) heat storage condensers. *Energy* 59, 265–276.
- Cheng, W., Ding, M., Yuan, X., Han, B.-C., 2017. Analysis of energy saving performance for household refrigerator with thermal storage of condenser and evaporator. *Energy Convers. Manag.* 132, 180–188.
- Cheng, W., Zhang, R., Xie, K., Liu, N., Wang, J., 2010. Heat conduction enhanced shape-stabilized paraffin/HDPE composite PCMs by graphite addition: Preparation and thermal properties. *Sol. Energy Mater. Sol. Cells* 94, 1636–1642.
- Cofré-Toledo, J., Vasco, D.A., Isaza-Roldán, C.A., Tangarife, J.A., 2018. Evaluation of an integrated household refrigerator evaporator with two eutectic phase-change materials. *Int.*

Refrig. 93, 29–37.

CP, A., 2000. Refrigeration and Air Conditioning.

Cuevas, C., Lebrun, J., 2009. Testing and modelling of a variable speed scroll compressor. Appl. Therm. Eng. 29, 469–478.

Dandotiya, D., Banker, N.D., 2017. Performance enhancement of a refrigerator using phase change material-based condenser: an experimental investigation. Int. J. Air-Conditioning Refrig. 25, 1750032.

Dincer, I., Rosen, M.A., 2021. Thermal energy storage systems and applications. John Wiley & Sons.

Directive, C., 1992. 92/75/EEC of 22 September 1992 on the indication by labelling and standard product information of the consumption of energy and other resources by household appliances. Off. J. L 297, 10.

Dong, Y., Coleman, M., Miller, S.A., 2021. Greenhouse Gas Emissions from Air Conditioning and Refrigeration Service Expansion in Developing Countries. Annu. Rev. Environ. Resour. 46, 59–83.

Dupont, J.-L., Domanski, P., Lebrun, P., Ziegler, F., 2019. The role of refrigeration in the global economy-38. Informatory Note on Refrigeration Technologies.

Ekren, O., Celik, S., Noble, B., Krauss, R., 2013. Performance evaluation of a variable speed DC compressor. Int. J. Refrig. 36, 745–757.

Elarem, R., Mellouli, S., Abhilash, E., Jemni, A., 2017. Performance analysis of a household refrigerator integrating a PCM heat exchanger. Appl. Therm. Eng. 125, 1320–1333.

ENERGY, S., 1998. ENERGY STAR program. http://www.energystar.gov/index.cfm?c=Vent.pr_vent_fans.

Fernandez, A.I., Martínez, M., Segarra, M., Martorell, I., Cabeza, L.F., 2010. Selection of materials with potential in sensible thermal energy storage. Sol. Energy Mater. Sol. Cells 94, 1723–1729.

Gao, X., Zhang, W., Fang, Z., Hou, X., Zhang, X., 2020. Analysis of melting and solidification

- processes in the phase-change device of an energy storage interconnected heat pump system. AIP Adv. 10, 55021.
- Gin, B., Farid, M.M., 2010. The use of PCM panels to improve storage condition of frozen food. J. Food Eng. 100, 372–376.
- Gin, B., Farid, M.M., Bansal, P., 2011. Modeling of phase change material implemented into cold storage application. HVAC\&R Res. 17, 257–267.
- Gin, B., Farid, M.M., Bansal, P.K., 2010. Effect of door opening and defrost cycle on a freezer with phase change panels. Energy Convers. Manag. 51, 2698–2706.
- Hamad, G. Ben, Younsi, Z., Naji, H., Salaün, F., 2021. A Comprehensive Review of Microencapsulated Phase Change Materials Synthesis for Low-Temperature Energy Storage Applications. Appl. Sci. 11, 11900.
- Han, L., Ma, G., Xie, S., Sun, J., Jia, Y., Jing, Y., 2017. Preparation and characterization of the shape-stabilized phase change material based on sebacic acid and mesoporous MCM-41. J. Therm. Anal. Calorim. 130, 935–941.
- Hartmann, D., Melo, C., 2013. Popping noise in household refrigerators: Fundamentals and practical solutions. Appl. Therm. Eng. 51, 40–47.
- Holman, J.P., 1986. Heat transfer. McGraw Hill.
- Holman, J.P., 2021. Experimental Methods for Engineers EIGHTH EDITION.
- Hosseini, S.E., Wahid, M.A., 2016. Hydrogen production from renewable and sustainable energy resources: Promising green energy carrier for clean development. Renew. Sustain. Energy Rev. 57, 850–866.
- Hu, H., Jin, X., Zhang, X., 2017. Effect of supercooling on the solidification process of the phase change material. Energy procedia 105, 4321–4327.
- Ibrahim, N.I., Al-Sulaiman, F.A., Rahman, S., Yilbas, B.S., Sahin, A.Z., 2017. Heat transfer enhancement of phase change materials for thermal energy storage applications: A critical review. Renew. Sustain. Energy Rev. 74, 26–50.
- ISO 15502:2005 Household refrigerating appliances — Characteristics and test methods, 2005.

- Joybari, M.M., Haghghat, F., Moffat, J., Sra, P., 2015. Heat and cold storage using phase change materials in domestic refrigeration systems: The state-of-the-art review. *Energy Build.* 106, 111–124.
- Karthikeyan, A., Aakash Sivan, V., Maher khaliq, A., Anderson, A., 2021. Performance improvement of vapour compression refrigeration system using different phase changing materials. *Mater. Today Proc.* 44, 3540–3543.
- Kasinathan, D., Kumaresan, V., 2021. Study on the effect of inclusion of thermal energy storage unit in the energy performance of a household refrigerator. *Heat Mass Transf.* 57, 1753–1761.
- Kato, Y., 2007. CHEMICAL ENERGY CONVERSION TECHNOLOGIES FOR EFFICIENT ENERGY USE. In: Paksoy, H.Ö. (Ed.), *Thermal Energy Storage for Sustainable Energy Consumption*. Springer Netherlands, Dordrecht, pp. 377–391.
- Kenisarin, M.M., 2014. Thermophysical properties of some organic phase change materials for latent heat storage. A review. *Sol. Energy* 107, 553–575.
- Khan, Ibrahim, Saeed, K., Khan, Idrees, 2019. Nanoparticles: Properties, applications and toxicities. *Arab. J. Chem.* 12, 908–931.
- Khan, M.I.H., Afroz, H.M.M., 2011. An experimental investigation of the effects of Phase Change Material on Coefficient of performance (COP) of a household refrigerator. In: *Proceedings of the International Conference on Mechanical Engineering and Renewable Energy*.
- Kumar, P.M., Elakkiyadasan, R., Sathishkumar, N., Prabhu, G.A., Balasubramanian, T., 2020. Performance enhancement of a domestic refrigerator with nanoparticle enhanced PCM over the condenser side. *FME Trans.* 48, 620–627.
- Kumar, V., Ranjan, D., Verma, K., 2021. Global climate change: the loop between cause and impact. In: *Global Climate Change*. Elsevier, pp. 187–211.
- Kumar, V., Shrivastava, R., Nandan, G., 2016. Energy saving using phase change material in refrigerating system. *Third Int. Conf. Manuf. Excell.* 184–190.

- Kürklü, A., 1998. Energy storage applications in greenhouses by means of phase change materials (PCMs): a review. *Renew. Energy* 13, 89–103.
- Lane, George A, Lane, G A, 1983. *Solar heat storage: latent heat materials*. CRC press Boca Raton, FL, USA:
- Li, G., 2016. Sensible heat thermal storage energy and exergy performance evaluations. *Renew. Sustain. Energy Rev.* 53, 897–923.
- Liang, N., Shao, S., Tian, C., Yan, Y., 2010. Dynamic simulation of variable capacity refrigeration systems under abnormal conditions. *Appl. Therm. Eng.* 30, 1205–1214.
- Magendran, S.S., Khan, F.S.A., Mubarak, N.M., Vaka, M., Walvekar, R., Khalid, M., Abdullah, E.C., Nizamuddin, S., Karri, R.R., 2019. Synthesis of organic phase change materials (PCM) for energy storage applications: A review. *Nano-Structures & Nano-Objects* 20, 100399.
- Maiorino, A., Del Duca, M.G., Mota-Babiloni, A., Greco, A., Aprea, C., 2019. The thermal performances of a refrigerator incorporating a phase change material. *Int. J. Refrig.* 100, 255–264.
- Manini, P., 2001. Vacuum Insulation Panels (VIPs) Technology: A Viable Route to Improve Energy Efficiency in Domestic Refrigerators and Freezers. In: Bertoldi, P., Ricci, A., de Almeida, A. (Eds.), *Energy Efficiency in Household Appliances and Lighting*. Springer Berlin Heidelberg, Berlin, Heidelberg, pp. 122–127.
- Manting, F., Xuelai, Z., Jun, J.I., Weisan, H.U.A., Biao, L.I.U., Xuzhe, W., 2019. Progress in hydrated salt based composite phase change materials. *Energy Storage Sci. Technol.* 8, 709.
- Marques, A.C., Davies, G.F., Evans, J.A., Maidment, G.G., Wood, I.D., 2013. Theoretical modelling and experimental investigation of a thermal energy storage refrigerator. *Energy* 55, 457–465.
- Mastani Joybari, M., Haghghat, F., Moffat, J., Sra, P., 2015. Heat and cold storage using phase change materials in domestic refrigeration systems: The state-of-the-art review. *Energy Build.* 106, 111–124.

- Md Imran Hossen, K., Afroz, H., 2011. An Experimental investigation of the effects of phase change material on Coefficient of Performance (COP) of a household refrigerator.
- Mehling, H., Cabeza, L.F., 2008. Heat and cold storage with PCM. *Heat mass Transf.* 11–55.
- Mohamed, S.A., Al-Sulaiman, F.A., Ibrahim, N.I., Zahir, M.H., Al-Ahmed, A., Saidur, R., Yılbaş, B.S., Sahin, A.Z., 2017. A review on current status and challenges of inorganic phase change materials for thermal energy storage systems. *Renew. Sustain. Energy Rev.* 70, 1072–1089.
- Nazir, H., Batool, M., Bolivar Osorio, F.J., Isaza-Ruiz, M., Xu, X., Vignarooban, K., Phelan, P., Inamuddin, Kannan, A.M., 2019. Recent developments in phase change materials for energy storage applications: A review. *Int. J. Heat Mass Transf.* 129, 491–523.
- Omara, A.A.M., Abuelnuor, A.A.A., Dafaallah, M.A.A., Ali, A.M.A., Alshoubli, M.A.M., 2018. Energy and Exergy analysis of solar water heating system integrated with phase change material (PCM). In: 2018 International Conference on Computer, Control, Electrical, and Electronics Engineering (ICCCEEE). pp. 1–5.
- Omara, A.A.M., Mohammedali, A.A.M., 2020. Thermal management and performance enhancement of domestic refrigerators and freezers via phase change materials: A review. *Innov. Food Sci. Emerg. Technol.* 66, 102522.
- Opolot, M., Zhao, C., Liu, M., Mancin, S., Bruno, F., Hooman, K., 2020. Influence of cascaded graphite foams on thermal performance of high temperature phase change material storage systems. *Appl. Therm. Eng.* 180, 115618.
- Oró, E., Miró, L., Farid, M.M., Cabeza, L.F., 2012. Thermal analysis of a low temperature storage unit using phase change materials without refrigeration system. *Int. J. Refrig.* 35, 1709–1714.
- Oró, E., Miró, L., Farid, M.M., Martin, V., Cabeza, L.F., 2014. Energy management and CO₂ mitigation using phase change materials (PCM) for thermal energy storage (TES) in cold storage and transport. *Int. J. Refrig.* 42, 26–35.
- Pavithran, A., Sharma, M., Shukla, A.K., 2021. An investigation on the effect of PCM incorporation in refrigerator through CFD simulation. *Mater. Today Proc.* 46, 5555–5564.

- Pingali, P., 2007. Westernization of Asian diets and the transformation of food systems: Implications for research and policy. *Food Policy* 32, 281–298.
- Pirvaram, A., Sadrameli, S.M., Abdolmaleki, L., 2019. Energy management of a household refrigerator using eutectic environmental friendly PCMs in a cascaded condition. *Energy* 181, 321–330.
- Qureshi, Z.A., Ali, H.M., Khushnood, S., 2018. Recent advances on thermal conductivity enhancement of phase change materials for energy storage system: A review. *Int. J. Heat Mass Transf.* 127, 838–856.
- Rahman, R., Hossain, M.A., Das, S.K., Hasan, A., 2014. Performance improvement of a domestic refrigerator by using PCM (phase change material). *Glob. J. Res. Eng.*
- Raveendran, P.S., Murugan, P.C., 2021. Energy Conservation on Vapour Compression Refrigeration System using PCM. In: *IOP Conference Series: Materials Science and Engineering*. IOP Publishing, p. 12106.
- Raveendran, S., Sekhar, J., 2016. Exergy analysis of a domestic refrigerator with brazed plate heat exchanger as condenser. *J. Therm. Anal. Calorim.*
- Rostami, S., Afrand, M., Shahsavari, A., Sheikholeslami, M., Kalbasi, R., Aghakhani, S., Shadloo, M.S., Oztop, H.F., 2020. A review of melting and freezing processes of PCM/nano-PCM and their application in energy storage. *Energy* 211, 118698.
- Sharma, A., Tyagi, V. V, Chen, C.R., Buddhi, D., 2009. Review on thermal energy storage with phase change materials and applications. *Renew. Sustain. Energy Rev.* 13, 318–345.
- Sidik, N.A.C., Kean, T.H., Chow, H.K., Rajaandra, A., Rahman, S., Kaur, J., 2018. Performance enhancement of cold thermal energy storage system using nanofluid phase change materials: A review. *Int. Commun. Heat Mass Transf.* 94, 85–95.
- Sonnenrein, G., Elsner, A., Baumhögger, E., Morbach, A., Fieback, K., Vrabec, J., 2015. Reducing the power consumption of household refrigerators through the integration of latent heat storage elements in wire-and-tube condensers. *Int. J. Refrig.* 51, 154–160.
- Trias, F.X., Olliet, C., Rigola, J., Pérez-Segarra, C.D., 2018. A simple optimization approach for

- the insulation thickness distribution in household refrigerators. *Int. J. Refrig.* 93, 169–175.
- Veerakumar, C., Sreekumar, A., 2016. Phase change material based cold thermal energy storage: Materials, techniques and applications – A review. *Int. J. Refrig.* 67, 271–289.
- Verma, S., Singh, H., 2020. Vacuum insulation panels for refrigerators. *Int. J. Refrig.* 112, 215–228.
- Vine, E., du Pont, P., Waide, P., 2001. Evaluating the impact of appliance efficiency labeling programs and standards: process, impact, and market transformation evaluations. *Energy* 26, 1041–1059.
- Wahid, M.A., Hosseini, S.E., Hussen, H.M., Akeiber, H.J., Saud, S.N., Mohammad, A.T., 2017. An overview of phase change materials for construction architecture thermal management in hot and dry climate region. *Appl. Therm. Eng.* 112, 1240–1259.
- Wang, R.Z., Xu, Z.Y., Ge, T.S., 2016. 1 - Introduction to solar heating and cooling systems. In: Wang, R.Z., Ge, T.S. (Eds.), *Advances in Solar Heating and Cooling*. Woodhead Publishing, pp. 3–12.
- Wang, X., Lu, E., Lin, W., Liu, T., Shi, Z., Tang, R., Wang, C., 2000. Heat storage performance of the binary systems neopentyl glycol/pentaerythritol and neopentyl glycol/trihydroxy methyl-aminomethane as solid–solid phase change materials. *Energy Convers. Manag.* 41, 129–134.
- Waterman, A.T., 1917. XXI. On the positive ionization from certain hot salts, together with some observations on the electrical properties of molybdenite at high temperatures. London, Edinburgh, Dublin *Philos. Mag. J. Sci.* 33, 225–247.
- Yanping, Y., Wenquan, T., Xiaoling, C., Li, B., 2011. Theoretic prediction of melting temperature and latent heat for a fatty acid eutectic mixture. *J. Chem. Eng. Data* 56, 2889–2891.
- Yusufoglu, Y., Apaydin, T., Yilmaz, S., Paksoy, H.O., 2015. Improving performance of household refrigerators by incorporating phase change materials. *Int. J. Refrig.* 57, 173–185.

Zeinelabdein, R., Omer, S., Gan, G., 2018. Critical review of latent heat storage systems for free cooling in buildings. *Renew. Sustain. Energy Rev.* 82, 2843–2868.

Zhang, H., Baeyens, J., Cáceres, G., Degrève, J., Lv, Y., 2016. Thermal energy storage: Recent developments and practical aspects. *Prog. Energy Combust. Sci.* 53, 1–40.

APPENDIX (A)

CALIBRATION OF ENERGY DATA LOGGER

A.1. Results of Calibration of Energy Data Logger.

Household Device	Universal digital multimeter UNI-T UT89X			Zhurui power recorder (PR10)			Watt Error%
	Ampere	Voltage	Watt	Ampere	Voltage	Watt	
Television	0.551	217.70	119.95	0.552	217.37	119.99	0.03
Refrigerator	1.043	232.20	242.18	1.041	231.79	241.29	0.37
Microwave	3.172	221.11	701.36	3.181	220.33	700.87	0.07
Steam iron	5.822	223.00	1298.37	5.849	222.30	1300.23	0.14
Hair dryer	6.878	218.03	1499.61	6.882	217.21	1494.84	0.32
Vacuum cleaner	8.460	226.5	1916.19	8.441	227.50	1920.38	0.22
Average watt error %							0.19

APPENDIX (B)

CALIBRATION OF PRESSURE GAUGE

B.1. Results of Calibration of Pressure Gauges.

Low pressure calibration (psi)			High pressure calibration (psi)		
Hongsen low side	Elitech PGW-500	error %	Hongsen high side	Elitech PGW-500	error %
-13.5	-13.453	0.35	80	80.2	0.37
-10	-9.977	0.23	92	91.8	0.22
-2.5	2.490	0.40	106	106.5	0.47
5.5	4.523	0.42	115	114.5	0.44
12	11.98	0.17	125	124.8	0.16
Average error %		0.35	Average error %		0.33

APPENDIX (C)

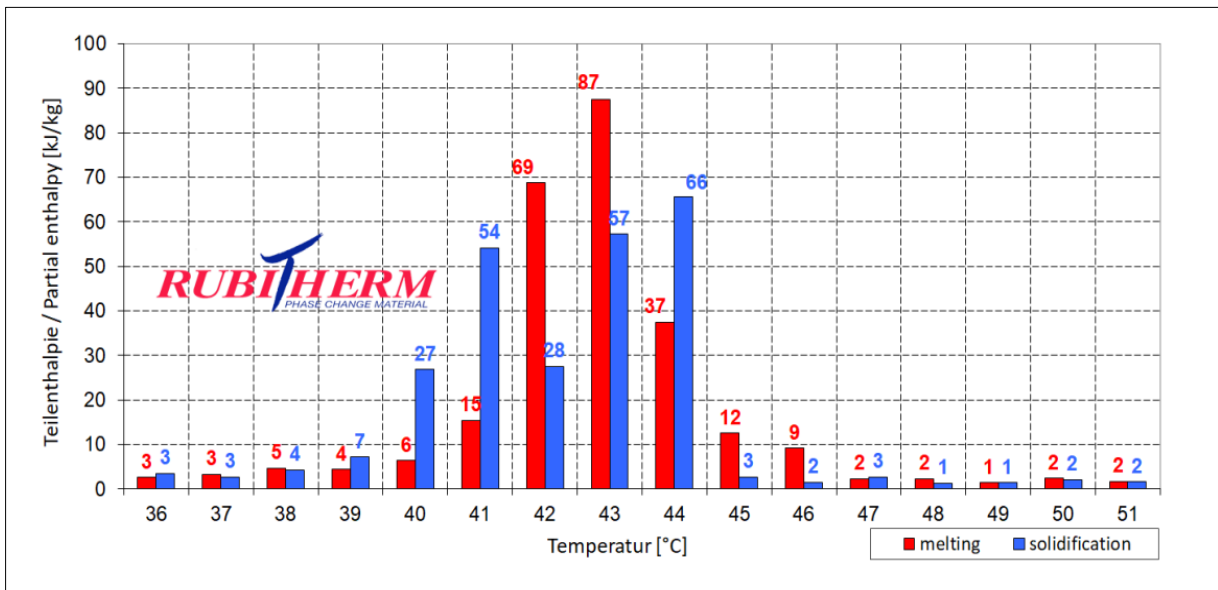
CALIBRATION OF TEMPERATURE SENSORS

C.1. Results of Calibration of Temperature Sensors.

Locations	Temperatures		
	RTD sensor	J-type Thermocouple	error %
Discharge of compressor	73.43	73.31	0.163
Top of condenser	48.88	48.98	0.204
Middle of condenser	40.27	40.40	0.322
Bottom of condenser	27.71	27.64	0.253
Inside fridge cabinet	2.10	2.11	0.474
Outlet of evaporator (fridge)	-15.04	-15.11	0.463
Inside freezer cabinet	-22.15	-22.22	0.315
Inlet of evaporator (freezer)	-29.90	-30.03	0.433
Average error %			0.328

APPENDIX (D)

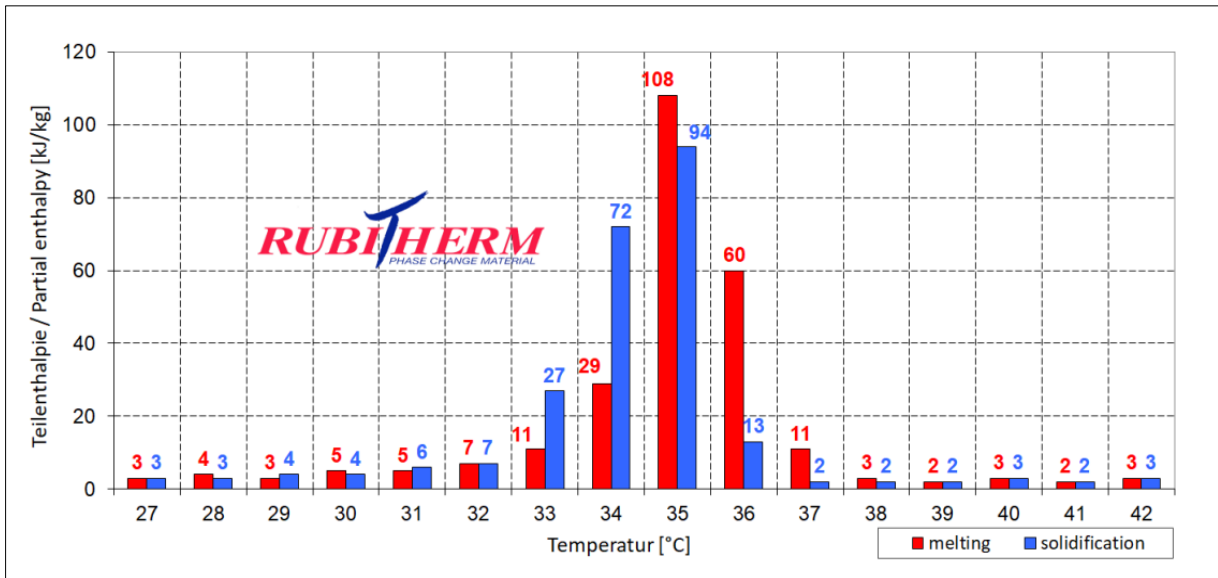
DSC GRAPH FOR RT44HC PCM



D.1. DSC graph of latent heat of fusion vs. temperature for RT44HC.

APPENDIX (E)

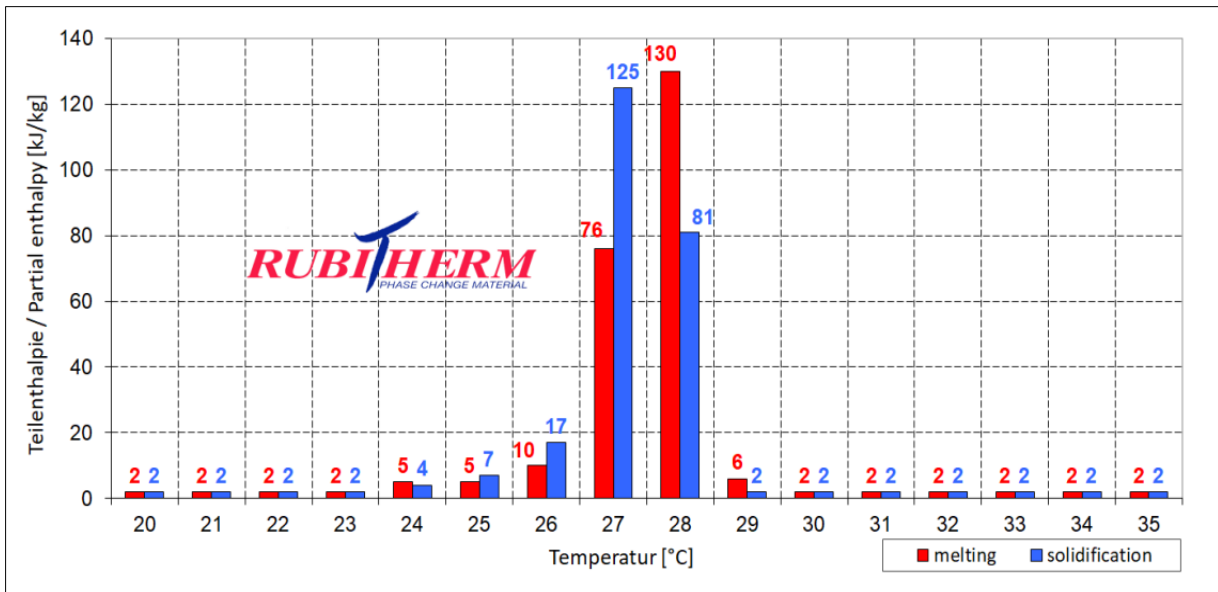
DSC GRAPH FOR RT35HC PCM



E.1. DSC graph of latent heat of fusion vs. temperature for RT35HC.

APPENDIX (F)

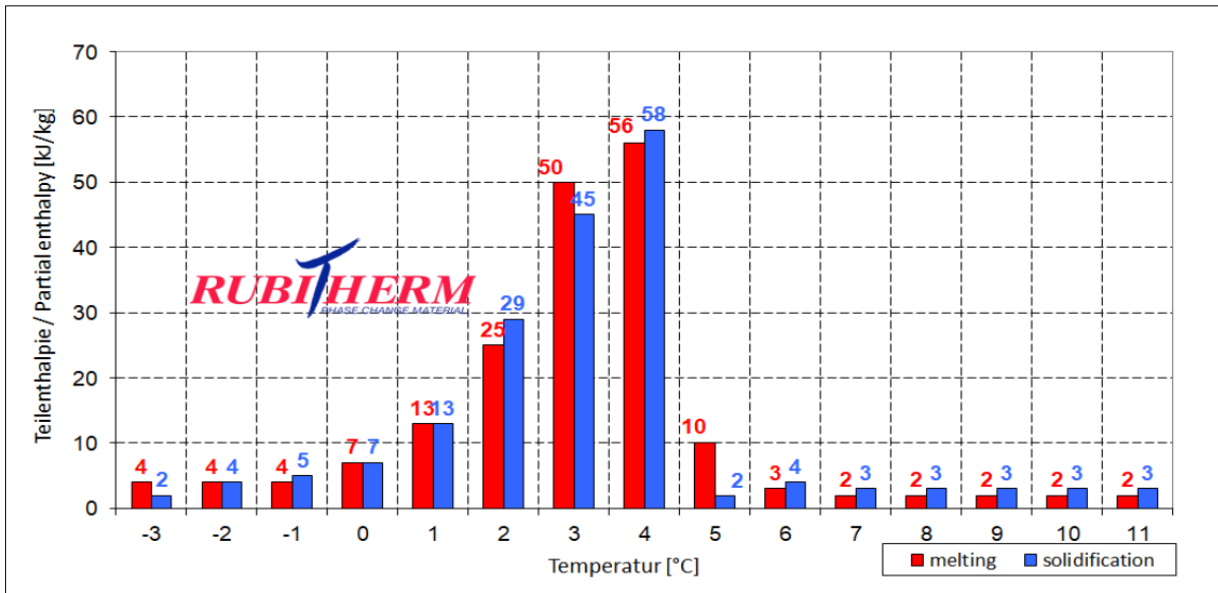
DSC GRAPH FOR RT28HC PCM



F.1. DSC graph of latent heat of fusion vs. temperature for RT28HC.

APPENDIX (G)

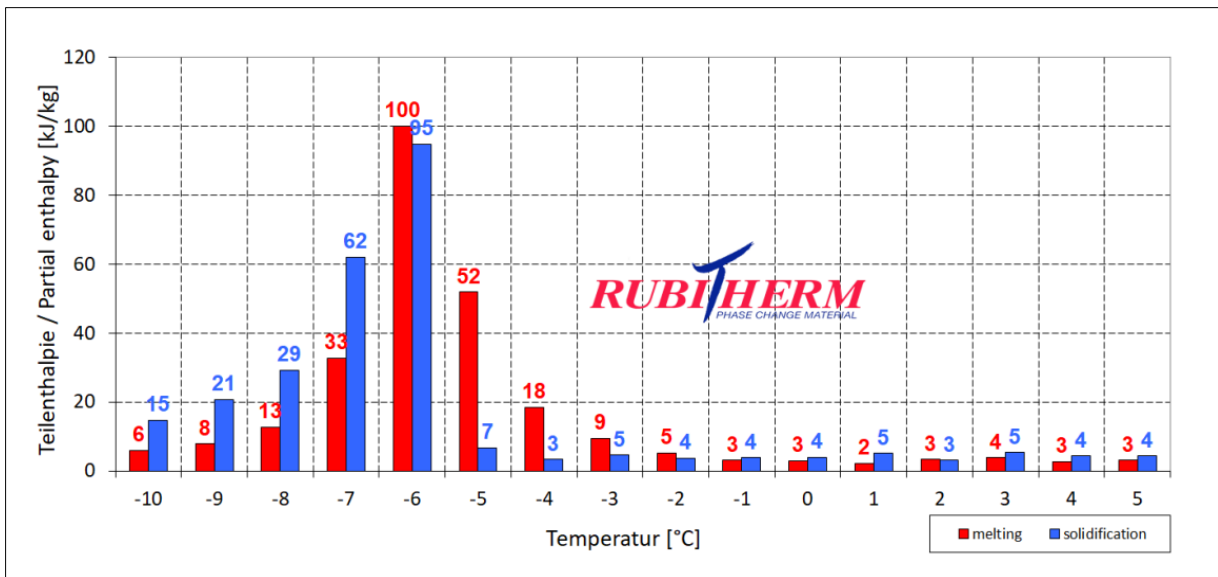
DSC GRAPH FOR RT4 PCM



G.1. DSC graph of latent heat of fusion vs. temperature for RT4.

APPENDIX (H)

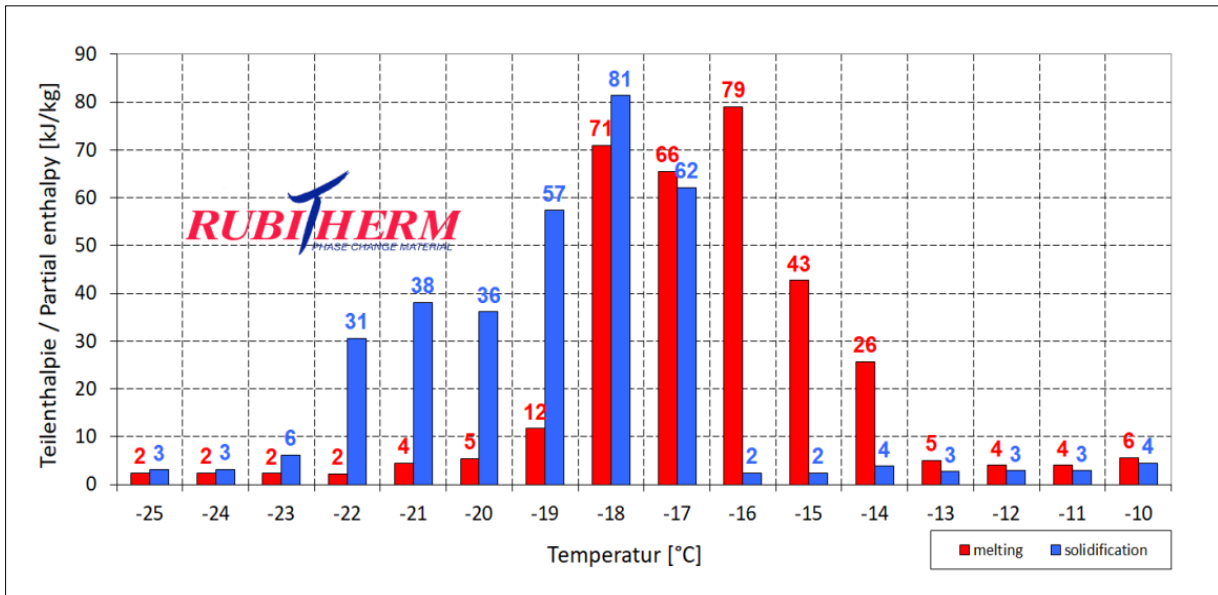
DSC GRAPH FOR SP-7 PCM



H.1. DSC graph of latent heat of fusion vs. temperature for SP-7.

APPENDIX (I)

DSC GRAPH FOR SP-17 PCM



I.1. DSC graph of latent heat of fusion vs. temperature for SP-17.

APPENDIX (J)

SAMPLE CALCULATION OF MASS FOR CONDENSER

J.1. Calculation of Mass Required for the Condenser

In this section, the condenser heat rejection for HR case is determined. Based on Eq. (3.5), the \dot{M}_{ref} , inlet specific enthalpy h_2 of condenser and outlet specific enthalpy h_3 of condenser are required. The \dot{M}_{ref} can be calculated using Eq. (3.4). In Eq. (3.4) the work done by compressor w and energy consumption E are also required.

The w can be obtained using Eq. (3.2). In this equation, the enthalpy for the suction of the compressor h_1 is required. The enthalpies are determined using the Danfoss Coolselector®2 program by condenser and evaporator pressures and temperatures, as given in Table 5.2. Additionally, the energy consumption was obtained from the data logger. The results are below.

$$h_1 = 536.6 \text{ kJ/kg}$$

$$h_2 = 661.3 \text{ kJ/kg}$$

$$h_3 = 265.9 \text{ kJ/kg}$$

$$E = 0.121 \text{ kW}$$

Thus, the work done is:

$$w = h_2 - h_1$$

$$w = 661.3 - 536.6$$

$$w = 124.7 \text{ kJ/kg}$$

And, the refrigerant mass flow rate is:

$$\dot{M}_{ref} = \frac{E}{w}$$

$$\dot{M}_{ref} = \frac{0.121}{124.7}$$

$$\dot{M}_{ref} = 0.000973 \text{ kg/s}$$

Then, the condenser heat rejection is:

$$Q_H = \dot{M}_{ref} \times (h_2 - h_3)$$

$$Q_H = 0.000973 \times (661.3 - 265.9)$$

$$Q_H = 0.385 \text{ kW}$$

Finally, according to Eq. (3.23), the amount of mass required for condenser is:

$$M = \frac{Q_H \times T_{on}}{h_f}$$

$$M = \frac{0.385 \times 8.80 \times 60}{250}$$

$$M = 0.813 \text{ kg}$$

APPENDIX (K)

SAMPLE CALCULATION OF MASS FOR EVAPORATORS

K.1. Calculation of Mass Required for the Evaporators

Based on Eq. (3.7), the evaporators heat extraction for HR experiment included \dot{M}_{ref} , inlet specific enthalpy h_4 of freezer evaporator and outlet specific enthalpy h_1 of fridge evaporator. The \dot{M}_{ref} and the outlet specific enthalpy h_1 of fridge evaporator (suction of the compressor) are found in the **Appendix J**. However, the inlet specific enthalpy h_4 of the freezer evaporator is the same as the outlet specific enthalpy h_3 of the condenser due to the capillary tube.

$$h_1 = 536.6 \text{ kJ/kg}$$

$$h_4 = 265.9 \text{ kJ/kg}$$

Hence, the evaporators heat extraction is:

$$Q_L = \dot{M}_{ref} \times (h_1 - h_4)$$

$$Q_L = 0.000973 \times (536.6 - 265.9)$$

$$Q_L = 0.262 \text{ kW}$$

Finally, according to Eq. (3.24), the required mass for the evaporators:

$$M = \frac{Q_L \times T_{on}}{h_f}$$

$$M = \frac{0.262 \times 8.80 \times 60}{300}$$

$$M = 0.476 \text{ kg}$$

APPENDIX (L)

UNCERTAINTY ANALYSIS

L.1. Uncertainty Analysis for the Temperature Sensors

L.1. Example of temperature sensor readings.

x_i (°C)	$x_i - \bar{x}$	$(x_i - \bar{x})^2$
48.9	-0.23	0.0529
48.7	-0.03	0.0009
48.5	0.17	0.0289
48.6	0.07	0.0049
48.7	-0.03	0.0009
48.5	0.17	0.0289
48.9	-0.23	0.0529
48.6	0.07	0.0049
48.7	-0.03	0.0009
48.6	0.07	0.0049

\bar{x} (°C)	48.67
Number of readings (N)	10

The uncertainty of temperature sensors can be determined by:

$$U = \sqrt{\frac{\sum_{i=1}^n (x_i - \bar{x})^2}{N \times (N-1)}}$$

$$U = \sqrt{\frac{0.181}{10 \times (10-1)}}$$

$$U = \pm 0.044$$

L.2. Uncertainty Analysis for the Elitech PGW-500 Pressure Gauge

L.2. Example of pressure gauge readings.

x_i (bar)	$x_i - \bar{x}$	$(x_i - \bar{x})^2$
0.358	0.015	0.000225
0.358	0.015	0.000225
0.395	- 0.022	0.000484
0.358	0.015	0.000225
0.395	- 0.022	0.000484
0.358	0.015	0.000225
0.358	0.015	0.000225
0.395	- 0.022	0.000484
0.395	- 0.022	0.000484
0.358	0.015	0.000225

(\bar{x}) (bar)	0.373
Number of readings (N)	10

The uncertainty of temperature sensors can be determined by:

$$U = \sqrt{\frac{\sum_{i=1}^n (x_i - \bar{x})^2}{N \times (N-1)}}$$

$$U = \sqrt{\frac{0.003286}{10 \times (10-1)}}$$

$$U = \pm 0.006$$

APPENDIX (M)

SAMPLE CALCULATION OF COP

M.1. COP Calculation

In this part, the COP for the HR test is calculated using Eq. (3.21). This equation involved four specific enthalpies at the inlet and outlet of the compressor and evaporators. The enthalpies have been identified in the **Appendices J and K**.

Therefore, the COP is:

$$COP = \frac{\text{Refrigeration effect}}{\text{Compressor work done}} = \frac{h_1 - h_4}{h_2 - h_1}$$

$$COP = \frac{536.6 - 265.9}{661.3 - 536.6}$$

$$COP = 2.17$$

LIST OF PUBLICATIONS



JP Journal of Heat and Mass Transfer

© 2023 Pushpa Publishing House, Prayagraj, India

<http://www.pphmj.com>

<http://dx.doi.org/10.17654/0973576323028>

Volume 33, 2023, Pages 135-154

P-ISSN: 0973-5763

PERFORMANCE ENHANCEMENT OF A HOUSEHOLD REFRIGERATOR USING SINGLE AND DOUBLE PHASE CHANGE MATERIALS (PCM) ON THE EVAPORATOR: EXPERIMENTAL STUDY

Darawan Bazyan Dhahir* and Ahmed Mohammed Adham

Department of Technical Mechanical and Energy Engineering

Erbil Technical Engineering College

Erbil Polytechnic University

Erbil, Iraq

e-mail: darawan99L@gmail.com

Abstract

A refrigerator is the most common and efficient method for preserving food and medicine, although its continuous operation consumes a considerable amount of household energy. Accordingly, optimizing its energy consumption is required. Thus, this study investigated a household refrigerator's overall functionality with phase change materials (PCMs) on the evaporator. The tests involved the application

Received: March 3, 2023; Accepted: April 12, 2023

Keywords and phrases: household refrigerator, evaporator, phase change material, coefficient of performance.

*Corresponding author

How to cite this article: Darawan Bazyan Dhahir and Ahmed Mohammed Adham, Performance enhancement of a household refrigerator using single and double phase change materials (PCM) on the evaporator: experimental study, JP Journal of Heat and Mass Transfer 33 (2023), 135-154. <http://dx.doi.org/10.17654/0973576323028>

This is an open access article under the CC BY license (<http://creativecommons.org/licenses/by/4.0/>).

Published Online: May 18, 2023



زانكۆی پۆلیتیه كنیکی ههولیر ERBIL POLYTECHNIC UNIVERSITY

بهرزکردنهوهی ئهدای ساردكهرهوهیهکی مأل به بهكارهینانی مادهكانی گۆرینی قوناغ
(Phase Change Materials, PCMs) و نانۆگهردیلهكان (Nanoparticles)

تیزیکه

پیشكهشی ئهنجومهنی كۆلیژی تهكنیکی ئهنذاریاری ههولیر كراوه له زانكۆی پۆلیتیهكنیکی ههولیر له
بهشیکه جیهجیكردنی مهرجهكان بۆ پروانامهیی ماستهر له ئهنذاریاری میكانیک و ووزه

لهلایهن

دارهوان بازیان ظاهر

بهكالۆریۆس له ئهنذاریاری ساردكردنهوه و ههواسازی

به سهپرپرشتیاری

پ. د. احمد محمد ادهم

ههولیر - كوردستان

گهلاویژ ۲۰۲۳

پوخته

ساردكهرموه باوترين و كاراترين ريگايه بو پاراستنى خوراك و دهرمان، هرچهنده كاركردى بهردهوامى بريكى بهرچاو وزه بهكاردهينيت. بويه، هم تويزينهويه ليكولينهوه و هلسهنگاندى بو نهداى گشتى ساردكهرموهيهكى مالان كرد بهبهكارهينانى مادهكانى گورينى قوناغ (PCMs) و نانوكهرديلهكان (Nanoparticles). مادهكانى گورينى قوناغ به تاك و به كو خراانه سهر بههلمكهر (ههلمگرتنى ساردى بههلمكهر، ECS) و كوندنيسهر (ههلمگرتنى گهرمى كوندنيسهر، CHS). ههرهها ساردكهرموهيهك به دووانه ههلمگرتنى وزه (DES) و ههلمگرتنى وزه تيكه لآو (CES) پيشنياركرا. يهكهميان (CHS) و (ECS) و دووهميان (CHS) و (ECS) و پانيلهكانى (PCM) له كابينهى سهلاجهدا لهخوگرتبوو. مادهكانى گورينى قوناغ پارافينى تورگانيك، هايدراتى خوئى ناتورگانيك و ناوى پاكراوه بوون. بهكارهينانى وزه لهلايهن ساردكهرموهكان بهپنى ستانداردهكانى (ISO) ههلهسهنگيندرا. نايژوبوتان (R600a) مادهى ساردكهرموه بوو له سيستههمهكدا. تاقيردنهوهكان برى بوون له بهكارهينانى چهندين (PCM) بو كوندنيسهر و بههلمكهرهكان. (PCM) لهگهل نانوكهرديلهكانى ئوكسيدى مس (CuO) به تنيا لهسهر كوندنيسهر تاقيركرايهوه. له نهجامدا، له ريگهى شيكارى و تاقيردنهويهكى بهر فر اوانهوه، كارايى گشتى ساردكهرموهكه باشتر بوو. (CHS) به شيويهكى كارىگهر تواناى ساردى (COP) باشتر كرد و پلهى گهرمى كابينهكانى پاراست، له كاتيكدا (ECS) به شيويهكى كارا وزهى پاشهكهوت كرد و ههلاوسانى پلهى گهرمى لهناو كابينهكاندا كهمكردهوه. گرنگترين باشتركردنهكان لهلايهن تاقيردنهوهكانى (DES) و (CES) بوون بههوى تيكهلكردنى لايهنه خراپ و باشهكانى بهكارهينانى (PCM) لهسهر كوندنيسهر، بههلمكهر و كابينهى سهلاجه به جيا. پاشهكهوتكردى وزه بو كهيسهكانى (CHS)، كهيسهكانى (ECS)، (DES)، و (CES) ۱۰.۸۷-۲۱.۲۴%، ۲۳.۴۷-۱۵.۲۱%، ۲۴.۲۹%، و ۲۶.۴۲% بوو. باشتربوونى (COP) بو تاقيردنهوهكانى (CHS)، تاقيردنهوهكانى (ECS)، (DES)، و (CES) ۷.۵۶-۱.۵۸%، ۴.۳۵-۵.۵۰%، ۸.۸۱%، و ۹.۱۰% بوو. هرچهنده پلهكانى گهرمايان بهرزبووتهوه، بهلام گورانى پلهكانى گهرما له كابينهكانى سهلاجه و بهفرگردا به ريزهه ۱۵.۵۳-۵۶.۵۳% و ۰.۶۱-۲۶.۴۶% دابهزيوه.